THÈSE POUR OBTENIR LE GRADE DE DOCTEUR DE L'UNIVERSITÉ DE MONTPELLIER

En Biologie

École doctorale Sciences Chimiques et Biologiques pour la Santé (CBS2)

Unité de recherche UMR 5294 CNRS Laboratory of Pathogen Host Immunity

A Unique Mechanism of Action of an Acyclic Nucleoside Phosphonate as Potent Inhibitor of Malaria Parasite cGMP Dependent Protein Kinase

Présentée par Marie ALI

07/09/2023

Sous la direction de Rachel CERDAN

Devant le jury composé de

Catherine LAVAZEC, DR, Institut Cochin, CNRS UMR8104	Rapportrice
Olivier SILVIE, DR, CIMI, INSERM U1135	Rapporteur
Françoise BENOIT-VICAL, DR, LCC, INSERM ERL1289	Présidente du jury
Bruno PRADINES, DR, IHU	Examinateur
Sharon WEIN, IR, UM, CNRS UMR5294	Co-encadrante
Rachel CERDAN, PR, UM, UMR5294	Directrice de thèse

UNIVERSITÉ DE MONTPELLIER

“Yesterday is but today’s memory and tomorrow is today’s dream.”

Gebran Khalil Gebran

Acknowledgment

Writing the acknowledgement made me realize the reality of the end of my chapter in the lab. I have been incredibly fortunate to be surrounded by so many amazing people, and outstanding researchers. It saddens me to leave, but rest assured, I will always pop up, unannounced and uninvited.

First and foremost, I would like to express my deepest gratitude to my thesis director, Rachel Cerdan, for her support, guidance, and mentorship throughout my research journey. Your expertise, patience, and dedication were instrumental in shaping the outcome of this thesis.

This journey couldn't have been completed without my amazing supervisors, Sharon Wein Gratraud, and Kai Wengelnik. Sharon you have always shown trust and support, regardless of my requests, thank you for instilling in me the necessary methodology and rigor for conducting a scientific project. Managing two Maries for this long, make you a super woman! Kai, you embody the tough love saying. It is the hardest, but the purest and most valuable form of love. Behind your intimidating façade lies the wisest, sweetest, most caring person I have ever met. I have grown scientifically by your side. Thanks for the enthusiasm you demonstrate during our scientific discussions, and the advices you have given me.

This project could not have taken place without the collaboration of Suzanne Peyrottes and Thomas Cheviet. Thank you for your immense contribution to this project, your (hyper)responsiveness, and your availability. Me requesting the compound was an easy task, but I know how hard you worked for generating it, and for that, mille merci.

My sincere appreciation to the members of my thesis committee, Bruno Pradines, Yvon Sterkers and Arthur Talman, for their valuable insights, critical feedback, and the time they dedicated to reviewing and improving this work.

I extend my gratitude to the reviewers, Catherine Lavazec and Olivier Silvie, for evaluating this thesis. Thanks to the examiners, Françoise Benoit-Vical and Bruno Pradines, for accepting the task of assessing this work and contributing their expertise to this project.

For the friendship formed along the journey, Eitac Murshudzada, Casilda Muñoz, Coralie Duclovel, Inayat Bhardwaj, Pawan Kumar, Quentin Chevalier, Rafael Miyazawa Martins, my baby Albanian brother Réa Dura, and my northern ally Reem El Monla. You all have a place

engraved in my heart, I never once felt, “This is too hard, I can’t anymore”. You made spending the nights in the lab one of the most pleasant experiences a PhD student can have. I cherished every second. Of course, I cannot forget to thank the best office mate anyone can ever have Yann Bordat, and my pranking partner Marjorie Bienvenue.

A big thank you to Jose Juan Lopez Rubio, Maryse Lebrun, Mauld Lamarque, Sebastien Besteiro, Anthoine Claessens, Georges Lutfalla, Laure Yatim and Ana Rita Batista Gomes. You pushed us to become, in my humble opinion, great researchers. Thank you for spreading positivity, sharing your knowledge and implementing so many meetings where we had to present. I was able to develop immunity to the stress of presenting.

Thanks to my close ones and my family for their encouragement and the love they have shown me, especially my parents for their financial support throughout my never-ending studies. Thanks to my friends, to my “forced to be twin sister”, Mona Bourgess. The me I see through your eyes is such an amazing person that I strive to become, I am really lucky to have you as my forever. To my baby sisters, Roy Aghnatios and Ralph Chahwane, thank you for the fun, the unconditional support, and the long journeys you made to always be by my side when I needed you. To my big sisters Marleine Tamer and Raneen Ibrahim, as the eldest in my family I am used to taking care of others. But how lucky was I to find two amazing souls who adopted me, took care of me, and never allowed me to be alone in the lab.

Most importantly to Veronica Ghoughasian, you were with me in every important step of my life. You pushed me beyond boundaries, and you created the person I am today. You are my idol, you always fought your battles, never backed down, even until the end. I want to keep making you proud so you could keep shouting “This is my granddaughter! She’s a bit crazy, but truly amazing!”.

This work would not have been possible without the collective contributions and support of all those mentioned and many others who, in various ways, played a part in this research.

To the one and only, whenever the experiments didn’t work and we needed a higher power interference.

THANK YOU.

Table of Content

Summary 13

Résumé 14

List of Figures 17

List of Tables 19

Abbreviation List 21

General Introduction 25

Chapter I: Malaria 27

1. Introduction 27
2. Malaria Etiology 27
3. *Plasmodium* Life Cycle 29
   - A. Parasite Development in the Human Host 31
     - i. Hepatic Stage 31
     - ii. Intraerythrocytic Cycle 33
     - iii. Key Pathways 35
       - a. Invasion Pathway 35
       - b. Egress Pathway 36
   - B. *P. falciparum* in the Mosquito Host 37
     - i. Parasite Development 37
     - ii. Signaling Pathway Involved in Gametogenesis 38
4. Malaria Symptoms and Pathology 40
   - A. Asymptomatic Malaria 41
   - B. Uncomplicated Malaria 41
   - C. Complicated Malaria 42
5. Epidemiology of the Disease 43

6. The War Against Malaria....44
A. Vector Control....44
B. Diagnostic....45
C. Vaccination....46
D. History of Antimalarial Drugs....48
i. The Current Antimalarial Drugs....49
a. The Arylaminoalcohol....49
b. 4- Aminoquinoline....50
c. The 8-Aminoquinoline....52
d. Artemisinin, and its Derivatives....55
e. The Antifolates: Sulfadoxine-Pyrimethamine and Proguanil....57
f. Doxycycline....58
g. Hydroxynaphthoquinones....59
ii. Into the Future....64
a. Inhibitor of *Plasmodium* Elongation Factor 2....66
b. Inhibitor of *Plasmodium* P- Type NA^+ ATPase....66
c. Inhibitor of Dihydroorotate Dehydrogenase....67
Chapter II: Exploring New Horizons of Acyclic Nucleoside Phosphonate 69
1. Introducing a Possible New Antimalarial Compound: UA2239, an Acyclic Nucleoside Phosphonate....69
2. UA2239 Unexpected Mechanism of Action on *P. falciparum* 71
Chapter III: Exploring the Possible UA2239 Interaction 75
1. UA2239, a Cyclic Guanosine Monophosphate Analogue....75
2. Possible Targets of UA2239....77
A. The Guanylate Cyclases 77
B. The Phosphodiesterases....80

C. The cGMP-Dependent Protein Kinase G 83
i. Human cGMP-Dependent Protein Kinase G 83
ii. *Plasmodium* cGMP-Dependent Protein Kinase G, and its Allosteric Activation 85
Thesis Objectives 89
The Results 93
Chapter I: UA2239 Target Validation and Characterization 95
1. Introduction 95
2. Results 95
A. UA2239 does not Target *P. falciparum* DNA Synthesis 95
B. Identification of UA2239 Target 96
C. Validation of PKG as the Target of UA2239 99
i. Generation of *Pf*ePKG Transgenic Parasites 99
ii. Let's Talk Controls 103
iii. Genetic Validation of *P. falciparum* as UA2239 Target 104
iv. Phenotypic Validation of UA2239 Target 105
D. Characterizing the Evolution of Resistance, the Fitness Toll 108
i. Surviving the Challenge: *Pf*ePKG D597Y 108
ii. Uncovering the Subtle Fitness Toll 109
E. Assessing Antimalarial Drug's Efficacy on UA2239-Resistant Strains 110
F. *P. falciparum* Mechanism of Resistance Against UA2239 113
3. Conclusion 115
Chapter II: UA2239 Characteristic as an Antimalarial Drug 117
1. Introduction 117
2. Results 117
A. Exploring Cross-Resistance to C2, a *Pf*PKG Inhibitor 117
B. Combining UA2239 with C2 118

C. Unveiling the Entry Mechanism of UA2239.....120

B. Assessment of UA2239 Efficacy Across Different Stages of the Malaria Parasite's Intraerythrocytic Cycle.....121

C. UA2239 Effect on *P. berghei* Gametocytes.....123

3. Conclusion.....124

Material & Methods 127

Cell Biological Methods..... 129

1. Thawing of *P. falciparum* Parasites.....129
2. Freezing of *P. falciparum* Parasites.....129
3. *P. falciparum* Culture 129
4. *P. falciparum* Synchronization 130

i. 70%-Percoll Synchronization 130

ii. 5%-Sorbitol Synchronization.....130

5. Ring-Stage Survival Assay.....130
6. Flow Cytometry.....131
7. Immunofluorescence Assay 132
8. Transfection.....132

A. Transfection by Direct Electroporation. 132

B. Transfection by Invasion of DNA-Loaded Erythrocytes. 133

9. *In vitro* Drug Sensitivity Assay 133
10. Isobologram 134
11. Stage Specificity Assay 134
12. Time Course Assay 134
13. Activity of *Plasmodium berghei* Male Gametocyte Exflagellation 135

Molecular Biology 136

1. Insertion of the Sequence of Interest into pBluescript.....136

A. *P. falciparum* cGMP-dependent Protein Kinase G 136

B. *P. falciparum* Phosphodiesterase-β into pBluescript 138

2. Insertion of the Guide RNA in the pDC2-cas9-sgRNA-*h*DHFR Plasmid 140

C. Colony Screening- PCR1 141

D. Analysis of Transgenic Parasites- PCR2 141

E. Quantitative PCR 142

Conclusion & Discussion 143

1. Exploring the Mechanism of Action of UA2239 145

2. Pharmacological Properties of UA2239 149

Annexes 153

Table containing all the primers used for this study 155

The Different *E. coli* Codonized *Pf*pkg (699bp) Sequences 157

The Different *E. coli* Codonized *Pf*pdeβ (150bp) Sequences 159

References 161

Summary

Elimination of malaria relies on the development of new antimalarial compounds belonging to a new chemical class and with a novel mechanism of action. In collaboration with a team of medicinal chemists, we identified purine analogs of a new Acyclic Nucleoside Phosphonates (ANPs) family with potent antimalarial effect. The lead compound UA2239 has a strong activity *in vitro* on *Plasmodium falciparum* growth with an IC_{50} value of 74 nM (in 3D7 strain) and *in vivo* in *Plasmodium berghei*-infected mice with an efficient dose to inhibit 50% of the parasite growth, ED_{50} of 0.5 mg/kg after intraperitoneal administration.

During this thesis, our objective was to decipher the mechanism of action of UA2239 compound. We were able to reach our objective through the generation of UA2239 resistant parasites by compound pressure for 7 months, followed by the analysis of the whole genome sequence of these resistant clones. *Plasmodium falciparum* cyclic GMP-dependent protein kinase G (*Pf*PKG) was identified as the target of UA2239. This enzyme contains four regulatory cGMP-binding domains, one of which does not bind cGMP, followed by the kinase domain. *Pf*PKG is an essential enzyme implicated in the different stages of the parasite life cycle. It has been shown to be implicated in the invasion and egress pathways of merozoites, but also in the gliding activity of ookinetes and sporozoites.

We characterized the effects of UA2239 at the molecular and phenotypic levels. First, we validated *Pf*PKG as a molecular target of UA2239 by introducing into parasites the single nucleotide mutations found in resistant clones. We deciphered the mode of action of UA2239 and showed that the compound has a completely new way of inhibiting *Pf*PKG by targeting one of the regulatory domains, thus blocking cGMP-mediated activation of PKG, whereas other known PKG inhibitors interact with the catalytic site. We also discussed the mechanism of resistance induced by *Pf*PKG mutations

In parallel, we showed how the compound enters the red blood cell and that UA2239 blocks the merozoite egress during the intraerythrocytic. We also were able to discover that UA2239 has an irreversible effect on both trophozoites and schizonts.

In conclusion, UA2239 has potent effects on *Plasmodium* and its unique mechanism of action makes it a promising novel antimalarial.

Résumé

L'élimination du paludisme repose sur le développement de nouveaux composés antipaludiques appartenant à une nouvelle classe chimique et possédant un nouveau mécanisme d'action. En collaboration avec une équipe de chimistes médicinaux, nous avons identifié des analogues de purine d'une nouvelle famille de nucléosides phosphonates acycliques (ANP) ayant un puissant effet antipaludique. Le composé principal UA2239 a une forte activité *in vitro* sur la croissance de *Plasmodium falciparum* avec une valeur IC_{50} de 74 nM (dans la souche 3D7) et *in vivo* chez des souris infectées par *Plasmodium berghei* avec une dose efficace pour inhiber 50% de la croissance du parasite, ED_{50} de 0,5 mg/kg après administration intrapéritonéale.

Au cours de cette thèse, notre objectif était de décrypter le mécanisme d'action du composé UA2239. Nous avons pu atteindre notre objectif grâce à la génération de parasites résistants à l'UA2239 par pression du composé pendant 7 mois, suivie de l'analyse de la séquence du génome entier de ces clones résistants. La protéine kinase G dépendante du GMP cyclique de *Plasmodium falciparum* (*Pf*PKG) a été identifiée comme la cible principale de l'UA2239. Cette enzyme contient quatre domaines régulateurs de liaison au GMPc, dont l'un ne lie pas le GMPc, suivis du domaine kinase. *Pf*PKG est une enzyme essentielle impliquée dans les différentes étapes du cycle de vie du parasite. Il a été démontré qu'elle est impliquée dans les voies d'invasion et de sortie des mérozoïtes, mais aussi dans l'activité de glissement des ookinètes et des sporozoïtes. Nous avons caractérisé les effets de l'UA2239 aux niveaux moléculaire et phénotypique. Tout d'abord, nous avons validé *Pf*PKG en tant que cible moléculaire de l'UA2239 en introduisant dans les parasites, les mutations ponctuelles trouvées dans les clones résistants. Nous avons décrypté le mode d'action de l'UA2239 et montré que le composé bloque le cycle de vie du parasite la sortie du mérozoïte pendant le cycle intra-érythrocytaire. Nous avons montré comment le composé pénètre dans le globule rouge et que l'UA2239 a un effet irréversible et spécifique à chaque étape. Enfin, nous discutons du mécanisme de résistance induit par les mutations *Pf*PKG. Ce nouveau composé a probablement une toute nouvelle façon d'inhiber la *Pf*PKG en ciblant l'un ou plusieurs domaines régulateurs, bloquant ainsi l'activation de la PKG médiée par le GMPc, alors que d'autres inhibiteurs connus de la PKG interagissent avec le site catalytique. En conclusion,

UA2239 a des effets puissants sur *Plasmodium* et son mécanisme d'action unique en fait un nouvel antipaludique prometteur.

List of Figures

Fig. 1. Ultrastructure of *Plasmodium* intraerythrocytic stages 28
Fig. 2. Schematic representation of *Plasmodium* life cycle.. 31
Fig. 3. Schematic representation of *Plasmodium* hepatic stage 32
Fig. 4. *Plasmodium* asexual intraerythrocytic cycle 34
Fig. 5. The stages of gametocyte development in *P. falciparum* 35
Fig. 6. *P. falciparum* RBC invasion pathway cascade 36
Fig. 7. *P. falciparum* egress pathway cascade 37
Fig. 8. *Plasmodium* development in the mosquito host 38
Fig. 9. Indigenous cases in 2000 and their status by 2021 43
Fig. 10. Timeline of main antimalarials and occurring resistance 48
Fig. 11. Schematic representation of chloroquine mechanism of action 51
Fig. 12. Schematic representation of primaquine mechanism of action 54
Fig. 13. Folate pathway and Antifolate drugs against this pathway malaria 57
Fig. 14. Scheme of intraerythrocytic *P. falciparum* depicting doxycycline dose dependent mechanism of action 59
Fig. 15. Atovaquone mechanism of action in the mitochondrial respiratory chain in *Plasmodium* 60
Fig. 16. The pipeline of future possible antimalarial drugs. 65
Fig. 17. Chemical structure of M5717 and its key biological and physical properties. 66
Fig. 18. Chemical structure of KAE609 and its key biological and physical properties. 67
Fig. 19. Chemical structure of DSM265 and its key biological and physical properties 68
Fig. 20. Chemical structures of acyclic nucleoside phosphonates with antiviral 69
Fig. 21. Preliminary results for UA2239 71
Fig. 22. The effect of UA2239 on the development of *P. falciparum* 72
Fig. 23. Similarities in the chemical structures of cGMP and UA2239. 73
Fig. 24. cGMP involvement in the *Plasmodium* cycle. 76
Fig. 25. *P. falciparum* stage specific involvement of cyclic nucleotide signaling components and protein kinases. 77
Fig. 26. Guanylate cyclases 79
Fig. 27. Phosphodiesterases 81

Fig. 28. Structure of the human Protein kinase G 85
Fig. 29. *Plasmodium* protein kinase G. 86
Fig. 30. *Plasmodium* PKG inhibitors. 88
Fig. 31. UA2239 does not target DNA synthesis. zoites. N=2. Hpi: Hours Post-Invasion. 96
Fig. 32. The SNPs identified through WGS of the resisNA extracted and underwent WGS....99
Fig. 33. Identification of UA2239 target in *P. falciparum*. 100
Fig. 34. Diagnostic PCRs for the transgenic population of *Pf*ePKG.....102
Fig. 35. *In vitro* UA2239 activity on the different control strains used in this study.....104
Fig. 36. Visualization of the parasitophorous vacuole membrane of *P. falciparum* schizonts.
.....107
Fig. 37. *Pf*ePKG D597Y mutation causes a strong fitness cost for the parasite.....109
Fig. 38.The mutation conferring resistance to UA2239 cause a fitness cost 110
Fig. 39. Sensitivity of UA2239 resistant clones to dihydroartemisinin (DHA) 112
Fig. 40. Diagnostic PCRs for *Pf*ePDEβ integration 114
Fig. 41. *In vitro* interaction between UA2239 and C2, an inhibitor of *Pf*PKG.....119
Fig. 42. Schematic representation of the methodology of two techniqures 122
Fig. 43. Time course of *P. falciparum* growth inhibition.....123
Fig. 44. Impact of UA2239 on *P. berghei* gametocyte exflagellation after intraperitoneal (i.p)
administration.....124
Fig. 45. *In vitro* interaction between UA2239 and Furosemide, a new permeability pathway
(NPP) inhibitor.....121
Fig. 46. The genomic locus of the *P. falciparum* 3D7 PKG 136
Fig. 47. Preparing the pBluescript containing the donor *Pf*PKG DNA.....137
Fig. 48. Alignment of *Pf*PKG and *Pf*ePKG wild type sequences aligned.....138
Fig. 49. Preparing the pBluescript containing the donor DNA for *Pf*ePDEß 139
Fig. 50. Alignment of *Pf*PPDEß and *Pf*ePDEß wild type sequences aligned.....140
Fig. 51. Constructing the pDC2-Cas9-gRNA plasmid for *Pf*PKG. 141
Fig. 52. X-ray 3D structure of *Pf*PKG C 147
Fig. 53. *Pf*PKG conformational changes upon cGMP binding in the CNB-D domain of *Pf*PKG .
.....148

List of Tables

Table 1. Artemisinin derivatives available as co-formulations.....56

Table 2. Classes of currently used antimalarial drugs. 63

Table 3. *In vitro* antimalarial activity of UA2239 on resistant strains (Resistant) and *Pf*ePKG or *Pf*ePDEβ mutated strains (Transgenic)..105

Table 4. Antimalarial activity of chloroquine on UA2239 resistant and transgenic strains. .111

Table 5. Antimalarial activity of UA2239 and C2 on C2- and UA2239-resistant strains, respectively. 118

Table 6. *In vitro* stage-dependent susceptibility of *P. falciparum* (3D7) to UA2239.....122

Abbreviation List

ACT	artemisinin-based combination therapy
AIS	auto-inhibitory sequence
AMA	Apical Membrane Antigen
ANP	acyclic nucleoside phosphonate
ART	artemisinin
ATP	adensine triphosphate
bp	base pair
C2	compound 2
cAMP	cyclic adenosine monophosphate
CDC	center for disease control and prevention
CDPK	Ca2+ dependent protein kinase
cGMP	cyclic guanosine monophosphate
CNB	cyclic nucleotide binding domains
CPR	cytochrome P450 NADPH-reducatse
CQ	chloroquine
CRT	chloroquine resistant transporter
CSA	chondroitin sulfate A
CSP	circumsporozoite protein
CYP2D6	cytochrome P450 2D6
DDT	dichloro-diphenyl-trichloro-ethane
DHA	dihydroartemisnin
DHFR	dihydrofolate reductase

DHODH	dihydroorotate dehydrogenase
DHPS	dihydropteroate synthase
DOX	doxycycline
EBA	erythrocyte binding antigen
EMP	erythrocyte membrane protein
Eph	Epherin
ER	endoplasmic reticulum
FV	food vacuole
G6PDd	glucose-6-phosphate dehydrogenase deficient
GC	guanylate cyclase
h	hour
*h*DHFR	*human* dihydrofolate reductase
hpi	hour post invasion
HRP	histidine-rich protein
HSPG	heparan sulfate proteoglycan
IC50	50% inhibition concentration
IFA	immunofluorescence assay
iRBC	infected RBC
IRS	indoor residual spraying
ITN	insecticide-treated nets
LRP	lipoprotein receptor related protein
LSM	larval source management
mdr	multidrug resistance

mGC	transmembrane GC
MQ	mefloquine
MSP	merozoite surface protein
NK	natural killer
NPP	new permeability pathway
O=PQm	quinoneimines
OH-PQ	hydroxylated-PQ
PDE	phosphodiesterase
PKA	protein kinase A
PKG	protein kinase G
PPP	Parasite Plasma Membrane
PPM	parasite protein phosphatase
PQ	primaquine
PV	parasite vacuole
PVM	parasitophours vacuole membrane
PYR	pyronaridine
QN	quinine
RBC	red blood cell membrane
RBCm	RBC membrane
RDT	rapid diagnostic test
RH	reticulocyte binding protein homologue
ROS	reactive oxygen species
SERA	serine-like repeat antigen

SERCA	SARCO/endoplasmic reticulum calcium
sGC	soluble GC
SNP	single nucleotide polymorphism
SUB	subtilisin-like protease
TQ	tafenoquine
TRAP	thrombospondin-related anonymous protein
VE	vaccine efficacy
WGS	whole genome sequencing
WT	wild type

General Introduction

Chapter I: Malaria

1. Introduction

The term "malaria" originates from the Italian "*mala aria",* meaning bad air, reflecting to how malaria was thought to be transmitted in the mid-18th century. Throughout the years, the intermittent fevers has served as specific symptom to document the evolution of malaria[1]. The first descriptions of these symptoms date to ancient time. However, the official cause of the disease was not discovered until 1880 by the French Surgeon, Dr. Charles Louis Alphonse Laveran[1]. While he was examining blood smears of sick soldiers, he observed the presence of granules of black pigment which were absent in both healthy people and patient suffering from other diseases. Later on, this pigmentation was linked to the presence of parasites inside the Red Blood Cells (RBCs). His tenacious hard work led to the description of four distinct stages of the malaria parasite (rings, trophozoites, schizonts and gametocytes)[1]. Nonetheless, the discoveries of Dr. Laveran were met with skepticism until 1885, when Marchiafava and Celli, two Italian researchers confirmed Dr. Laveran's earlier findings and gave the parasite the name "*Plasmodium*"[1]. Finally, in 1907, Dr. Laveran was rewarded the Nobel prize for the identification of the intraerythrocytic forms of the causative agent of malaria. Since then, extensive studies have been conducted to better understand the biology of the parasite and the resulting disease.

2. Malaria Etiology

Malaria is a vector borne disease caused by a parasite from the genus *Plasmodium*, an obligate endo-parasite. This genus is part of the Apicomplexa phylum, which regroups more than 6 000 described species[2], such as *Toxoplasma, Babesia***,** and *Cryptosporidium*, among others.

Several apicomplexan parasites are of great medical, veterinary, agricultural and economic importance as they affect humans and animals. The most intriguing apicomplexan is *Plasmodium* as it is responsible for one of the deadliest infectious diseases in the world. To date, there are over 200 species of *Plasmodium* described[3]. *Plasmodium* species have shown a high degree of host specificity, and only six of them can infect humans. *Plasmodium falciparum* (*P. falciparum*) and *Plasmodium vivax* (*P. vivax*) are responsible for most of the current malaria cases, with *P. falciparum* being the most lethal species. The four other species

that can infect humans are *Plasmodium malariae* (*P. malariae), Plasmodium ovale curtisi* and *Plasmodium ovale* wallikeri and the recently added *Plasmodium knowlesi* (*P. knowlesi*) which originally infects monkeys. The remaining *Plasmodium* species can infect a wide variety of vertebrate animals, including apes, rodents, chickens, and snakes.

Plasmodium possesses the typical organelles found in eukaryotic organisms, such as a nucleus, endoplasmic reticulum, Golgi apparatus, mitochondria. Additionally, it has some organelles that are unique to Apicomplexans **(Fig. 1)**, which are listed below.

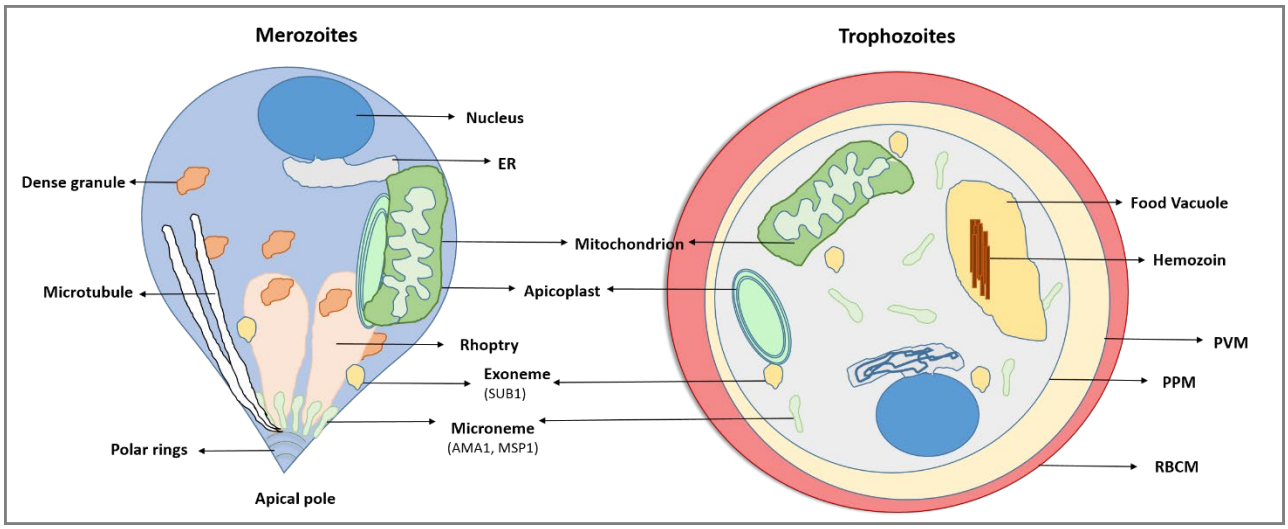

Fig. 1. Ultrastructure of *Plasmodium* intraerythrocytic stages. AMA1: Apical Membrane Antigen-1; ER: Endoplasmic Reticulum; MSP1: Merozoite Surface Protein-1; PPM: Parasite Plasma Membrane; PVM: Parasitophorous Vacuole Membrane; RBCM: Red Blood Cell Membrane, SUB1: Subtilisin-like protease-1.

- The parasitophorous vacuole membrane (PVM) is formed around the parasite during its cell invasion. It creates an environment suitable for the parasite development. During the hepatic stage the PVM protects the parasite from being degraded by the endocytic/lysosome system, and from cell intrinsic defenses such as apoptosis and selective autophagy[4]. Additionally, in both the hepatic stage and the intraerythrocytic cycle the PVM acts as conduit for communication and nutrient acquisition[5].
- The apicoplast is a derived non-photosynthetic plastid found in all Apicomplexa, except in *Cryptosporidium*. The Apicomplexa acquired this organelle by secondary endosymbiosis of a plastid, from a *Cyanobacterium*[6]. Even though the apicoplast evolution in the Apicomplexa resulted in its loss of all photosynthetic abilities, it still retained an important number of prokaryotic metabolic pathways. These pathways include the synthesis of:

fatty acids (precursors for membrane lipid synthesis), iron sulfur clusters (co-factors for essential biological functions), heme and isoprenoids (critical for diverse cellular process such as prenylation of proteins involved in vesicular trafficking)[7]. In the intraerythrocytic cycle the only essential role of the apicoplast was shown to be the synthesis of isoprenoids[8]. These functions make the apicoplast essential for the parasite, which makes it an interesting drug target.

- The apical complex is a unique organelle at the apex of the Apicomplexa phylum, hence its name. It is composed of secretory vesicles: the micronemes, the rhoptries and the dense granules[9]. This complex is involved in multiple functions, such as host cell invasion, protein secretion, and gliding motility[9]. It also contributes to the formation of the parasitophorous vacuole[10].
- The exonemes are newly discovered apical secretory organelles[11], they store the Subtilisin-like protease 1 (SUB1). This protease plays a role in the egress of invasive merozoite from both the hepatic stage[12] and the intraerythrocytic stage[13,14].

Alongside the organelles commonly found in Apicomplexa, *Plasmodium* possesses its own distinct organelles:

- The digestive vacuole or food vacuole (FV) is a lysosome-like acidic organelle. Its role is to degrade hemoglobin by the proteases. Briefly, hemoglobin is transferred from the RBCs cytoplasm to the parasite FV through cytostomes[15]. Once inside the FV, the hemoglobin will be digested by proteases and this degradation will supply *Plasmodium* with amino acids[15]. Another product of this digestion is heme. It is a toxic by-product, which will be detoxified by biocrystallization to hemozoin[15] **(Fig. 1).**
- The new permeability pathways (NPPs) are channels established at the erythrocyte membrane from 15 h after invasion[16]. They allow the entry of a wide range of nutrients such as anions, small non-electrolytes and also macromolecules[16]. They play a crucial role in the survival and development of the parasite within the host cell.

3. *Plasmodium* Life Cycle

The milestone in completing the life cycle of *Plasmodium* occurred on the 20th of August 1897, when Surgeon Major Ronald Ross discovered the malaria life cycle within female *Anopheles*

mosquitoes. These mosquitoes are the host of the sexual form of *Plasmodium* and are responsible for the transmission of the parasite to its second host.

Of the approximately 500 *Anopheles* species known worldwide, the Center for Disease Control and Prevention (CDC) reported that only 30 to 40 of them can transmit malaria in their natural habitats[17,18]. The species vary depending on the region and the environment. For example, in Africa, the dominant species are *Anopheles gambiae* and *Anopheles funestus,* while in South Asia and the Arabian Peninsula, *Anopheles stephensi* is dominant[19]. This latter species has been reported by WHO to be very adaptable and invasive and the organization is working on stopping its further spread. *Plasmodium* exhibits a heteroxenous complex life cycle, which involves two different hosts: the female *Anopheles* mosquito serving as the definitive host for sexual reproduction of the parasite, and the vertebrate host, acting as the intermediate host for asexual reproduction. Along the cycle, the parasite features various forms specifically adapted to establishing infection, proliferating and, finally, mediating transmission (**Fig. 2**).

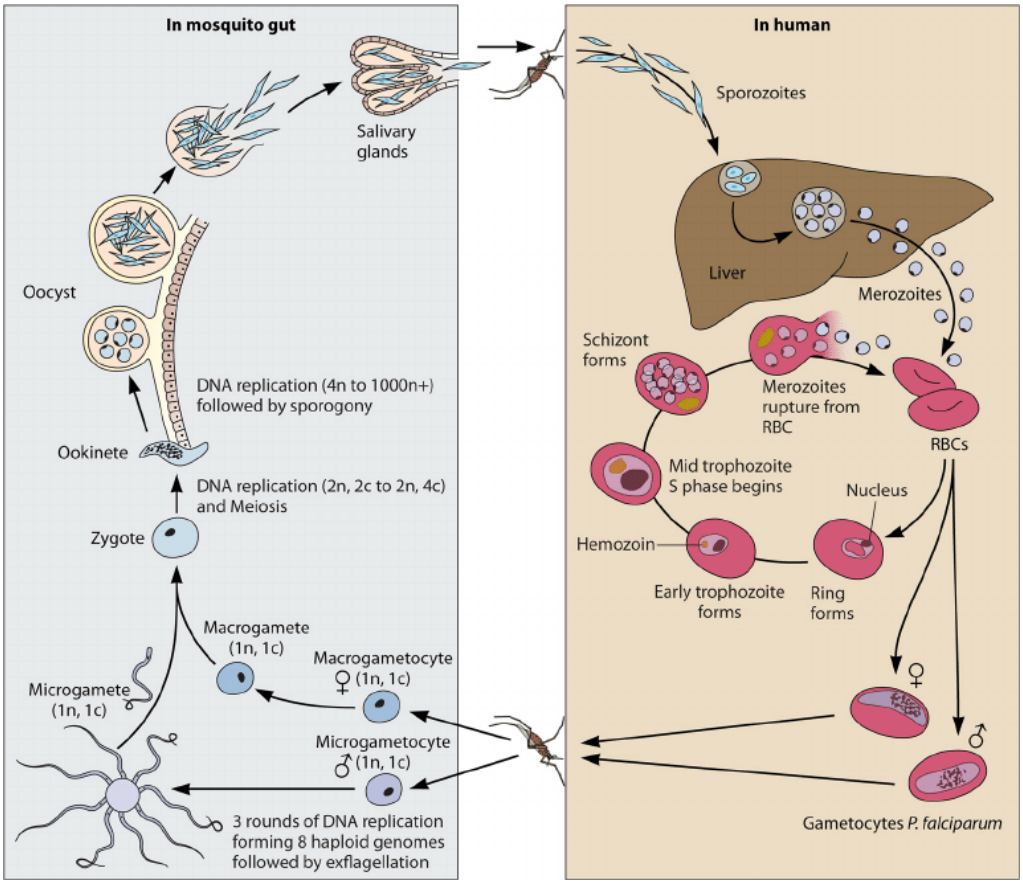

Fig. 2. Schematic representation of *Plasmodium* life cycle (Andrew H Lee *et al*, 2014) [20]**.** The transmission of malaria starts when a female Anopheles mosquito (left) transfers *Plasmodium* parasite to a human host (right). Following an initial stage in the liver, the parasite enters an asexual cycle within the red blood cells. From these intraerythrocytic parasites, sexual forms can develop, allowing transmission to another mosquito. Within the mosquito, the parasites undergo both meiotic and mitotic replication, resulting in the formation of sporozoites. These sporozoites have the ability to infect another human host. RBC: Red Blood Cell.

A. Parasite Development in the Human Host

i. Hepatic Stage

During a blood meal, the mosquito injects saliva containing vasodilators and coagulant to facilitate the ingestion of blood. At the same time, 20-200 parasites at sporozoite stage contained in the salivary gland of the mosquito will be inoculated in the skin[21]. The sporozoites use their motor driven mechanism to move through the dermis until they reach a blood vessel and enter the bloodstream[22,23].

Once in the bloodstream, these sporozoites have an exclusive tropism for hepatocytes. The sporozoites express at their surface the circumsporozoite protein (CSP) and the thrombospondin-related anonymous protein (TRAP). The parasites will use these proteins to

bind to the hepatocyte receptors heparan sulfate proteoglycans (HSPGs) [24,25] and the low density lipoprotein receptor related protein (LRP-1)[26] found on the surface of the hepatocytes. Other interactions include the parasite *P52* protein binding to the transmembrane receptor Epherin A2 (EphA2), the latter is essential for sporozoite invasion and concomitant PVM formation[27]. These interactions are essential for the continuation of the parasite life cycle making them potential targets for antimalarial drugs. In fact, the first approved malaria vaccine targets the CSP in this stage; more details about the vaccine will be presented later in this manuscript.

During this invasion, the sporozoites trigger the formation of the PVM[28]. The PVM will create a suitable environment, the parasitophorous vacuole (PV), where the parasite will be able to begin its asexual replication called exoerythrocytic schizogony. One sporozoite can develop into 10 000 merozoites[29]. Once the merozoites are mature, they will rupture the PVM. The merozoites will then bud off from the infected hepatocyte in vesicles named the merosomes[30] (**Fig. 3**). Each merosome contains 10 to 1 000 hepatic merozoites and is surrounded by modified host hepatocyte cell membrane, allowing the merosome to hide from the immune system (Kupffer cells) on their way to the bloodstream[30]. When the merosomes reach the bloodstream, the merozoites are released to initiate the intraerythrocytic cycle[30].

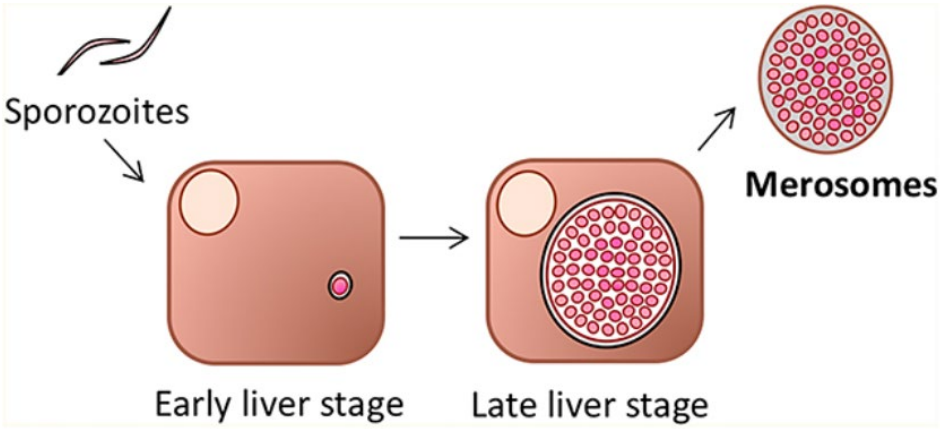

Fig. 3. Schematic representation of *Plasmodium* hepatic stage (Melanie J. Shears *et al,* 2020)[30].

This phase is asymptomatic and its duration varies depending on the *Plasmodium* species. For instance, *P. falciparum* hepatic stage process takes 6-7 days[31]. In the cases of *P. vivax* and *P. ovale,* they possess a unique feature, some of their sporozoites can differentiate into a dormant state known as hypnozoites[31]. Hypnozoites can remain inactive for extended periods of time (weeks, months, even years) before reactivating, leading to a malarial relapse[31]. This

phenomenon of relapse poses a significant challenge to the control and elimination of malaria.

ii. Intraerythrocytic Cycle

The intraerythrocytic cycle begins with the invasion of RBCs by the merozoites that have just been released into the bloodstream. While invading the RBCs, the merozoite invaginates into the RBC membrane (RBCm), resulting in the creation of the PVM, and the establishment of the PV[32]. The parasite will export and incorporate proteins in both of these membranes. This remodeling serves to facilitate the access of nutrients, and help the infected RBC (iRBC) escape the immune system[33].

Following invasion, the parasite undergoes maturation from its initial ring form to its trophozoite form within 24 hours post invasion (hpi) (**Fig. 4**). During this maturation, the parasite metabolic activity increases as it prepares for subsequent phase of asexual replication known as erythrocyte schizogony[20]. This process starts with the replication of the DNA, leading to the production of multiple copies of the parasite's genome. Each genome is then packaged into separate daughter merozoites, resulting in the formation of the schizont form[20] (**Fig. 4**). Each ring generates up to 32 new merozoites[20]. When the merozoites are mature, they will initiate the egress pathway. This pathway starts with the PVM rounding up and then rupturing, releasing the merozoites into the RBC cytoplasm. Then the RBCm rupture, releasing finally the merozoites into the bloodstream, and thus start another cycle of invasion-multiplication-dissemination.

The intraerythrocytic cycle duration depends on the species, the most abundant species: *P. falciparum, P. vivax*, *P. ovale* have a 48 hours (h) cycle, whereas *P. knowlesi*, and *P. malariae* have a 24 and 72h cycles, respectively.

The rupture of the RBCs and the release of waste and toxic factors like the hemozoin lead to the symptoms of malaria such as fever, anemia, chills, and headache[34].

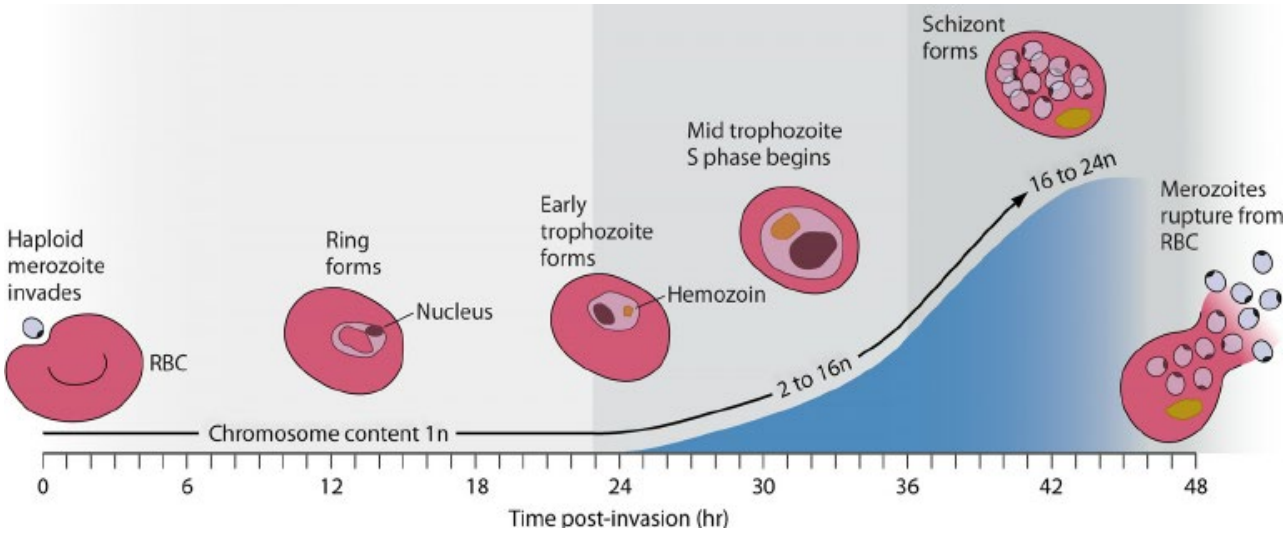

Fig. 4. *Plasmodium* asexual intraerythrocytic cycle (Andrew H Lee *et al*, 2014)[20]**.** *Plasmodium*'s intraerythrocytic cycle involves a haploid merozoite (1N) invading a red blood cell (RBC) and developing into the "ring" form (0-24 hpi). As the parasite transitions to the trophozoite stage, its metabolic activity increases in preparation for DNA replication. The asynchronous replication produces multiple copies of the genome up to 32 merozoites (24N). The genomes will then be packaged into daughter merozoites ready for egress and invasion of new RBCs.

During the intraerythrocytic cycle, some parasites will commit to gametocytogenesis, leading to the formation of either macrogametocytes (female gametocytes) or microgametocytes (male gametocytes). The level of commitment to these sexual forms of the parasite varies between *Plasmodium* species, suggesting the involvement of genetics and epigenetics factors[35]. The gametocytes will mature through different stages (stage I-> stage V) (**Fig. 5. A-B**). In the case of *P. falciparum,* stage V is reached in 10 days. During a blood meal of an *Anopheles* mosquito, asexual forms and gametocytes at different stages are ingested, of which only stage V gametocytes will be able to continue their cycle in their definitive host. Once in the mid-gut of the mosquito, the gametes are activated and fertilization can occur.

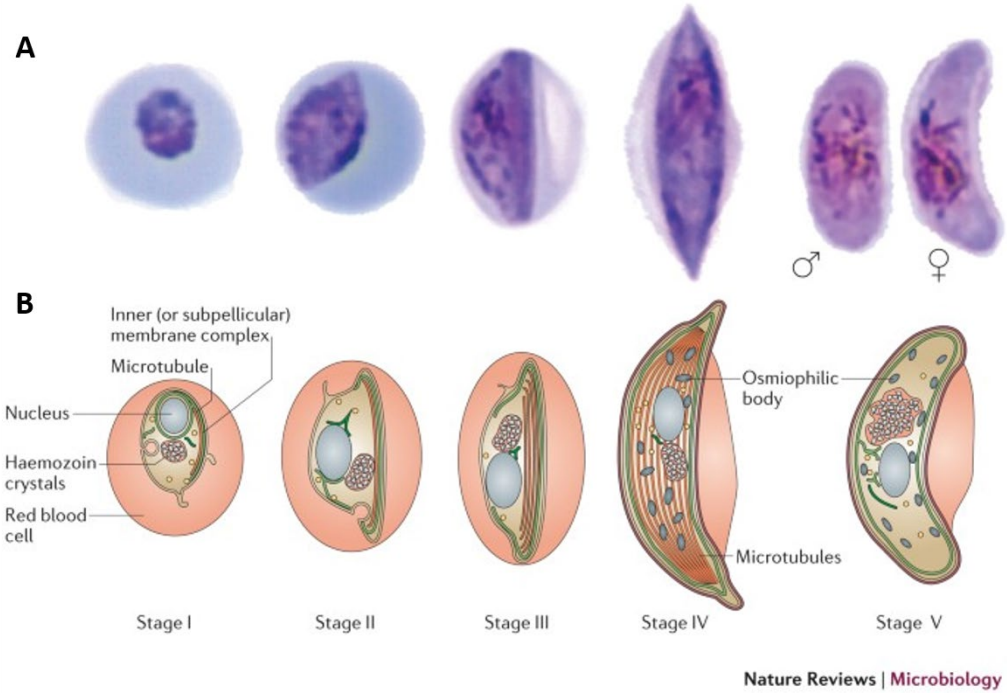

Fig. 5. The stages of gametocyte development in *P. falciparum* (Gabrielle A Josling *et al*, 2015)[36]. A) represents pictures taking of gametocytes at different time points in their development. **B)** Graphic representation of the different gametocyte stages. Each stage has a distinct shape which allows us to differentiate them. Stage I gametocytes have a round/ovale shaped similar to a young trophozoite. Stage II gametocytes are distinguished by being D-shaped. Stage III gametocytes are elongated with rounded ends. Stage IV gametocytes have pointed ends and are further elongated to the point of changing the shape of the RBC membrane. Stage V gametocytes allows us to differentiate the female and male gametocytes, with the female gametocytes having a more elongated banana shaped form, while the male gametocytes are potato shaped.

iii. Key Pathways

a. Invasion Pathway

The merozoites surface adhesins, which are essential proteins for the attachment of the merozoites to the RBCs are stored in micronemes and rhoptries. The discharge of these proteins is mediated by cyclic nucleotides and Ca^{2+} [37]. When merozoites are in the blood stream, they are exposed to factors which will cause the activation of protein kinases, that will modulate the phosphorylation of diverse target proteins necessary for merozoite invasion. In fact, the activation of *P. falciparum* Protein Kinase G (*Pf*PKG) and Protein Kinase A (*Pf*PKA) by cyclic guanosine monophosphate (cGMP) and cyclic adenosine monophosphate (cAMP) respectively, leads to a rapid increase in cytosolic Ca^{2+} which will activate several *P. falciparum* Ca^{2+} dependent protein kinases (*Pf*CDPKs)[38]. *Pf*CDPK1 plays a crucial role in micronemes discharge, a key step in erythrocyte invasion[39] (**Fig. 6**). Both of these latter signals

will cause the secretions of the adhesin proteins from the micronemes such as the apical membrane antigen-1 (AMA1), and the erythrocyte binding antigen-175 (EBA175). AMA1 is translocated to the merozoite membrane and it plays a crucial role in the formation of the tight junction between the merozoite and the RBC[37]. EBA175 binds to its RBC receptor, Glycophorin A, and causes the release of rhoptry proteins, such as the reticulocyte binding protein homologue (RH)[40], inside the RBC. These secreted proteins are involved in sealing the engagement between the merozoite and the RBC in the invasion process[40] (**Fig. 6**).

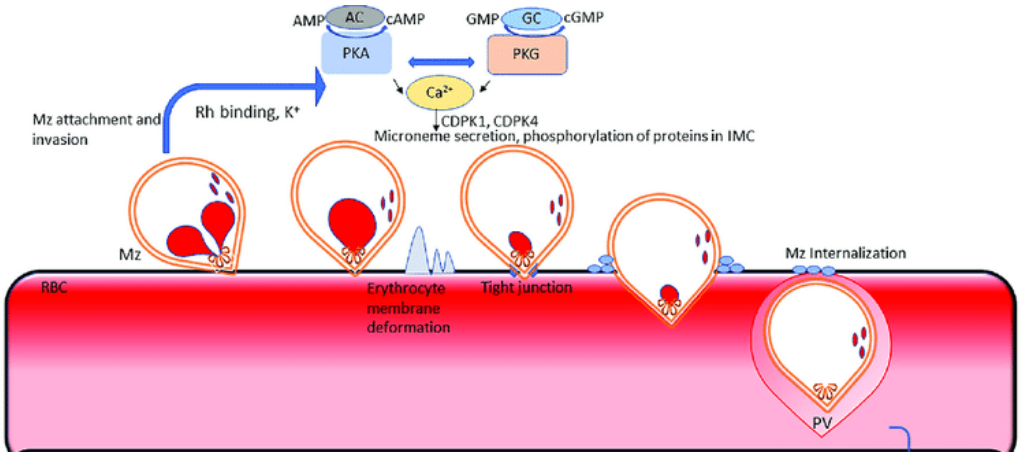

Fig. 6. *P. falciparum* RBC invasion pathway cascade (adapted from Manish Sharma *et al*, 2021)[41]. The merozoites invasion cascade is initiated by the low concentration of K^+., that will cause the carbonic anhydrase to increase the production of HCO_3^- and H^+. HCO_3^- will activate the soluble Adenylyl cyclase-ß (ACß). Guanylate cyclase (GC) is also activated by a yet to be discovered stimulus. The cyclases will generate cAMP and cGMP that in turn will activate PKA and PKG, respectively. These proteins will cause the phosphorylation of diverse proteins, such as the CDPKs and the increase in the internal Ca^{2+} in the parasite. Then the Ca^{2+} will cause micronemes and rhoptries secretion which is necessary for the merozoite invasion. Mz: merozoites; Rh: rhoptries; CDPK: Calcium dependent protein kinase; PKA: cAMP-dependent Potein Kinase; PKG: cGMP-dependent Protein Kinase.

b. Egress Pathway

The parasite protein phosphatase 1 (*Pf*PP1) plays an essential role in stimulating guanylate cyclase α (CGα) activity[42]. GCα will synthesis cGMP, the increase of the concentration of cGMP will cause subsequently the activation of *Pf*PKG. Like in the invasion pathway, the *Pf*PKG activation will cause a rapid mobilization of cytosolic Ca^{2+} that will activate members of the CDPK family[42]. *Pf*CDPK5 was proven to be required for efficient egress[42]. Along with *Pf*PKG, *Pf*CDPK5 triggers the intracellular release and activation of several effector molecules that

disrupt the bounding membranes within minutes during blood stage merozoite egress[43]. The mobilization of Ca^{2+} will cause the rounding up of the PVM[44]. In parallel, *Pf*PKG activity and Ca^{2+} are required for discharge of *Pf*SUB1 from the exonemes into the PV lumen[44,47] **(Fig. 7)**. *Pf*SUB1 is essential for all morphological changes associated with egress, including PVM rupture and RBCm permeabilization[14]. One of the substrates of *Pf*SUB1 is the PV-resident cysteine protease called *P. falciparum* serine-like repeat antigen-6 (SERA6). This protein plays a role in the degradation of ß-spectrin, a protein of the RBC cytoskeleton, leading to the destabilization of the RBCm[14]. Another known *Pf*SUB1 substrate is *P. falciparum* merozoite surface protein-1 (*Pf*MSP1) **(Fig. 7).** *Pf*MSP1 plays a role in merozoite viability and in egress[48].

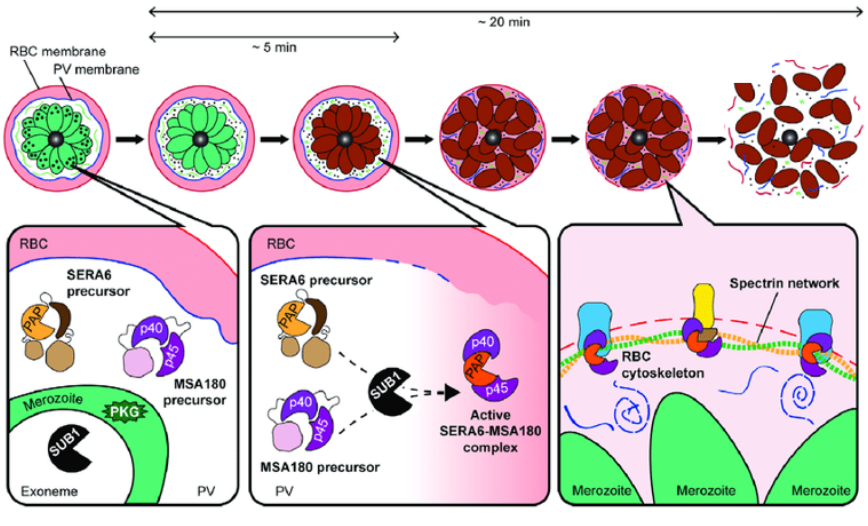

Fig. 7. *P. falciparum* egress pathway cascade (Michelle S Y Tan *et al*, 2021)[49]. *Pf*PKG was shown to be an essential protein during merozoites egress. *Pf*PKG phosphorylates *P. falciparum* subtilisin-like protease (*Pf*SUB1). *Pf*SUB1 will process *P. falciparum* serine-like repeat antigen (*Pf*SERAs), which in turn are involved in merozoite egress and secretion of apical organelle[50,51]. PKG: G-dependent Protein Kinase; MSA: Merozoite Surface Antigen.

B. *P. falciparum* in the Mosquito Host

i. Parasite Development

When a female *Anopheles* mosquito bites the human host for a blood meal, she ingests the macrogametocytes and microgametocytes. Within the mosquito, the sexual development of *Plasmodium* occurs in various compartments. The first development starts in the mosquitos' midgut, where the drop in temperature and the xanthurenic acid will activate the gametocytes and induce *Plasmodium* developmental changes[52]. The macrogametocyte activation takes 10 minutes, and is characterized by its rounding up and egress forming the

macrogametes[53] (**Fig. 8**). Microgametocyte activation is more complex, the first 15 to 20 minutes include 3 rounds of DNA replication, alternating with 3 rounds of endomitotic division[54]. Once the multiplication cycles are completed, the microgamete will round up, and the single organizing center of microtubules will develop into becoming 8 motile basal bodies[55]. Their exflagellation occurs once they are fully developed[56] (**Fig. 8**)**.**The motile microgametes are then able to fertilize the macrogamete creating a motile diploid zygote (10-25h post gamete fusion) (**Fig. 8**). The zygote will migrate to the midgut epithelium and matures into a diploid ookinete which will then cross the midgut cells and matures into a diploid oocyst. During 10 to 14 days, the oocysts are going through sporogonic development, thus generating hundreds of haploid sporozoites[57]. The sporozoites will then egress from the *Anopheles* midgut oocysts, and migrate through the circulatory system and eventually invade the salivary glands, where they can be transmitted to human during the mosquito blood meal[57].

The mosquito forms of the parasite (zygote, oocyst and ookinetes) are the only diploid forms, in the human host, the parasite has only a haploid chromosome baggage.

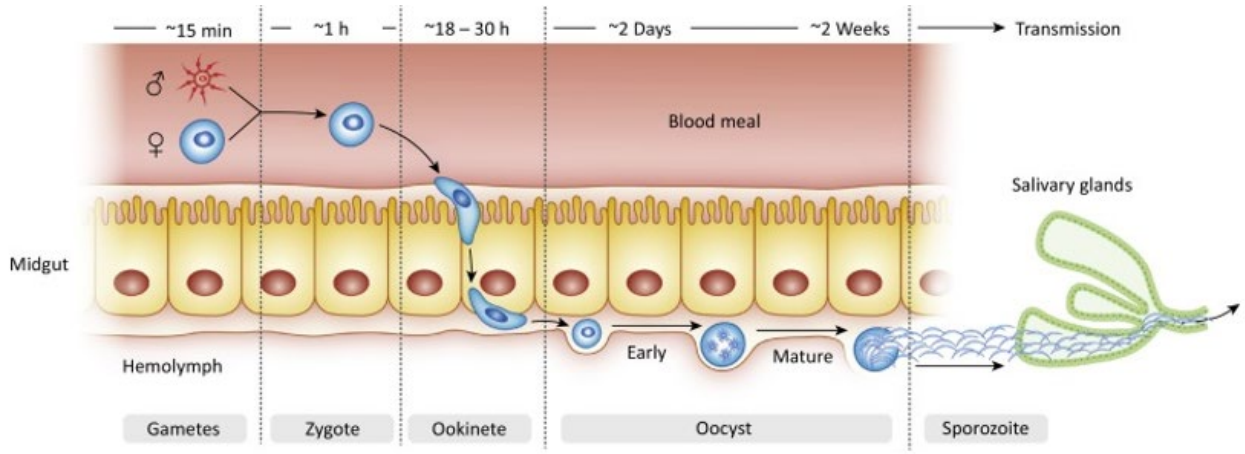

Fig. 8. *Plasmodium* development in the mosquito host (Ryan C. Smith *et al*, 2016)[58].

ii. Signaling Pathway Involved in Gametogenesis

Gametocytes undergo activation by well-defined environmental triggers within seconds of being taken up by a feeding mosquito. This activation process is mediated by a drop in temperature and the concomitant exposure to a chemical stimulus from the mosquito, xanthurenic acid (XA)[52]. In the case of *P. falciparum* XA enhances GC activity, leading to an increase in cGMP concentration. Consequently, cGMP activates *Pf*PKG, triggering the

gametogenesis process.

*Pf*PKG controls the synthesis of phosphatidyl 4-phosphate (PI4P) from phosphatudyl-1D-*myo*-inositol (PI) and its subsequent conversion to phosphatidylinositol - (4,5) - bisphosphate (PIP_2) through phosphorylation of the phosphoinositol kinases involved in these steps, phosphatidylinositol 4-kinase (PI4K) and phosphatidylinositol 4-phosphate 5-kinase (PIP5K)[52] **(Fig. 9)**. In parallel to PKG activation, the phosphoinositide-specific phospholipase C (PI-PLC) is also stimulated upon gametocyte activation by XA. This stimulation leads to the hydrolysis of PIP_2 into diacylglycerol (DAG) and inositol-(1,4,5)-trisphosphate (IP_3) **(Fig. 9)**. Although no IP_3 receptor channel orthologue has been identified in *Plasmodium*, it is suggested that IP_3 triggers the opening of Ca^{2+}-channels in the endoplasmic reticulum, resulting in an increase of intracellular Ca^{2+} concentration[52] .

The increase of intracellular Ca^{2+} is sensed by the CDPKs. In female macrogametocytes, CDPK1 plays a crucial role in releasing translational repression of messenger RNAs (mRNAs) that encode proteins essential for zygote-to-ookinete conversion [52].

In male parasites, CDPK4 acts as another Ca^{2+} effector **(Fig. 9)**. Chemical inhibition of CDPK4 was shown to inhibit the egress of *P. falciparum* microgametes *in vitro* and transmission of *P. berghei* to the mosquito *in vivo*[52].

Additionally, a plasmodial facilitates chromatin transcription protein termed FACT-L is associated with DNA replication in microgametes[52]. Downstream of these events, the loss of mitogen-activated protein kinase Map-2 and cell division cycle protein CDC20 interferes with chromatin condensation, axoneme motility and cytokinesis during the formation of the male flagellar microgametes. Furthermore, the depletion of the metallo-dependent protein phosphatase PPM1 in *P. berghei* results in impaired exflagellation, while the depletion of the Ca^{2+}-dependent phosphatase Calcineurin affects male gametogenesis and subsequent fertilization in the rodent malaria parasite[52] **(Fig. 9)**.

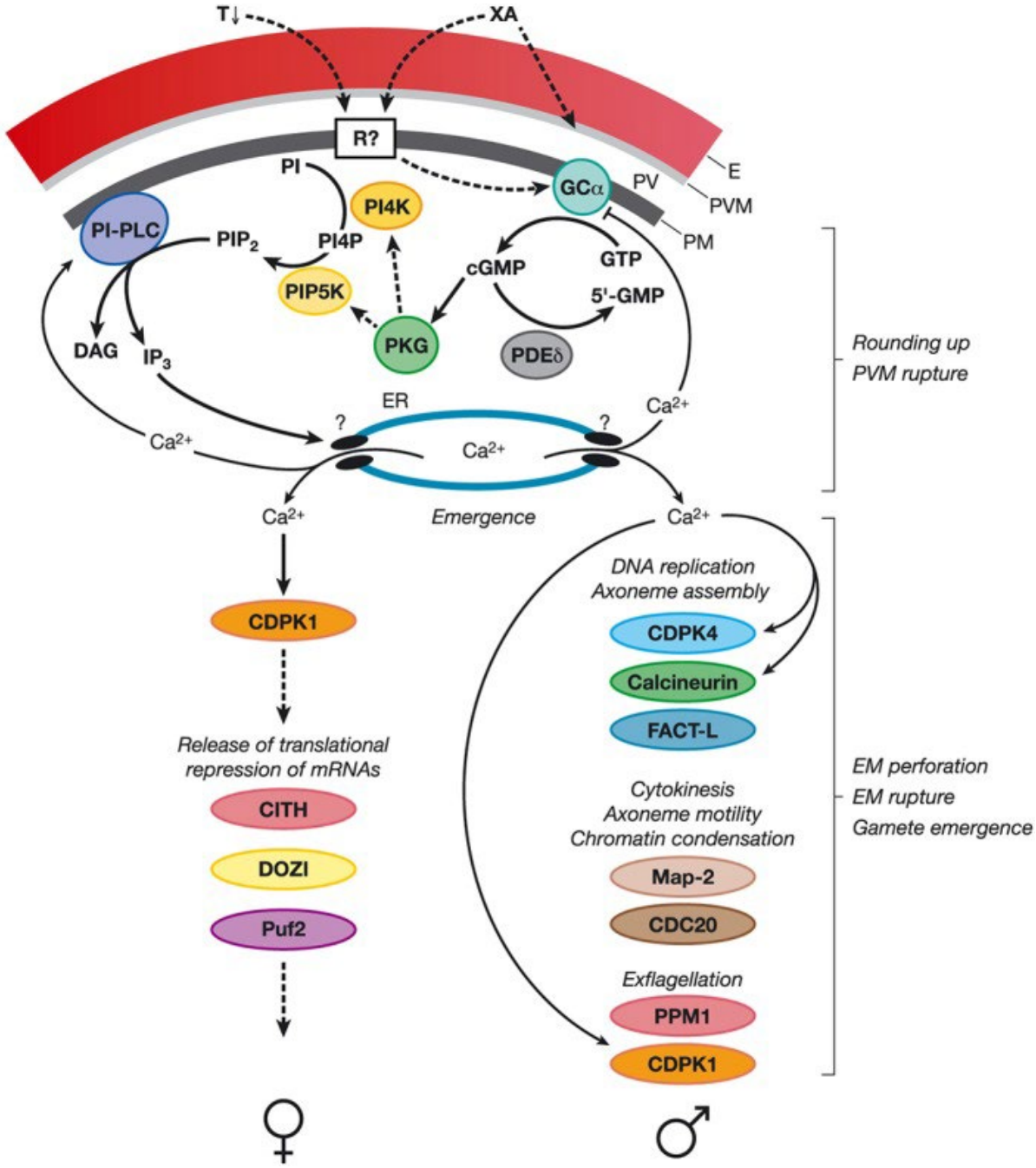

Fig. 9. The signaling pathways involved in gametogenesis (Sandra Bennink *et al*, 2016)[52].

4. Malaria Symptoms and Pathology

The intraerythrocytic phase is the symptomatic phase of the disease. It is due to the rupture of the RBCs and the release of RBC and parasite debris such as the hemozoin, a pyrogenic that causes the activation of innate immune cells including monocytes and tissue macrophages[59]. The immune cells then secrete pro-inflammatory cytokines causing a fever and other pathological effects[59]. The severity of the symptoms is used to classify 3 types of malaria: asymptomatic malaria, uncomplicated malaria and complicated malaria.

A. Asymptomatic Malaria

Some people, although infected with *Plasmodium*, do not present any clinical disease. They represent the asymptomatic cases of malaria. These asymptomatic cases are generally found in people residing in endemic countries and are a consequence of an immune response developed by continuous exposure to the parasite over several years resulting in a naturally acquired immunity to malaria[60]. *P. falciparum* erythrocyte membrane protein-1 family (*Pf*EMP1) is a major surface antigen in mediating the antibody-immune response, and this response ends up clearing the majority of iRBCs [61, 62]. *Pf*EMP1 is encoded by 60 *var* genes. Depending on the *var* genes expressed, an antigenically distinctive *Pf*EMP1 will be expressed. The *Pf*EMP1 family is restricted to the intraerythrocytic stages, and is expressed on the surface of RBC about 16 hpi[63]. Pregnant women are generally more susceptible to malaria due to their higher concentration of cortisol, which causes the inhibition of natural killer (NK) cell activity. The NK cells are the first cells in the peripheral blood to start fighting the parasite. They play an essential role in the innate immune response to malaria infection[64]. However, pregnant women in endemic countries who developed a strong immune response before pregnancy can also develop asymptomatic malaria. They still need to be treated otherwise they could lead to poor pregnancy outcomes (abortion, low birth weight…) [65].

In the end, asymptomatic malaria is in most cases not diagnosed, and patients are therefore not treated. This results in continuous transmission of gametocytes to the mosquito and thus to other humans. This situation is one of the problems malaria eradication programs are facing.

B. Uncomplicated Malaria

The uncomplicated malaria is represented by non-specific combination of repeated symptoms starting with a cold phase, also known as the shivering phase. This phase is followed by a hot phase, also known as the fever stage, the patient has fever, headaches and vomiting. In young children, this phase carries a high risk of developing seizures[66]. In the final phase, called the sweating phase, the patient's fever falls and body temperature returns to normal. The repetition of hot, wet, and cold phases is due to the synchronous lysis of the iRBCs. In the case of *P. falciparum*, *P. vivax* and *P. ovale* fever occurs every 48h, whereas in the case of *P. knowlesi* and *P. malariae* it occurs every 24 and 72h, respectively. Not all patients with malaria have all three phases. Some have only one or two of them and others

have all of them but with varying degrees of severity.

Unfortunately, these symptoms are similar to those of many other common viral infections, such as influenza and cold. This makes it challenging to diagnose malaria without proper testing, hence the importance of rapid diagnostic tests in the management of malaria treatment **(**see below**)**. Indeed, without treatment, there is a risk of developing complicated malaria. It should be noted that children under 5 years old, HIV patients and pregnant women who have uncomplicated malaria show the same symptoms but they are at higher risk of developing complicated malaria.

C. Complicated Malaria

Complicated malaria is due to a rapid multiplication of the parasite, iRBCs rupture and the sequestration of iRBCs to endothelial cells in the visceral capillaries. Complicated malaria causes severe anemia due to hemolysis, abnormalities in blood coagulation[67], metabolic acidosis[68], low blood pressure caused by cardiovascular collapse[69], acute kidney injuries[70], hemoglobinuria and cerebral malaria (CM) [71]. CM is caused generally by *P. falciparum*, and is defined by WHO as an unarousable coma lasting more than 1 h after a seizure. It accounts for 20% of adult deaths and 15% of childhood deaths worldwide.[72] At this point, despite treatment the mortality rate in children is 12-15%[73]. For this reason, *P. falciparum* is regarded as the most lethal species of *Plasmodium*.

Complicated malaria is particularly prevalent among African children under the age of 5, they account for the highest mortality rate (76%) from this disease[74]. The vulnerability of this age group to malaria is attributed to the loss of the maternal immunity and the lack of a fully developed immune system.

Additionally, Pregnant women are at higher risk of developing complicated malaria compared to non-pregnant women[75]. In severe cases and if left untreated, pregnant women may develop severe anemia and placental malaria[76]. In placental malaria, the parasite sequesters in the placenta to the host receptor chondroitin sulfate A (CSA) through *Pf*EMP1. This can lead to interference with the fetus development and contribute to an increase in the risk of stillbirths, abortions, premature delivery, and low birth weight[77], making placental malaria strongly associated to maternal and infant mortality.

5. Epidemiology of the Disease

Malaria is considered one of the most severe public health problems worldwide, it was even referred to as a serial killer in a commentary published in 2002[78]. It has been suggested that more humans have died of malaria than any other diseases in the history of mankind[79]. In 2021, the reported number of deaths due to malaria was 619 000. The aim to eradicate malaria hasn't been reached yet and currently half of the world's population reside in areas threatened by risk of malaria transmission[74] **(Fig. 10)**. Furthermore, the distribution of the six species that infect humans in these areas is very diverse. *P. falciparum* is predominant in African regions, whereas *P. vivax* is more prevalent in the Americas, Southeast Asia and Eastern Mediterranean[80]. The remaining species are regarded as very rare and are under-studied.

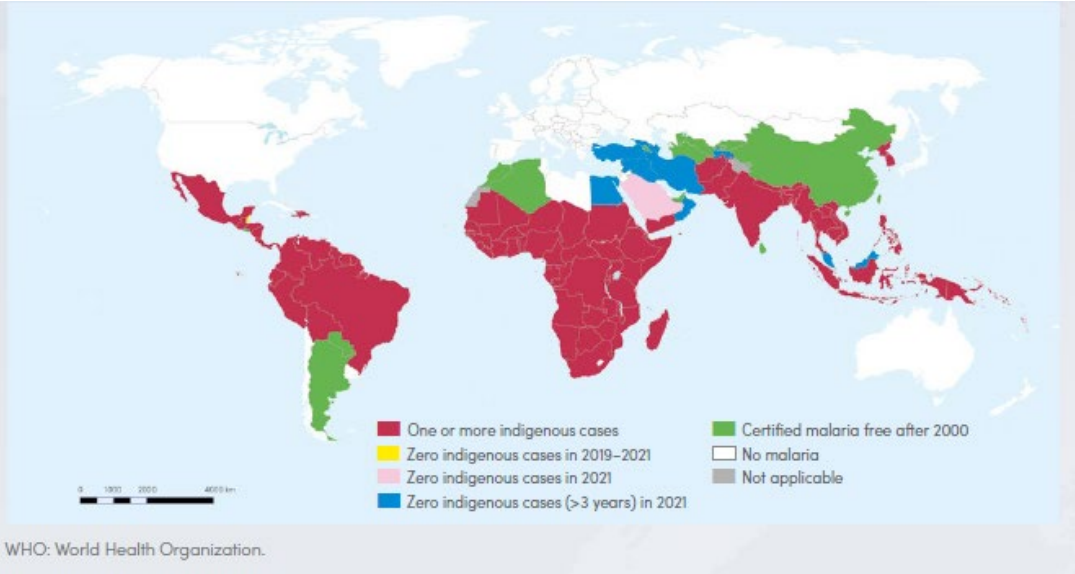

Fig. 10. Indigenous cases in 2000 and their status by 2021 (WHO malaria report, 2022)[81].

According to the most recent WHO malaria report, the incidence rate of malaria in 2021 was declared to be approximately 247 million cases, which is slightly higher than the 245 million cases reported the previous year[74]. WHO stated that reductions in malaria cases have stalled long before COVID -19 pandemic[82], and even though during the pandemic, efforts were done to prevent disruption in malaria control, the results were a bit disappointing with an increase in the malaria burden in many countries[83]. The increase of malaria burden was linked to the disruption in the provision of malaria prevention, diagnosis and treatment services. To prevent a potential disaster, many countries are currently focusing on strengthening their malaria control programs.

A new ray of hope in the fight against malaria has been introduced in 2021, as WHO endorsed for the first time the long-awaited malaria vaccine: RTS, S/ AS01 (Mosquirix™). Unfortunately, the efficacy of the vaccine was shown to be modest in children[84]. Thus, the use of antimalarial drugs remains the primary approach for both preventing and treating malaria. However, the development of resistant strains limits the effectiveness of these drugs and underscores the urgent need for new antimalarial drugs with novel mechanisms of action to overcome this problem.

6. The War Against Malaria

Malaria control is defined as the reduction of malaria transmission to a level where it is no longer a public health problem. Malaria control has been and still is organized by a global platform for coordinated action against malaria, the rollback malaria partnership to END malaria[85]. The organization was launched in 1998 in an effort to provide a coordinated global response to this disease. The burden of malaria varies across different countries, and even within regions of the same country, the burden is not uniformly distributed. Control operations therefore need to be adapted accordingly, taking into account factors such as the economy, epidemiology, infrastructure, education and cultural context of each country.
Different methods of malaria control exist, including vector control and the use of antimalarial drugs. However, as we will see below each of these control methods has its limitations.

A. Vector Control

The vector control strategies aim to interrupt the transmission of the disease by targeting malaria-transmitting mosquitoes. *Anopheles* and larval controls are two common vector control strategies utilized by WHO in attempt to control the spread of malaria. Fortunately, vector control strategies implemented by WHO have been proven to be effective in the prevention of malaria[86]. A study conducted from 2014 to 2018 provides evidence that the mass distribution of vector control tools led to a substantial reduction in biting rates by malaria vectors[87]. The study reported a 93% decrease in indoor biting and a 49% decrease in outdoor biting as a result of these interventions[87].

Currently WHO recommends the use of both insecticide-treated nets (ITNs), and/or indoor residual spraying (IRS) to prevent malaria. ITNs function by creating a physical barrier between people and mosquitoes while also reducing mosquito populations through the

presence of insecticides on the nets. On the other hand, IRS requires indoor application of the insecticide to all possible mosquito resting places. A key challenge with these methods is the development of insecticide resistance[88]. As an example, the Dichloro-Diphenyl-Trichloro-ethane (DDT), the insecticide of choice for IRS, helped eliminating malaria in some parts of Asia, Europe and Latin America. However, the major A*nopheles* species in Africa were able to develop resistance to DDT[89]. Resistance has also been reported in other countries outside such as India, China and Vitetnam[89].

Another method is the larval source management (LSM). Unlike ITNs and IRS which primarily target adult mosquitoes, LSM focuses on controlling the breeding sites of immature mosquitoes. These breeding sites typically consist of stagnant water bodies. By targeting these larval habitats, LSM aims to interrupt the mosquito life cycle and reduce the population of malaria-transmitting mosquitoes[90].

LSM encompasses two approaches: i) permanent habitat modification through land reclamation which involves creating land by removing water from muddy areas, and ii) habitat manipulation, which involves adding regular insecticide or introducing natural predators to the *Anopheles* into water bodies.

Unlike ITNs and IRS, LSM approaches do not rely heavily on insecticides. This reduces the likelihood of larvae developing resistance to the insecticides used and ensures the long-term effectiveness of these interventions. Moreover, since LSM targets the immature stages of mosquitoes, it has the potential to control mosquito bites both indoors and outdoors. Implementing LSM alongside other malaria control measures can enhance the overall effectiveness of vector control programs and contribute to the goal of malaria elimination.

B. Diagnostic

An early diagnosis and prompt treatment of infected individuals is crucial to interrupt the transmission cycle and control malaria. Malaria diagnosis can be achieved through clinical symptoms interpretation, microscopy, DNA detection, and rapid diagnostic tests (RDTs). The gold standard for malaria diagnosis is examining blood smears of suspected infected individuals under a microscope, but this method is limited in case of a very low parasitemia and requires qualified staff.

The second tool to diagnose malaria is the rapid diagnostic tests (RDTs). They are low-cost, easy-to-use and they can provide rapid results. RDTs rely on the detection of specific malaria antigens in the blood of infected people. Some RDTs can recognize one species (*P. falciparum* or *P. vivax*) and others can detect multiple species. These tests significantly improve the quality of malaria management, especially in remote areas with limited access to good quality microscopy services. However, RDTs have limitations, including reduced sensitivity, as they cannot detect an infection in case of a low parasitemia, resulting in a false negative[91]. Another limitation of RDTs is related to certain types of tests that specifically detect the histidine-rich protein 2 (HRP2), a protein produced by only *P. falciparum.* HRP2 can persist in the bloodstream even after successful treatment, leading to prolonged detection of the protein, making it difficult to distinguish between treated and current infections and this can result in false positives[92]. Nonetheless, the development of newly designed RDTs provides hope for the accurate diagnosis of malaria, as they have demonstrated more sensitivity than that achieved through routine microscopy[93].

The last method is the PCR which is principally used to confirm the infection or re-infection, and to identify the *Plasmodium* species, especially *P. vivax* and *P. ovale,* which require specific treatment to eliminate hypnozoites. However, the lack of PCR equipment in healthcare services in endemic countries limit the effectiveness of this method.

C. Vaccination

Vector control and early diagnosis have helped shape hope for malaria eradication. However, the emergence of insecticide-resistant mosquitoes poses a threat to malaria control. At this rate, an effective malaria vaccine would be an important tool in achieving malaria control. A vaccine supports both individual and public health, and is therefore considered as a great tool in the eradication of an infectious disease. The smallpox vaccine is a good example, having successfully eradicated the disease in 1980[94].

In the case of malarial vaccines, they are classified depending on which stage they target: pre-erythrocytic vaccines, blood stage vaccines, and transmission blocking vaccines. One pre-erythrocytic vaccine has been of interest: the RTS,S/AS01, which targets *Pf*CSP on the sporozoite surface, preventing the invasion of the hepatocytes and consequently blocking the continuation of the parasite life cycle.

This vaccine has been in development since 1987, and was the first malarial vaccine approved to be tested in phase 3 clinical trials in 2009. The phase 3 took place between March 27, 2009 and January 31, 2014 in 7 sub-Saharan African countries[95]. During which 3 doses and a booster dose of RTS,S/AS01 vaccine was given to two populations: infants (6-12 weeks old) and children (5-17 months). The vaccine efficacy (VE) against clinical malaria was 25.9% in infants and 36.3% in children, and in case of severe malaria the VE was 17.3% for infants and 32.2% for children[95]. These very modest results in addition to the reported decrease in the VE over time against clinical malaria[95], indicate that the vaccine's effectiveness in preventing malaria is very limited. Another concerning aspect is that the RTS,S/AS01, which is based on 3D7 *P. falciparum* strain sequence, has a higher efficacy against parasite with a genotype that matches the 3D7 strain, and is therefore not effective against other types of malaria[96].
While the WHO has recommended since 2021 the RTS,S/A01 vaccine for children living in endemic countries[81], it is important to recognize that this vaccine alone is not expected to achieve malaria eradication.

To address these issues, a new version of the vaccine, the R21, which contains more CS antigens fused to a fragment of the hepatitis B virus, is being tested. The vaccine was tested on children (5-17 months) in Nanoro, Burkina Faso. The vaccination took place before or at the start of the malaria season with 3 doses and one booster dose administered 12 months after the 3 doses[97]. This study showed a VE maintained at 80% during 12 months after the booster dose, and in case of no booster the VE decreased to 75% during the 24 months after the 3 doses[98]. There was some limitation during this study: a small sample size, the study location where highly seasonal malaria transmission happens, and the timing when the vaccine was administered (before or start of the peak). More trials will be needed but the R21 vaccine results seem to be more promising than the RTS,S/A01. Still its specificity to *P. falciparum* makes it hard to eradicate other species of malaria, and therefore until a vaccine that immunize against several malarial species is found, the prophylaxis and treatment of malaria will still rely on the use of drugs.

RTS,S/A01 is a recombinant based vaccine, other type of malarial vaccine are being pursued such as attenuated whole sporozoite vaccines (WSV). The VE in humans of these WSV were shown to be dose dependent[99,100], more studies are currently being undergone to better investigate these type of vaccines. Another type of vaccine that entered the preclinical studies

is viral-vectored based vaccines. These vaccines use a harmless virus (vector) to deliver the protein of interest *Pf*RH5. The results obtained showed a need for a high concentration to achieve and sustain an immune response in monkeys[101]. Efforts to improve *Pf*RH5 vaccine candidates are ongoing.

D. History of Antimalarial Drugs

During World War II in the South Pacific regions, malaria was considered to be a leading cause of disease among the soldiers. Antimalarial drugs have been the backbone in controlling malaria in endemic areas. Initially, antimalarial drugs were based on monotherapy, but nowadays, the treatment of malaria and chemoprevention are highly recommended to be a combination of at least two drugs, known as bitherapy **(Fig. 11)**.

Currently, the curative treatment of malaria relies on 14 antimalarial drugs, and the prophylactic treatment relies on 6 antimalarial drugs[102]. The majority of these drugs are administrated in bitherapy, although some, such as chloroquine, primaquine and mefloquine, can be used as monotherapy in specific cases[102]. The most notable bitherapy is the Artemisinin-based Combination Therapies (ACTs).

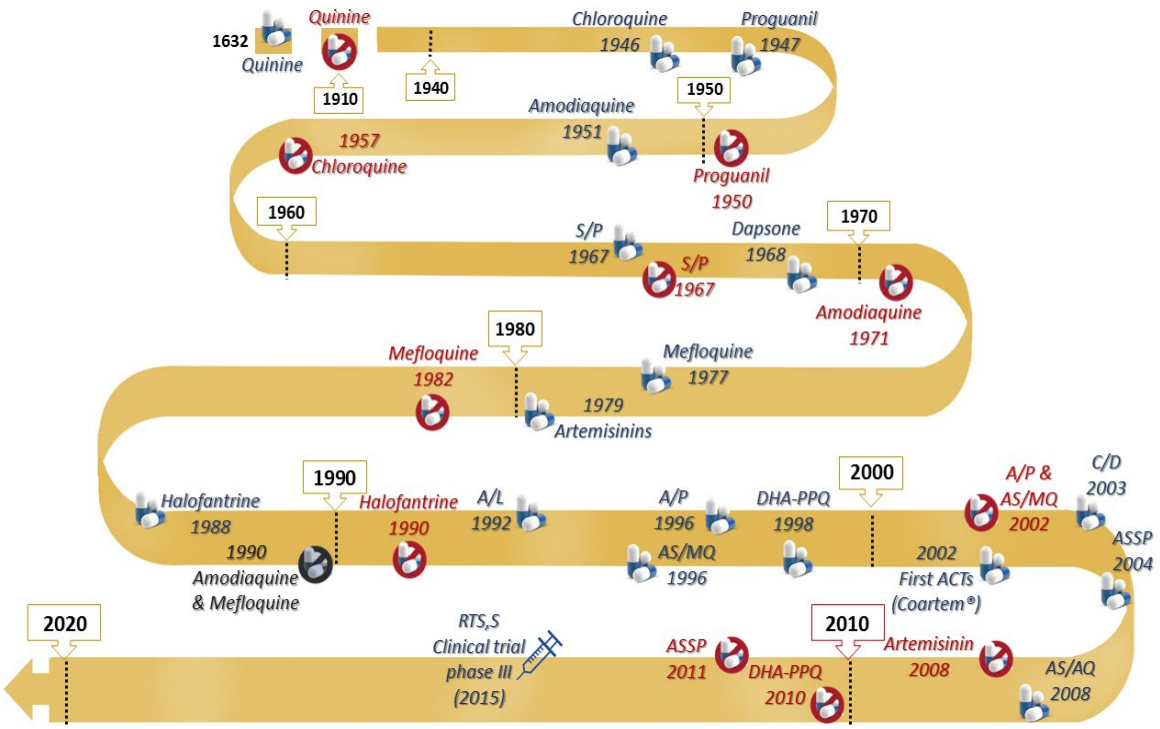

Fig. 11. Timeline of main antimalarials and occurring resistance (Thomas Cheviet *et al*, 2019)[103]. The blue pills represent the first time the drugs were used, the red circles represent the first reported drug resistance, black circles represent the drugs that are no longer used. AS/AQ: artesunate/amodiaquine; DHA-PPQ:

dihydroartemisinin-piperaquine; A/P: atovaquone/proguanil; A/L: artemether/lumefantrine; ASSP: artesunate sulfadoxine pyrimethamine; S/P: sulfadoxine/pyrimethamine; AS/MQ: artesunate/mefloquine; ACTs: artemisinin combination therapies; and C/D: chlorproguanil/dapsone.

i. The Current Antimalarial Drugs

a. The Arylaminoalcohol

1) Quinine

In 1820, the first antimalarial drug was isolated from the bark of the cinchona tree and was named Quinine (QN). QN was considered the drug of reference for intermittent fevers, one of the characteristic symptoms of malaria. The treatment of malaria with QN represented the first successful use of a chemical compound to treat an infectious disease[104]. It demonstrated remarkable efficacy against malaria, particularly in the treatment of complicated malaria. QN is a member of the arylamino alcohol family alongside mefloquine, halofantrine and lumefantrine. It has a rapid lethal effect on schizonts of all human *Plasmodium* species, it is also effective on *P. vivax* and *P. malariae* gametocytes[105]. Its mechanism of action is still not fully understood, but it is hypothesized that it has a similar one to the family of 4-aminoquinoline, which will be described below.

Later on, it was reported that QN caused serious side effects such as hypersensitive reactions[106], hypoglycaemia[107], thrombocytopenia[108], cardiac arrhythmias, and in worse cases fatalities were reported[109]. Adding to these side effects, the resistance to QN was reported in 1910 [110], the full mechanism of resistance is yet to be described. Nonetheless, researchers were able to identify a mutation in *P. falciparum* Na^+/H^+ exchanger (*Pf*nhe1) that could influence QN susceptibility[111].

The serious side effects and the emergence of resistance encouraged researchers to find some alternative improved ways to treat malaria. Despite the drawbacks, QN is still used to date but as a second line treatment in the management of severe malaria and is always coupled with another antimalarial drug: doxycycline. QN can also be used to treat first trimester pregnant women with uncomplicated malaria.

In the family of arylaminoalcohol, lumefantrine, a second derivative, is also still used. This drug is associated with artemether (see below) to treat malaria[112].

2) Mefloquine

The emergence of antimalarial drug-resistant strains at this time, pushed researchers to look for a replacement, and in 1970s, a more expensive QN analogue called mefloquine (MQ) was developed. This drug is effective against the blood stages of all malaria species. MQ inhibits the parasite protein synthesis through direct binding to the cytoplasmic ribosome (*Pf*80S)[113]. The resistance to mefloquine emerged 5 years after it was introduced and this resistance is associated with an increase in the *Pf*mdr1 copy numbers, which limited its use. The side effects of MQ including toxicity to the central nervous system, made the prescription of MQ possible only if the patient cannot be treated with other antimalarial[114], it is a last resort drug. Currently it is used in a combination therapy with artesunate, it is also used alone in case of chemoprevention[112]. MQ is not recommended for use in pregnant women, unless the potential benefits outweigh the risks[115].

b. 4- Aminoquinoline

In 1947, the 4-aminoquinoline antimalarial drugs were introduced, they are synthetic analogues of QN but they offer better efficacy, safety, and ease of production than their natural counterpart[116]. The 4-aminoquinoline family includes chloroquine, amodiaquine, piperaquine and pyronaridine.

1) Chloroquine

After world war II, chloroquine (CQ) was the most widely used drug as a chemoprophylaxis against all human *Plasmodium* infections and was also considered the drug of choice for the treatment of uncomplicated malaria. In an attempt to eradicate malaria, WHO suggested the massive use of CQ in 1957 by adding CQ to food products. The mechanism of action of CQ goes as follow: it will passively diffuse inside the acidic FV because it is not charged, then CQ will be protonated and once it is charged, it can't diffuse out and it will accumulate inside the FV **(Fig. 11)**.

As mentioned before, the FV is where the hemoglobin, the RBCs main constituent, will be digested into a toxic heme, that usually is detoxified for the survival of the parasite. However, CQ interferes in the conversion of the heme into hemozoin, and the accumulation of the heme will cause the death of the parasite and the iRBCs[117] **(Fig. 12)**. All of the other 4-aminoquinoline have a similar mechanism of action[118].

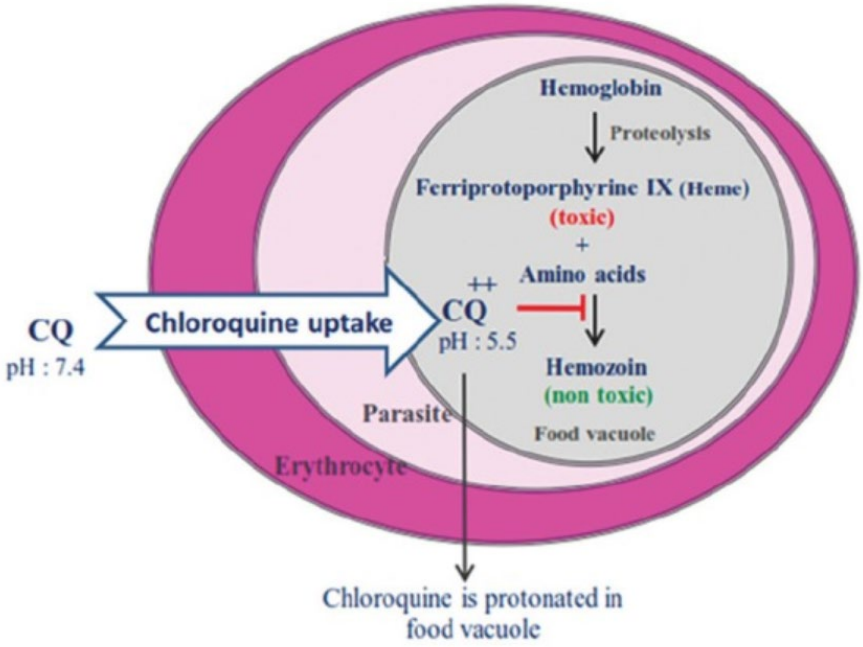

Fig. 12. Schematic representation of chloroquine mechanism of action (Arezoo Rafiee Parhizgar *et al*, 2017)[79]. CQ is transported to the food vacuole (FV) of the parasite, where it becomes trapped in its acidic form. CQ disrupts the process of converting heme into hemozoin, leading to the accumulation of heme. This accumulation of heme ultimately results in the death of the parasite and the infected red blood cell (iRBC).

In the early 1957s, CQ resistance was reported in South East Asia and South America, and eventually these resistant strains reached Africa. The mechanism of resistance in CQ resistant strains was defined to be the ability of the organism to survive in the presence of a higher concentration of the drug than the originally reported concentration. Moreover, the problem turned out to be more severe because the CQ resistant strains were also associated with resistance to the other molecules with the same mechanism of action[119]. The CQ resistance was discovered to be linked to mutations in the *P. falciparum* CQ Resistant Transporter (*Pf*CRT) gene[120]. *Pf*CRT is a 424 amino acid protein, and it is predicted to have 10 transmembrane helices in the membrane of the FV[120]. Mutations in the *Pf*CRT gene confer resistance by causing efflux of the drug outside the FV, resulting in a decrease in its concentration inside the FV and rendering it ineffective as an antimalarial drug against mutated strains. Another mutated gene that is also related to CQ resistance is *P. falciparum* multidrug resistant gene-1 (*Pf*mdr1). Even though *Pf*mdr1 is not directly related to this resistance, it still plays a role in modulating the level of resistance to CQ[121].

Currently CQ is recommended to be used to treat only *P. vivax* infection, or in the case of chemoprevention in central America, CQ is combined with Proguanil. In addition, it can be used in the treatment of pregnant women in their third trimester[122].

Concerning the other drugs of the 4-aminoquinoline family, amodiaquine is used in bitherapy with artesunate (another artemisinin derivative) to treat malaria, and in tri-therapy with Sulfadoxine and Pyrimethamine for chemoprevention[112].

2) Pyronaridine

Pyronaridine (PYR) is a structural hybrid to amodiaquine and aza-acridine moiety. Its synthesis was carried out in 1970 in China. Researchers have shown that PYR has a high efficacy in treating patients with uncomplicated *P. falciparum* strains including the strains resistant to CQ, and blood stage *P. vivax* [123,124]. The mechanism of action of PYR is related, like that of 4-aminoquinoline family, to the inhibition of hemozoin crystal formation, but it probably targets a different step in this metabolism[125], which would explain why CQ-resistant strains remain sensitive to PYR[126]. Moreover, it has been shown to have a lower toxicity than CQ and can also be administered to malaria infected pregnant women[127]. PYR is administrated in combination with other antimalarial, such as Sulfadoxine/Pyrimethamine or Artesunate, the latter is considered to be among the most efficient ACT for the treatment of malaria[127]. To date no resistance to the drug was observed[128].

c. The 8-Aminoquinoline

1) Primaquine

Primaquine (PQ) is an 8-aminoquinoline that was first synthesized at Columbia University in 1945. In addition to being effective on hypnozoites[129], it is also active on all human specie's sporozoites, on *P. vivax* blood schizonts and on *P. vivax* and *P. falciparum* gametocytes[130]. It wasn't until the 1950s that the large-scale studies on safety and efficacy began, and the interest in PQ arouse due to the repeated malaria relapses caused by *P. vivax* hypnozoites. Eventually, PQ use was approved by the Food and Drug Administration (FDA) in 1952.

The mechanism of action of PQ involves a 2-two-step biochemical relay: in the liver, PQ undergoes oxidation through the enzymes cytochrome P450 2D6 (CYP2D6) and cytochrome P450 NADPH-reductase (CRP) **(Fig. 13)**. Oxidation of PQ by CYP2D6 leads to the formation of hydroxylated-PQ metabolites (OH-PQm). These metabolites will go through a spontaneous

oxidation, resulting to the generation of quinoneimines (O=PQm) and the release of H_2O_2[131]. In turn, quinoneimine substrates for CPR will also be oxidized, leading to the accumulation of H_2O_2 **(Fig. 13).** The accumulated H_2O_2 exhibits anti-parasitic activity by oxidizing protein sulphydryl groups and damaging Fe- and FeS containing proteins that are essential for parasite survival **(Fig. 13)**. Alternatively, H_2O_2 can generate reactive oxygen species (ROS), such as superoxide and hydroxyl radicals[131], which most probably induce oxidative stress and parasite apoptosis. It has also been demonstrated that OH-PQm exerts antimalarial activity against liver parasite independently of CYP2D6[131].

The diverse efficacy of PQ makes it a good prophylaxis and treatment drug, but it's not recommended to be used on pregnant women due to the risk of severe hemolysis in glucose-6-phosphate dehydrogenase deficient (G6PDd) individual[132]. In addition to the previous, its limitation against erythrocytic parasites and the emergence of *P. vivax*-resistant strains to this drug reported in the 1982, restricted the current use of PQ to achieve radical cure for malaria caused by *P. vivax* and *P. ovale*[112]. The mechanism of resistance of PQ is yet to be elucidated.

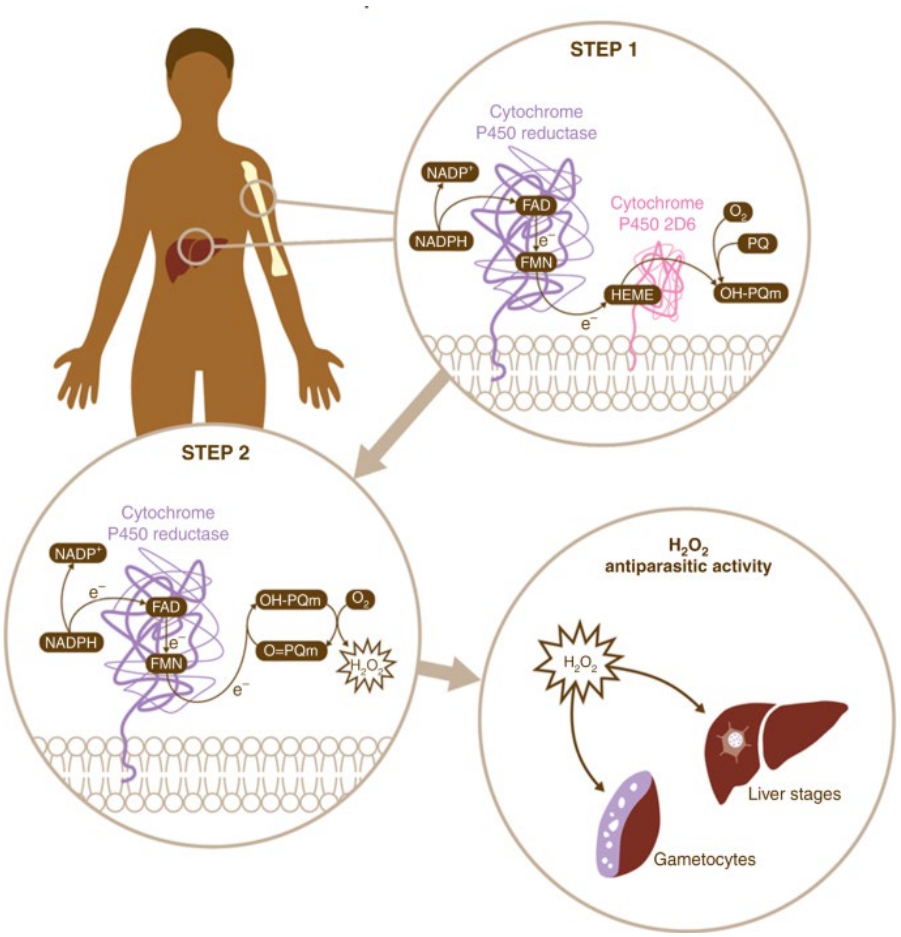

Fig. 13. Schematic representation of primaquine mechanism of action (Grazia Camarda *et al*, 2019)[131]. In the first step of its mode of action, PQ is converted into hydroxylated metabolites (OH-PQm) through the metabolic complex of CPR/CYP2D6. In the second step, these metabolites undergo spontaneous oxidation, forming quinoneimines (O=PQm) while generating H_2O_2. Human CPR receives two electrons from NADPH and utilizes FAD/FMN cofactors to facilitate one-electron transfers to the quinoneimines, reducing them back to their hydroxyl forms. This process perpetuates a catalytic cycle, leading to the accumulation of H_2O_2 at sites of metabolic transformation, such as the liver, bone marrow, and possibly other locations. *Plasmodium* parasites at these sites are eliminated through the action of H_2O_2[131].

2) Tafenoquine

Tafenoquine (TQ) is a newly licensed antimalarial drug (since 2018), it shows tolerability and efficacy in preventing recurrence of *P. vivax* malaria (active against hypnozoites)[133]. It is expected that TQ has better pharmacokinetic properties, which allows for single-dose treatment, compared to the standard 14-day Primaquine regimen. In addition, TQ was revealed to be active against liver- and blood- stage schizonts and gametocytes in both *P. falciparum* and *P. vivax*, which makes it suitable for malaria prophylaxis[133]. The mechanism of action remains unknown, still some clinical studies showed a possible similarity in its

mechanism of action to PQ[133]. Like PQ, one limitation of TQ is that it exhibits hemolytic toxicity in G6PDd individuals[133].

d. Artemisinin, and its Derivatives

Prior to the identification of the artemisinin, the Quechuas from Peru and Bolivia used the bark of the cinchona tree to produce a medicine remedy for fevers. Similarly, in another part of the world, the Chinese used the leaves of sweet wormwood (*Artemisia annua*) to similar purposes.

Between 1972 and 1982, Youyou Tu, a pharmaceutical chemist, and her team were able to identify and extract artemisinin (ART), the active substance from the leaves of the *Artemisia annua* plant. The discovery of ART was dubbed as one of the greatest discoveries in medicine in the second half of the 20th century, and Tu was rewarded a Nobel Prize in Physiology or Medicine for her discovery in 2015. Since the discovery of ART, many derivatives with better bioavailability and efficacy have been synthesized: dihydroartemisinin (DHA), artemether, artesunate, artemisone, arteether and artelinic acid. ART and its derivatives are classified as fast-acting drugs[134]. They rapidly kill the parasites resulting in a rapid disappearance of symptoms and making them especially effective against severe malaria. Unfortunately, these drugs have a very short half-life *in vivo* (2-5 h)[135], this can be the reason why the monotherapy with these drugs usually ends with a failure. Because of their fast-killing ability and the low prevalence of resistant parasites, the bitherapies used nowadays are the artemisinin-combination therapies (ACTs). These ACTs combine an artemisinin derivative with another antimalarial drug with a slow acting activity.

ACTs currently used include combinations such as artesunate coupled with either amodiaquine, mefloquine, sulfadoxine/pyrimethamine or pyronaridine/artesunate; artemether coupled to lumefantrine; and DHA coupled to piperaquine phosphate[102] (**Table 1**). They are globally recognized as the primary treatment of choice for uncomplicated *P. falciparum* malaria, serving as the standard first-line therapy[112].

	Partner drugs used	Manufacturer(s) and product proprietary-name
Artemisinin	Piperaquine	Artepharm (Artequick®)
	Naphthoquine	Kunming pharmaceuticals (Arco®)
Dihydroartemisinin	Piperaquine	Beijing Holley-Cotec (Duocotecxin®) Sigma-Tau (Eurartekin®) GPC ShenZhen (Combimal®) GVS labs (P-Alaxin®)
Artemether	Lumefantrine	Novartis Pharma (Coartem® and Riamet®)[a] Addis (Artemine®) Ajanta (Artefan®) Medinomics (Fantem®) Cipla (Lumartem® and Lumet®)
Artesunate	Amodiaquine	Sanofi Aventis (Coarsucam®)[a] Guilin Pharmaceuticals (Co-Artusan®)[a] Medinomics (MalmedFD®)
	Mefloquine	Mepha (Artequin®)
	Pyronaridine	Sin Phoong (Pyramax®)

[a]At the time of writing, only these three products (Coartem®, Coarsucam® and Co-artusan®) had achieved WHO pre-qualification

Table 1. Artemisinin derivatives available as co-formulations (Harin Ashley Karunajeewa *et al*, 2012)[136].

The mechanism of action of ART and its derivatives has been partially determined. It is thought to involve a two-step process. Initially, artemisinin is activated by heme-iron present within the parasite, leading to the cleavage of its endoperoxide bond[137,138]. This generates a free radical intermediate that can subsequently target and disrupt one or more vital proteins within the malaria parasite through alkylation and poisoning, ultimately resulting in parasite death[137]. ART has also been hypothesized to target *P. falciparum* adenosine triphosphatase-6 (*Pf*ATP6), the SARCO/endoplasmic reticulum calcium ATPase (SERCA) pump of malarial parasites[139].

Unfortunately, the parasite was able to develop a kind of resistance to this family of drugs. WHO called this resistance "artemisinin partial resistance". This resistance is partial because the mechanism of resistance developed affects only the ring stage of *Plasmodium* causing a delay in parasite clearance from the bloodstream of patients treated with ART. But ART is still effective and eventually the parasite will be cleared out of the body. A "full" ART resistance where all stages developed resistance to ART has not yet been reported.

The first reported cases of partial resistance were observed between 2006-2008 on the Thai-Cambodian border, in South-East Asia[140], and later spread to other endemic regions including Africa. The resistance was linked to non-synonymous single nucleotide polymorphisms (SNPs)

in the chromosome 13 *kelch* gene (*Pf*k13)[141]. The 4 most common SNPs are: Y493H, R539T, I543T and C580Y. The latter mutation is the most dominant in South-East Asia population[142]. All of these mutations were associated with increased parasite survival rates *in vitro* at ring stage and prolonged parasite clearance times *in vivo*[141,143]. The mechanism of resistance to ART has yet to be fully elucidated. Some studies showed a link between ART resistance and reduction in hemoglobin endocytosis[144]. This link between resistance and hemoglobin endocytosis, is due to *Pf*K13 role in the endocytosis pathway, which is required for the uptake of host cell hemoglobin[144]. Other studies showed a link of ART resistance due to the acceleration of the unfolded protein response pathways[145], improved ability to manage oxidative damages[146], increase in DNA replication at the ring stage[147] and an enhancement of the parasite antioxidant system[148].

e. The Antifolates: Sulfadoxine-Pyrimethamine and Proguanil

Antifolates, such as sulfadoxine-pyrimethamine (SP) and proguanil, target the folate biosynthesis pathway in *Plasmodium* parasites **(Fig. 14)**. SP is a combination of pyrimethamine, an inhibitor of dihydrofolate reductase (DHFR), and sulfadoxine, an inhibitor of dihydropteroate synthase (DHPS)[149].

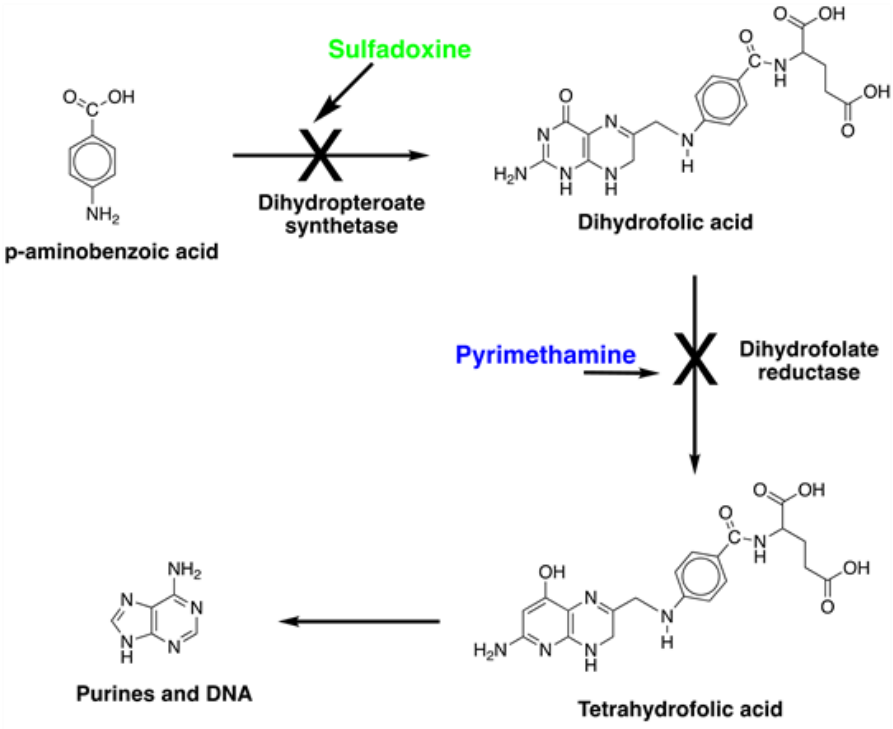

Fig. 14. Folate pathway and Antifolate drugs against this pathway malaria (Djogang Luce Karelle *et al*, 2021)[149].

These compounds work synergistically to block the synthesis of DNA[150] in the parasite by depleting the stores of tetrahydrofolate, a necessary cofactor for DNA synthesis[151]. Due to the development of resistance to CQ, many countries have adopted SP as the first-line treatment for malaria. SP in combination with artesunate is commonly used for the treatment of uncomplicated malaria in children and adults. Combination of proguanil with CQ is currently recommended to prevent malaria and is considered to be the treatment of choice to malaria infected pregnant women[152]. The use of these drugs is limited due to the emergence of resistant strains, but it is still used outside of Africa.

The resistance to SP was associated to point mutations in the DHFR: S108N, N51I, C59R, and a very high resistance is associated to I164L[153,154]. The resistance increases with the point mutations A437G and/or K540E, or A437G and/or A581G in the DHPS[154].

f. Doxycycline

Doxycycline (DOX) is a semi-synthetic broad-spectrum tetracycline antibiotic. Of all the tetracyclines, DOX has been shown to be the most effective as an antimalarial. In fact, DOX is approved by the FDA as prophylaxis (short term travelers < 4months) of *P. falciparum* in areas where CQ and/or SP resistant strains are found[155]. Additionally, DOX is used in combination with quinine for the treatment of uncomplicated malaria due to *P. falciparum* and *P. vivax*[102].

DOX has a slow acting schizonticide activity, with the parasite death occurring in the second cycle. This delay death can be explained by DOX mechanism of action on *Plasmodium*. At a dose of 1-3 µM, DOX has been shown to cause a ribosomal inhibition, therefore a blocking in protein translation in the apicoplast[156] **(Fig. 15)**. The metabolic functions of the apicoplast are not immediately affected by the drug. The apicoplast, even though defective, is still able to segregate and is inherited to the merozoites[156]. After RBC invasion, the defective apicoplast loses its functions (nuclear encoded protein importation, branching or further segregation to the next generation of merozoites), resulting in the death of the parasites in the second intra-erythrocytic cycle after treatment (48 h after treatment)[157]. There has not been any report of DOX resistant strain emerging, the slow acting characteristic DOX made its use limited. It is also not recommended for pregnant women and children younger than 8 years of age[158].

However, recently a group of researchers reported a first-cycle activity of DOX, when they used a higher dose for the treatment than previously >3 µM[156]. In fact, unlike 1 µM DOX which

targets the apicoplast protein translation, a 10 µM concentration was shown to kill the parasite in the first cycle *via* a metal-dependent mechanism that blocks apicoplast biogenesis **(Fig. 15)**, and a dose of > 20 µM caused a first-cycle effect, but the target was shown not to be the apicoplast **(Fig. 15)**[156]. These recent discoveries offer a potential solution to address the limitation of DOX and suggest the repurposing of DOX as a faster acting antimalarial at higher dosage levels.

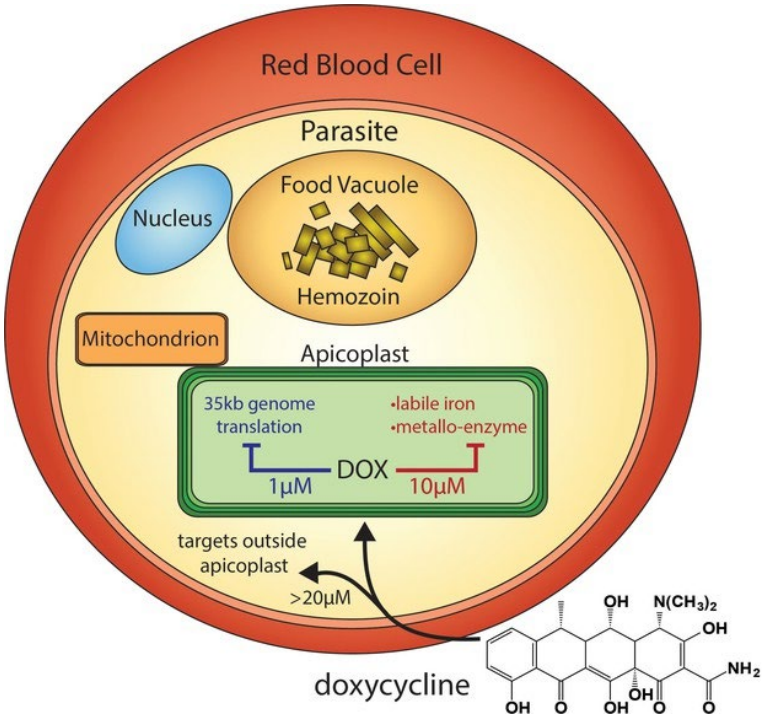

Fig. 15. Scheme of intraerythrocytic *P. falciparum* depicting doxycycline dose dependent mechanism of action (Megan Okada *et al*, 2020)[156]**.** Doxycycline demonstrates a concentration-dependent mechanism of actions at 1 µM, it inhibits apicoplast genome translation, employing a canonical delayed-death mechanism. At 10 µM, the apicoplast's novel metal-dependent mechanisms, contribute to Doxycycline efficacy. Beyond 20 µM, this compound exhibits off-target activity outside the apicoplast.

g. Hydroxynaphthoquinones

Extensive research has been conducted over the past 50 years to investigate the anti-malarial activity of hydroxynaphthoquinones[159]. Atovaquone is the member of this family who is currently used as an antimalarial in combination with proguanil (Malarone®) to protect and treat uncomplicated malaria in children and adults[159].

Atovaquone competitively inhibits the activity of ubiquinol and specifically targets the bc_1 complex in the mitochondrial electron transport chain (Complex III) **(Fig. 16)**[160]. This inhibition

leads to a loss of mitochondrial membrane potential[160]. Moreover, during the intraerythrocytic stage of infection, the parasite mitochondrion plays a crucial role in providing orotate for pyrimidine biosynthesis through the action of dihydroorotate dehydrogenase (DHODH) **(Fig. 16)**[160]. Consequently, the inhibition of the bc1 complex by Atovaquone disrupts the pyrimidine biosynthetic pathway[160]. This inhibition affects two essential processes, ultimately leading to the death of the parasite. Its specificity to *Plasmodium* respiratory chain is attributed to the structural distinctions between the coenzyme found in humans and that in *Plasmodium*. Atovaquone is effective against the intraerythrocytic cycle (schizonts) and liver stages parasites, excluding hypnozoites[160]. The limitation of Atovaquone is their low bioavailability and high plasma protein binding, new analogues are being developed to overcome these limitations[159]. Resistance to Atovaquone has been linked to a missense point mutation in cytochrome b[160].

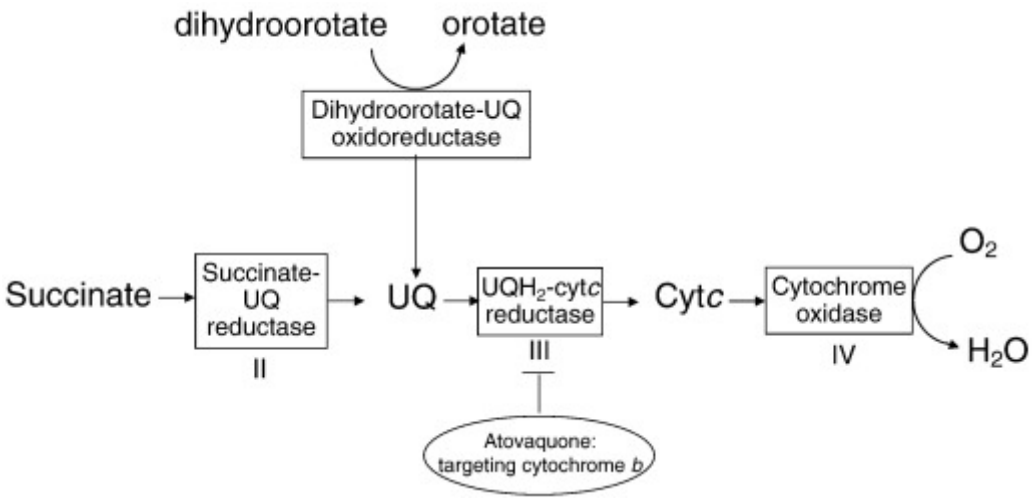

Fig. 16. Atovaquone mechanism of action in the mitochondrial respiratory chain in *Plasmodium* (Josephoe E. Siregar *et al*, 2015)[161]**.** The respiratory chain of *Plasmodium* consists of several key components, including active complex II (succinate-ubiquinone reductase), III (quinol-cytochrome c reductase, cytochrome bc_1), IV (cytochrome c oxidase), and dihydroorotate dehydrogenase (DHODH). Ubiquinone (UQ), also known as coenzyme Q, plays a crucial role in the mitochondrial respiratory chain of Plasmodium, it is the substrate of complex III. UQ serves as a connection point between pyrimidine metabolism and energy metabolism. Atovaquone is a competitor of UQ, it inhibits the movement of the iron-sulfur protein subunit of cytochrome b (CYT b) in complex III, which is necessary for the transfer of electrons to CYT c1 from ubihydroquinone bound to CYT b[161].

The following table (**Table 2)** summarizes the different chemical classes of currently used antimalarial drugs.

Drug	Family Classification	Structure	Target	Genes involved in resistance
Quinoline derivatives	Quinine	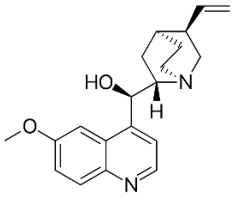	Chloroquine resistant transporter (hypothesis)	unk
	Chloroquine	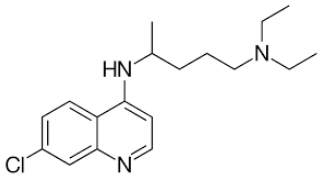	Chloroquine resistant transporter	*Pfcrt*, *Pfmdr1*
	Amodiaquine	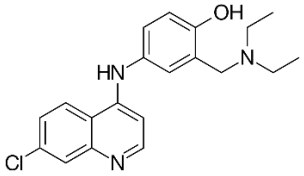	Chloroquine resistant transporter	*Pfcrt*, *Pfmdr1*
	Mefloquine	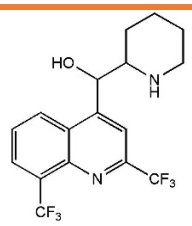	*Pf*80S ribosome	*Pfmdr1*
	Pyronaridine tetraphosphate	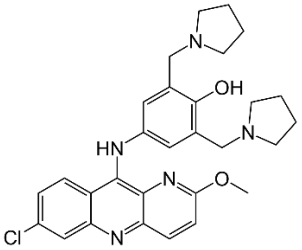	Hemozoin formation	Not reported
	Primaquine	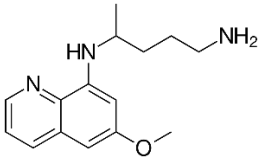	ROS-labile Fe-S groups[162]	unk
	Tafenoquine	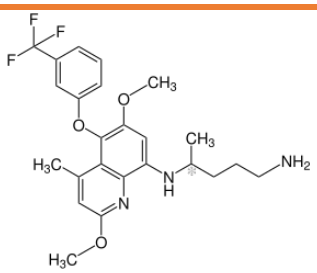	unk	Resistance not reported

Artemisinin Derivatives	Artemisinin	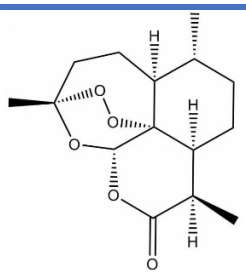	Heme detoxification pathway[163]	*Pfkelch13*
	Artesunate	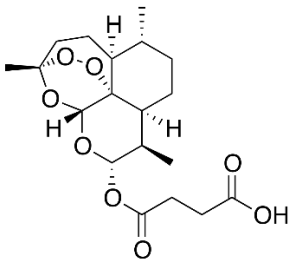	Heme detoxification pathway	*Pfkelch13*
	Artemether	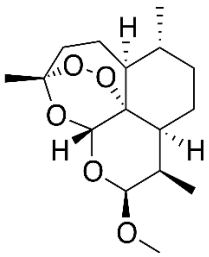	Heme detoxification pathway	*Pfkelch13*
	Dihydroartemisinin	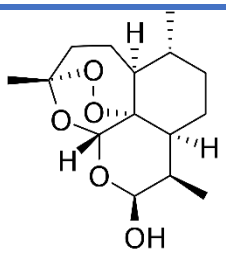	Heme detoxification pathway	*Pfkelch13*
Antifolates	Sulfadoxine	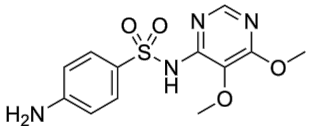	Dihydropteroate synthase	*Pfdhps*
	Pyrimethamine	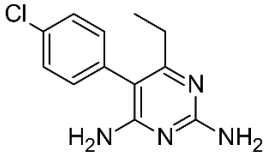	Dihydrofolate reductase	*Pfdhfr*
	Proguanil	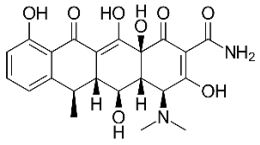	Dihydrofolate reductase	*Pfdhfr*

Tetracycline	Doxycycline	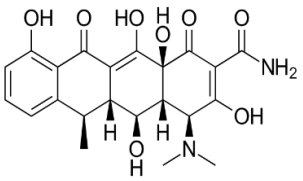	Apicoplast	Resistance not reported
Hydroxynaphthoquinones	Atovaquone	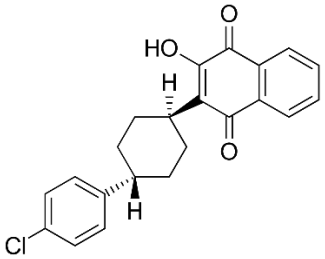	*Bc_1 complex*	Missense point mutation in cytochrome b

Table 2. Classes of currently used antimalarial drugs. The chemical structures are assembled according to their chemical classes. Their mode of action and reported resistance. Unk= unknown.

ii. Into the Future

The Medicine for Malaria Venture (MMV) is a nonprofit organization established in 1999 in the aim to reduce the burden of malaria. Since its creation, the organization has been front lining the discovery, development and delivery of new, effective and affordable antimalarial drugs. To ensure the selection of promising antimalarial drugs, MMV follows a set of criteria which includes the drugs to have a novel mechanism of action with no cross resistance to current drugs, being effective on both the asexual and sexual blood stages, and having a potential to be used as a chemoprevention[164].

The list of the antimalarial drugs currently supported by MMV is shown by the pipeline below **(Fig. 17)**.

Three new possible antimalarial drugs in the MMV pipeline with unique novel mechanism of actions were picked to be presented with more details.

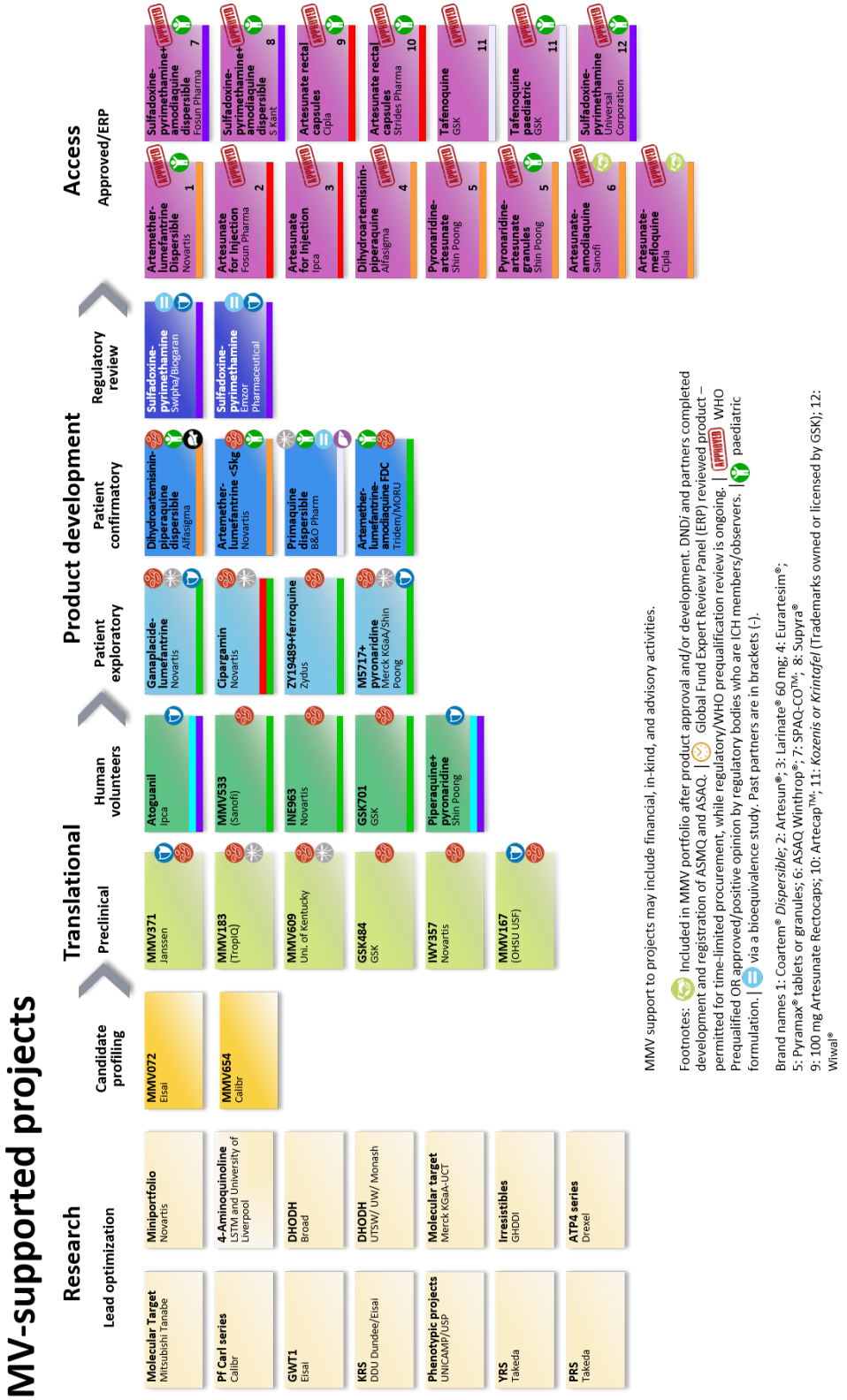

Fig. 17. The pipeline of future possible antimalarial drugs (MMV's pipeline of antimalarial drugs)[165].

a. Inhibitor of *Plasmodium* Elongation Factor 2

*Plasmodium e*longation factor 2 (*Pf*eEF2) catalyzes the guanosine triphosphate - dependent translocation of the ribosome along messenger RNA, and is essential for protein synthesis[166]. M5717 is the lead compound of a quinoline-4-carboamide antiplasmodial family **(Fig. 18)**. Preclinical *in-vitro* and *in-vivo* analyses indicated that M5717 has high selectivity for *Plasmodium* eEF2 and activity against multiple *Plasmodium spp* lifecycle stages, including liver-stage and both asexual and sexual blood-stage parasites[167]. It is currently being tested in patient exploratory phase (phase IIa) in combination with pyronaridine **(Fig. 17)**[168] .

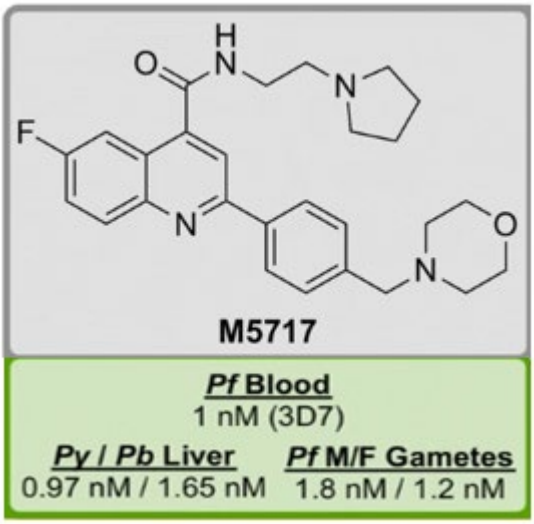

Fig. 18. Chemical structure of M5717 and its key biological and physical properties (adapted from Edwin G. Tse *et al*, 2019)[169].

b. Inhibitor of *Plasmodium* P- Type NA^+ ATPase

Erythrocytes maintain a low internal concentration of Na^+ levels. However, the malaria parasite disrupts the erythrocyte's cell membrane, allowing for the influx of Na^+ *via* parasite-induced NPPs[170]. This leads to the consequent increase of Na^+ concentration in the erythrocyte cytosol. To survive, the parasite needs to maintain a low erythrocytic Na^+ concentration. The influx of Na^+ concentration in the parasite is regulated by a P-type ATPase transporter called *P. falciparum* P-type NA^+-ATPase transporter (*Pf*ATP4), which serves as the primary mechanism for Na^+ efflux[170]. Inhibiting this transporter results in an accumulation of Na^+ concentration inside the parasite, ultimately leading to its death. An *Pf*ATP4 inhibitor,

KAE609 also known as Cipargamin **(Fig. 19),** is the optimized lead of the spiroindolones class and was awarded the MMV project of the year in 2009 and is currently in phase IIa (**Fig. 17**).

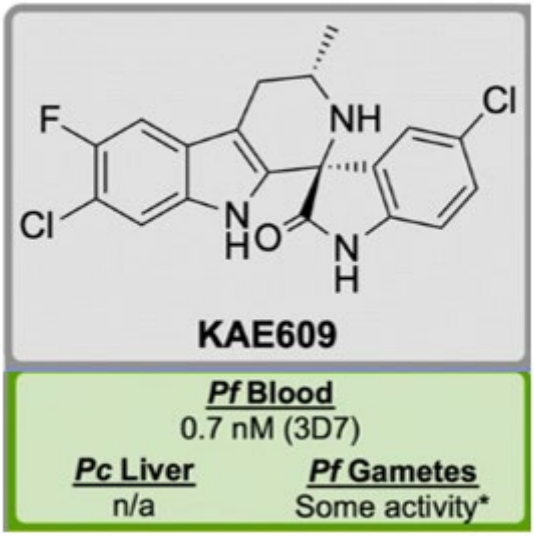

Fig. 19. Chemical structure of KAE609 and its key biological and physical properties (adapted from Edwin G. Tse *et al*, 2019)[169].

c. Inhibitor of Dihydroorotate Dehydrogenase

The mitochondrial dihydroorotate dehydrogenase (DHODH) is involved in the *de novo* pyrimidine biosynthesis pathway, and since *Plasmodium* cannot salvage preformed pyrimidine[171], DHODH is considered a good potential therapeutic target. A new optimized class of triazolopyrimidine compounds targeting the mitochondria was generated (DHODH inhibitor from Monach University) **(Fig. 17)**, with the lead compound being DSM265 **(Fig. 20)**. This compound is active against asexual hepatic and intraerythrocytic stages. Its efficacy was proven in a clinical study in which healthy volunteers were treated with DSM265 one day or seven days before direct venous inoculation of *P. falciparum* sporozoites. The treatment (400mg) had a 100% protection rate when administered the night before the inoculation, on the other hand, a partial protection was reported for the volunteer treated 7 days before inoculation[172].

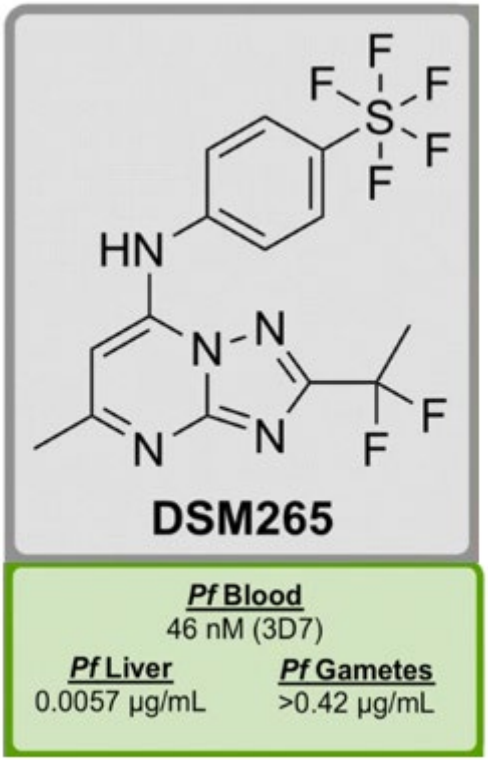

Fig. 20. Chemical structure of DSM265 and its key biological and physical properties (adapted from Edwin G. Tse *et al*, 2019)[169].

Chapter II: Exploring New Horizons of Acyclic Nucleoside Phosphonate

1. Introducing a Possible New Antimalarial Compound: UA2239, an Acyclic Nucleoside Phosphonate

Acyclic nucleoside phosphonates (ANPs) are a stable class of drugs composed of either purine or pyrimidine analogues. Initially, ANPs have been successfully used as antiviral agents inhibiting either RNA reverse transcriptase or DNA polymerase[173]. The first ANPs approved by the FDA were cidofovir and adefovir (**Fig. 21**). Cidofovir is used in the treatment of herpesvirus, polyomavirus, papillomavirus, adenovirus and poxvirus infections. It was also approved in the treatment of cytomegalovirus retinitis in acquired immunodeficiency syndrome (AIDS) patients. Adefovir was approved for the treatment of herpesvirus, hepadnavirus and retrovirus infections. Later on, ANPs have been introduced as treatment for dog lymphoma (Tanovea^{TM}) [174] (**Fig. 21**). Currently, ANPs are being investigated as possible treatments for parasitic infections[175,176,103].

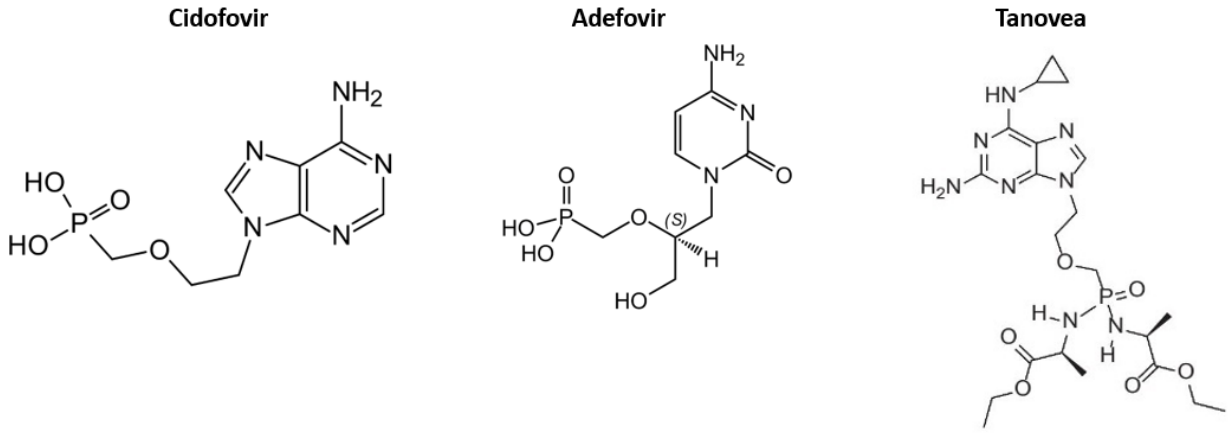

Fig. 21. Chemical structures of acyclic nucleoside phosphonates with antiviral (Cidofovir and Adefovir) and antitumor (Tanovea) activities.

The introduction of ANPs as possible antiparasitic drugs is based on the inability of protozoa such as *Plasmodium*, to synthesis purines *de novo*[177]. In fact, these parasites rely solely on the purine salvage pathway to support their continuous growth during the intraerythrocytic cycle[178].

In *Plasmodium*, hypoxanthine is considered as the main precursor of all purines, and depletion of hypoxanthine from the *in vitro* culture has shown to inhibit parasite gowth[179]. Moreover, the catalysis of the hypoxanthine relies on specific enzymes from the salvage pathway[180]. As an example, several ANP compounds were designed to inhibit *P. falciparum* hypoxanthine-guanine-xanthine phosphoribosyl transferase (*Pf*HGXPRT), an enzyme of this pathway, and are able to block parasites' growth in the micromolar range[181–184]. In the aim of malaria control, new drugs with novel mechanism of actions are urgently needed. To date there is no approved drug targeting purine salvage pathway for the treatment of malaria.

Regarding this project, the Suzanne Peyrottes' medicinal chemistry team, in collaboration with the Rachel Cerdan's team, has developed a new ANPs family containing β-Hydroxy- and β-Aminophosphonate Acyclonucleosides **(Fig. 22.A)**, to be tested and used as new antimalarial drugs[185]. Several compounds of this family were tested via a drug sensitivity assay, and eventually the lead compound in the series was a guanosine monophosphate analogue, UA2239[185]. This compound exhibited the lowest concentration to inhibit 50% of the parasite growth (IC_{50}) of 74 ± 8.6 nM[185] **(Fig. 22.B)**. UA2239 also inhibits parasite growth *in vivo* on *P. berghei*-infected mice at an efficient dose to inhibit 50% of parasite growth (ED_{50}) < 0.5 mg/kg **(Fig. 22.C)**[185]**.**

Moreover, the compound toxicity on human blood cell lines (K562 cells) was evaluated, and K562 cells are not affected by UA2239 up to 1 mM, indicating a high selectivity index towards iRBCs (**Fig.22.B).**

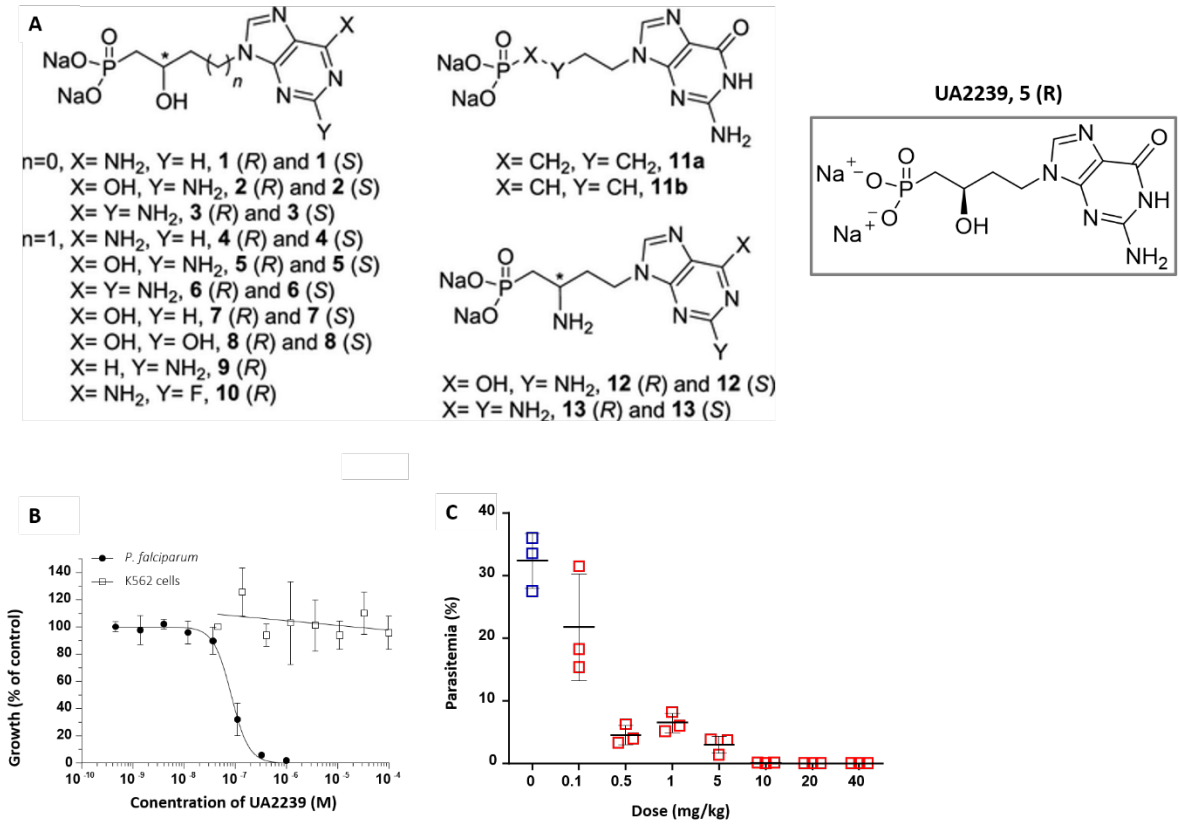

Fig. 22. Preliminary results for UA2239 (Thomas Cheviet *et al*, 2020)[185]. A) Structures of the studied compounds and the lead compound UA2239[185]. **B)** *In vitro* activity of UA2239 on *P. falciparum* 3D7 strain and K562 cells[185]. **C)** *In vivo* antimalarial activity of UA2239. *P. berghei*-infected mice were treated with UA2239 (red) or 0.9% NaCl (control, in blue) once a day from day 1 to day 4. Parasitemia was determined on day 5[185].

2. UA2239 Unexpected Mechanism of Action on *P. falciparum*

Although, ANPs have been described in the literature as inhibitors of DNA biosynthesis[175,176,103], we have yet to validate the mechanism of action of new ANPs such as UA2239 on *P. falciparum*. To investigate this, several phenotypic evaluations were performed. First, the development of *P. falciparum* synchronized cultures was monitored using Giemsa-stained thin blood smears for up to 60 hours post invasion (hpi). Both treated (2µM UA2239) and untreated cultures exhibited normal parasite development until they reached the schizont stages at 48 hpi **(Fig. 23.A)**. At this stage, the schizonts are expected to release 16-32 new parasites that would go and invade uninfected RBCs and new rings would start appearing, as we see for the control in **Fig. 23.A**. Unlike the normal development, in the treated cultures no new rings were observed and the parasites appeared to be stuck at the schizont stage **(Fig. 23.A)**. In the second experiment, the same conditions as the first experiment were applied, but instead of using Giemsa-staining, immunofluorescence assays

(IFAs) were conducted using Hoechst as a DNA stain. IFAs allowed better visualization of the individual merozoites **(Fig. 23.B)**, indicating that phenotypically, DNA replication seems to proceed normally until in the treated cultures.

However, the parasites appear to be blocked at the mature schizont stage, unable to undergo egress. It is worth noting that the possibility of impaired invasion of uninfected RBCs by the newly formed merozoites cannot be excluded.

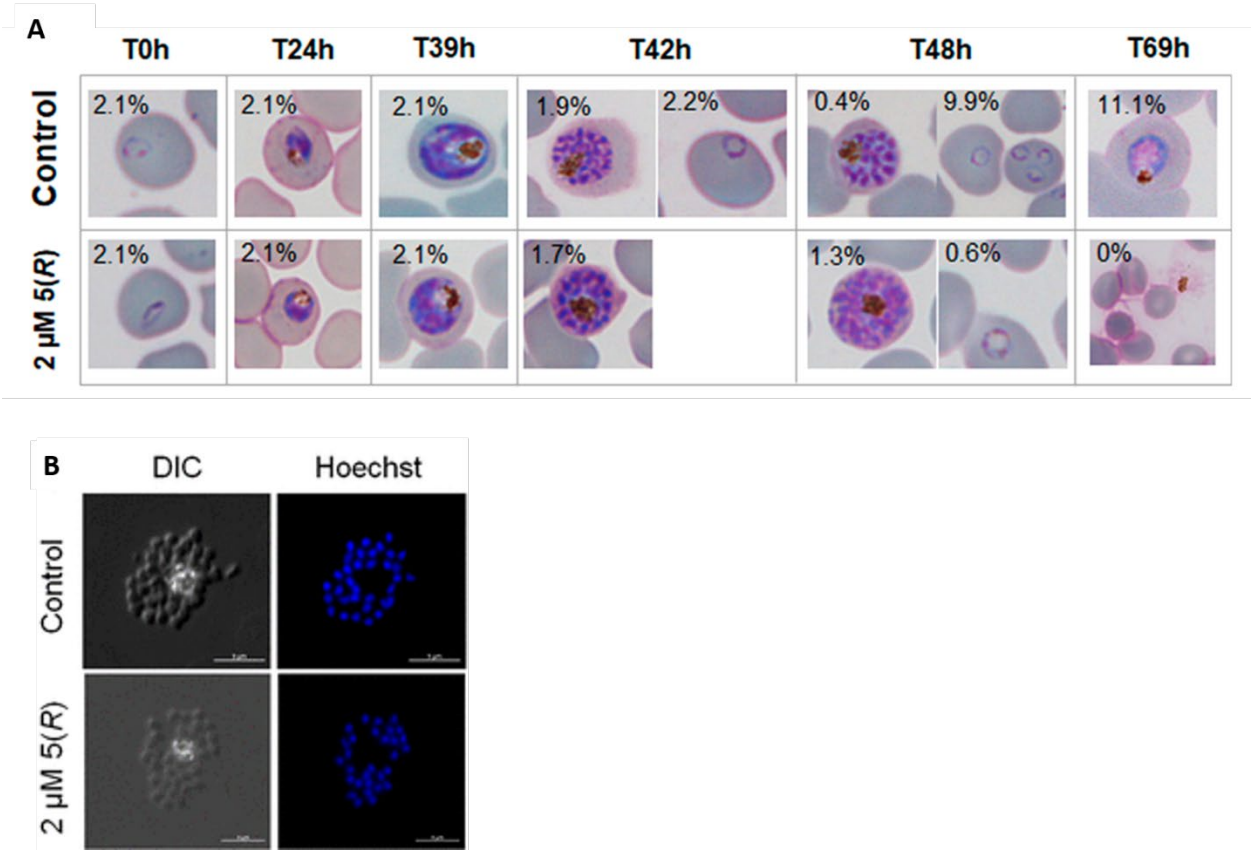

Fig. 23. The effect of UA2239 on the development of *P. falciparum*. All studies were done on tightly synchronized cultures. They were either untreated or UA2239 treated at a concentration of 2µM. **A)** Giemsa staining follow up until 60hpi of *P. falciparum* treated and untreated cultures. **B)** Immunofluorescence assay done on untreated and UA2239 treated cultures, using Hoechst to stain the different merozoite nucleus in the schizont.

Taken together these phenotypic results suggest that UA2239 operates through a distinct mechanism of action compared to other classes of antimalarial nucleoside analogue ANPs that primarily target DNA synthesis.

The observed inhibition of the parasite life cycle at the schizont stage by UA2239 raised intriguing questions regarding the possibility of this compound to target the egress pathway.

The egress pathway is a highly coordinated series of events involving proteases and other regulatory factors (as seen in the introduction). This prompted an investigation into the egress pathway of *Plasmodium*. The existing literature on this pathway highlights the significance of cyclic guanosine monophosphate (cGMP) as a crucial molecule involved in the egress of *Plasmodium* merozoites[186,47,194]. Given the structural similarities between cGMP and UA2239 **(Fig. 24)**, we hypothesized that UA2239 acts as a cGMP analogue, possibly targeting the *Plasmodium* enzymes associated with cGMP.

1

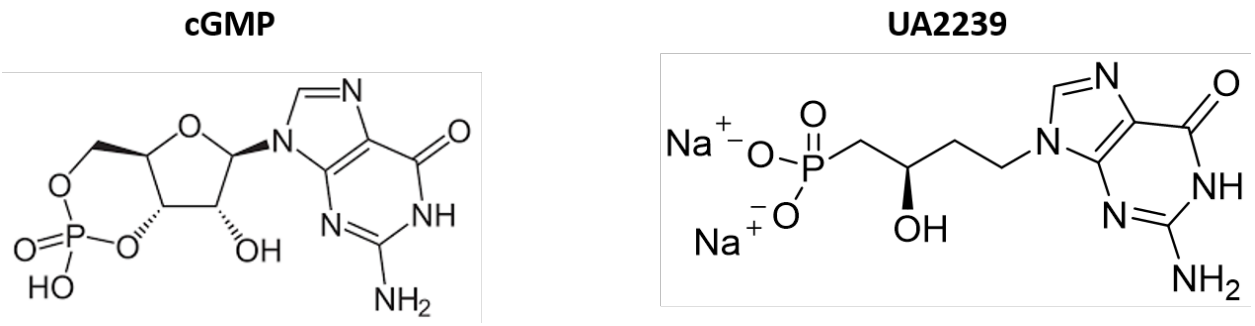

Fig. 24. Similarities in the chemical structures of cGMP and UA2239.

Chapter III: Exploring the Possible UA2239 Interaction

1. UA2239, a Cyclic Guanosine Monophosphate Analogue

cGMP was first identified in rat urines in 1963 and is a ubiquitous intracellular second messenger molecule[188]. It plays a crucial role in regulating various essential physiological processes in a wide range of organisms, ranging from the prokaryotes to the eukaryotes.
In humans, the synthesis of cGMP is catalyzed by the human guanylate cyclase (*h*GC)[189]. cGMP modulates various downstream effects, including vasodilation, retinal phototransduction, calcium homeostasis, and neurotransmission[189]. cGMP exerts its effect *via* cGMP gated cation channels, cGMP-dependent protein kinase G (*h*PKG), and cGMP-regulated phosphodiesterases (*h*PDEs)[189]. *h*PDEs are responsible for hydrolyzing cGMP into an inactive GMP form[189]. cGMP, along with another second messenger, cAMP, are involved in cell proliferation, cell cycle regulation, vasorelaxation in smooth muscle, retinal phototransduction, calcium homeostasis and neurotransmission[189,190]. Dysfunction in cGMP signaling can contribute to the development of various pathologies, including cardiovascular diseases.[191].

In the case of *Plasmodium*, the only known downstream effector of cGMP in *Plasmodium* is *Pf*PKG[192] **(Fig. 25)**. When the concentration of cGMP reaches a certain threshold within the cell, it binds to *Pf*PKG, leading to its activation[192]. Activated *Pf*PKG phosphorylates numerous intracellular protein substrates[192]. The activated protein is involved in motility of ookinete and sporozoites, initiation of the parasite egress pathway during the intraerythrocytic cycle, invasion of red blood cells, and gametocyte activation[192] **(Fig. 25)**. The concentration of cGMP is regulated by the activities of *Pf*GC, which synthesize cGMP from guanosine triphosphate (GTP) and of *Pf*PDEs which hydrolyze cGMP to guanosine monophosphate (GMP)[192] **(Fig. 25)**.

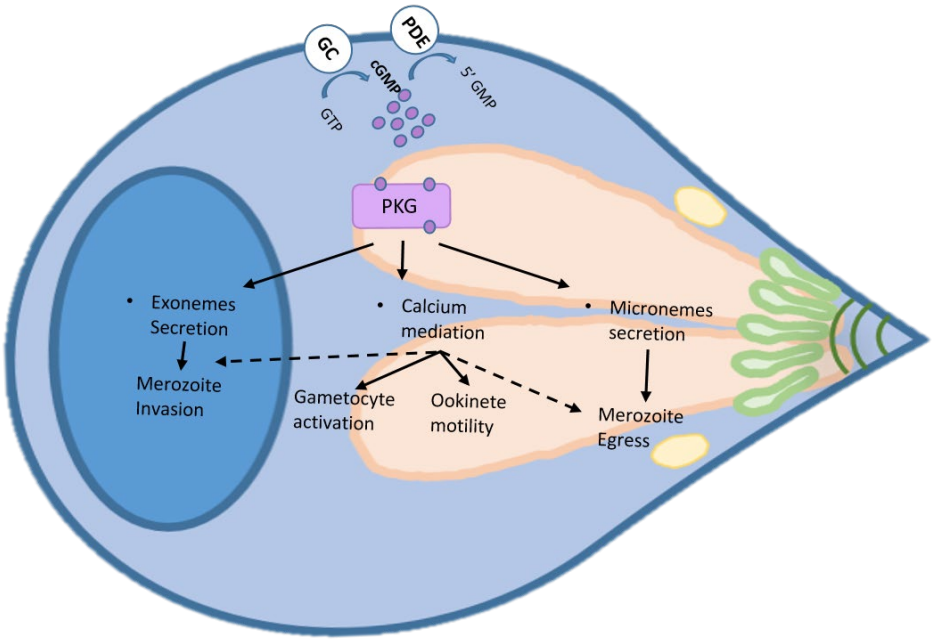

Fig. 25. cGMP involvement in the *Plasmodium* cycle.

Considering our hypothesis that UA2239, a guanine analogue, could target *Plasmodium* enzymes implicated in cGMP signaling, the potential targets of UA2239 could be *Pf*GC, *Pf*PDE, or *Pf*PKG. These three enzymes are involved in different stages of the parasite's life cycle, making them interesting targets for the development of antimalarial compounds **(Fig. 26)**.

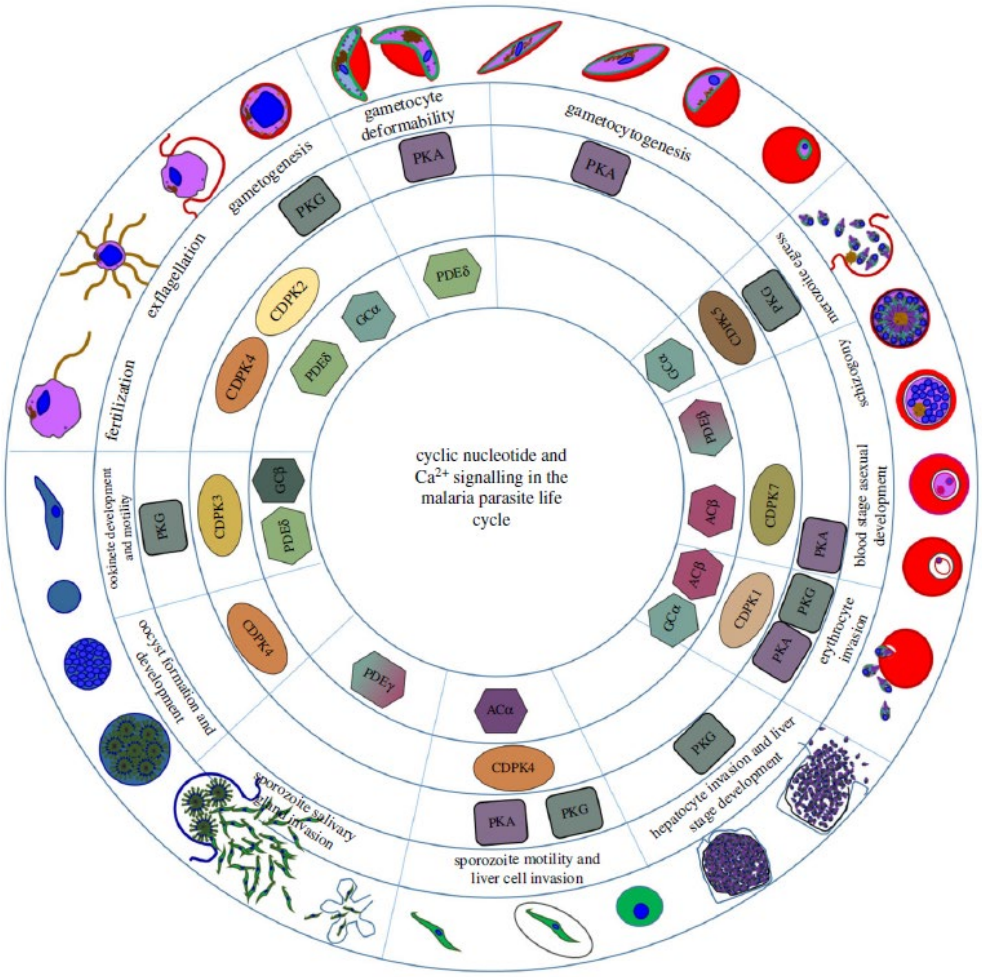

Fig. 26. *P. falciparum* stage specific involvement of cyclic nucleotide signaling components and protein kinases (David A. Baker *et al*, 2017)[192].

2. Possible Targets of UA2239

A. The Guanylate Cyclases

Guanylate cyclase (GC) catalyzes the conversion of GTP into cGMP, and is one of the two proteins regulating cGMP cellular levels[192].

Humans express both transmembrane GC (mGCs) and soluble GC (sGC). The mGCs family consists of seven single membrane-spanning proteins: mGC-A, mGC-B, mGC-C, mGC-D, mGC-E, mGC-F, and mGC-G[193]. Among the mGCs, mGC-D and G are not functional in cGMP synthesis[193]. The mGCs exist as homodimers except for mGC-C which was shown to be a homotrimer.[193] They contain an extracellular ligand-biding domain, a transmembrane domain, a kinase homology domain, a dimerization domain and a carboxy-terminal catalytic domain[193] **(Fig. 27.A)**. The latter domain is the most conserved between family members[193].

Moreover, the presence of the extracellular domain in these enzymes suggests that they potentially function as receptors for specific ligands.

The *s*GC is a heterodimer composed of one α and one β subunits. The two subunits of sGC have a similar organization consisting of an N-terminal heme binding domain, a dimerization domain (linker), and a carboxyl-terminal catalytic domain[193] **(Fig. 27.A)**. In the human two isoforms of sGC were reported. The most studied dimer, sGC-α_1/ sGC-β_1, is expressed in wide range of tissues[193]. The second dimer, sGC-α_2/ sGC-β_1, is mostly present in the lungs[194].
The primary and extensively studied endogenous activator of soluble guanylyl cyclase (sGC) is nitric oxide (NO). The activation of the protein is done through the binding of NO to both the prosthetic ferrous heme present in the sGC-β_1 subunit and to the non-heme sites of the sGC[195]. NO was initially identified as the endothelium-derived relaxing factor due to its powerful ability to induce vasodilation in response to vasodilators such as acetylcholine or bradykinin[193].

A

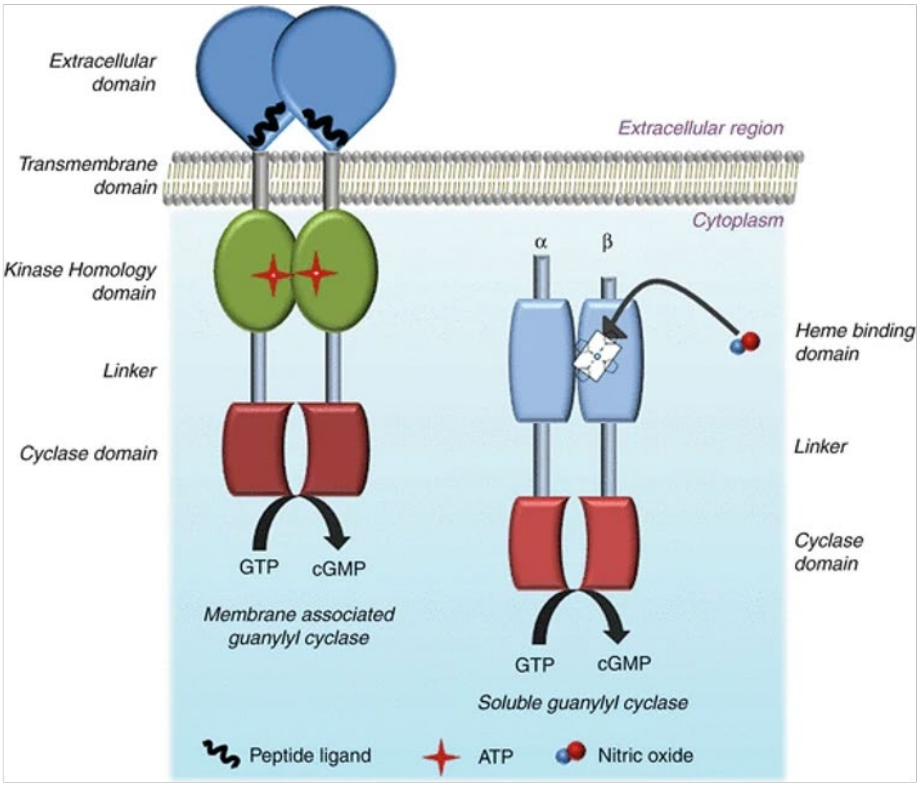

B

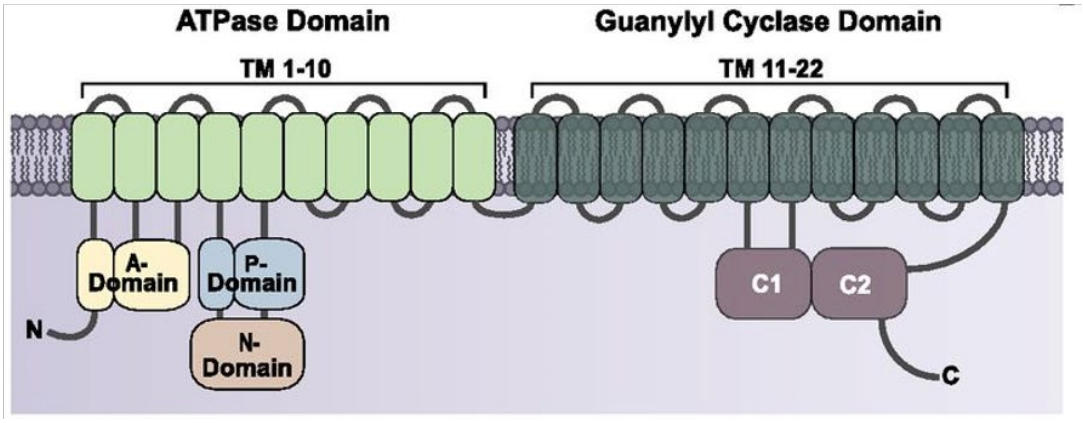

Fig. 27. Guanylate cyclases. A) Schematic representation of human GCs (Sandhya S. Visweswariah *et al*, 2012)[196]. **B)** Schematic representation of the predicted *Plasmodium* GCα (Stephanie D. Nofal *et al*, 2021)[197]. The N-terminal region of *Pf*GCα encodes a putative P-type ATPase that shows the closest similarity to type IV ATPases, known as P4-ATPases. The P-type ATPases consist of 10 transmembrane helices that facilitate ligand transport. This process involves several cytoplasmic components, including a N-domain that binds ATP, a P-domain containing a highly conserved aspartate residue that undergoes autophosphorylation to form an aspartyl phosphate intermediate, and an A-domain responsible for dephosphorylating the phosphorylation domain. N-domain: nucleotide binding domain; P-domain: phosphorylation domain; A-domain: actuator domain; C1 and C2: catalytic domain 1 and 2.

In *P. falciparum,* the genome encodes for two integral membrane GC paralogues[192]: *Pf*GCα (PF3D7_1138400) and *Pf*GCß (PF3D7_1360500). *Plasmodium*, its related apicomplexan and ciliate organisms possess a distinctive characteristic of having a guanylate cyclase physically connected to a P4-ATPase domain in the N-terminal **(Fig. 27.B)**, which is not found in other organisms[198]. *Pf*GC also has a C-terminal domain that exhibits a structure similar to G protein-dependent adenylyl cyclases. This domain consists of two catalytic domains (C1 and C2), each preceded by six transmembrane helices[198] **(Fig. 27.B)**. Within these twin catalytic domains, all of the conserved amino acid residues necessary for cGMP synthesis are present[198]. This structural arrangement is distinct from both types of mammalian GC[198]. *Pf*GCα deletion during the asexual cycle has been refractory[197], indicative of its essential role in blood stage development. On the contrary, *Pf*GCβ was shown to be dispensable during this stage and the gametogenesis. It has been deduced that the activity of *Pf*GCα in generating cGMP was enough for a normal gametogenesis. *Pf*GCβ has an essential role in the initiation of ookinetes gliding motility[199].

The cGMP generated after the activation will regulate its downstream effector, PKG, found in both human and *Plasmodium*[192] **(Fig. 25)**. Additionally, the human cGMP possesses another effector, the cGMP-modulated ion channels, which is absent in *Plasmodium*[200].
The second protein regulating cGMP cellular level is the family of phosphodiesterase (PDE).

B. The Phosphodiesterases

PDE play an essential and unique regulator role in the intracellular concentration of both cGMP and cAMP. PDEs catalyze the hydrolysis of these second messengers, and cause the termination of the cyclic nucleoside signaling.
The PDE superfamily is divided into three major classes on the basis of sequence similarity: class I, class II and class III. Class I PDEs constitute the majority of identified PDEs, they possess a conserved catalytic core of approximately 250-300 amino acids. Mammalian PDEs, as well as PDEs found in various organisms including Drosophila, nematodes, yeast, sponges, and parasites such as *Trypanosoma* and *Plasmodium*, are classified as class I PDEs[201]. These PDEs are structurally related, highly regulated, and functionally distinct[201].
Class II PDEs are a smaller group of PDEs and they are structurally distinct from class I PDEs. They have been identified in various lower eukaryotes, fungi and bacteria[202]. No class II PDEs have been identified in mammals[201].

The class III PDE, has been identified in *Escherichia coli*, the gene expressing this protein *cpdA* does not have any homology to either PDE class I or class II enzymes[203].

Human PDEs (*h*PDEs) consists of 11 families (PDEs 1-11) of proteins encoded by 21 different genes, each displaying multiple splice variants[204] **(Fig. 28.A)**. The *h*PDEs are divided in 3 groups based on the specificity to their substrates. The first group composed of *h*PDE-5, 6 and 9 specifically hydrolyzes cGMP[205]. The second group is composed of *h*PDE-4, 7 and 8 which are cAMP specific. The last group consists of *h*PDE-1, 2, 3, 10 and 11, the members of this group can hydrolyze both cyclic nucleosides[206]. *h*PDEs are structurally similar and consist of a N-terminal regulatory domain that vary considerably between the 11 subfamilies. This domain contains a cGMP and/or cAMP recognition sites; or a calmodulin binding domain (CaM); or a PAS domain. The C-terminal domain contains a catalytic domain that exhibits the greatest sequence homology in the 11 PDE families [207].

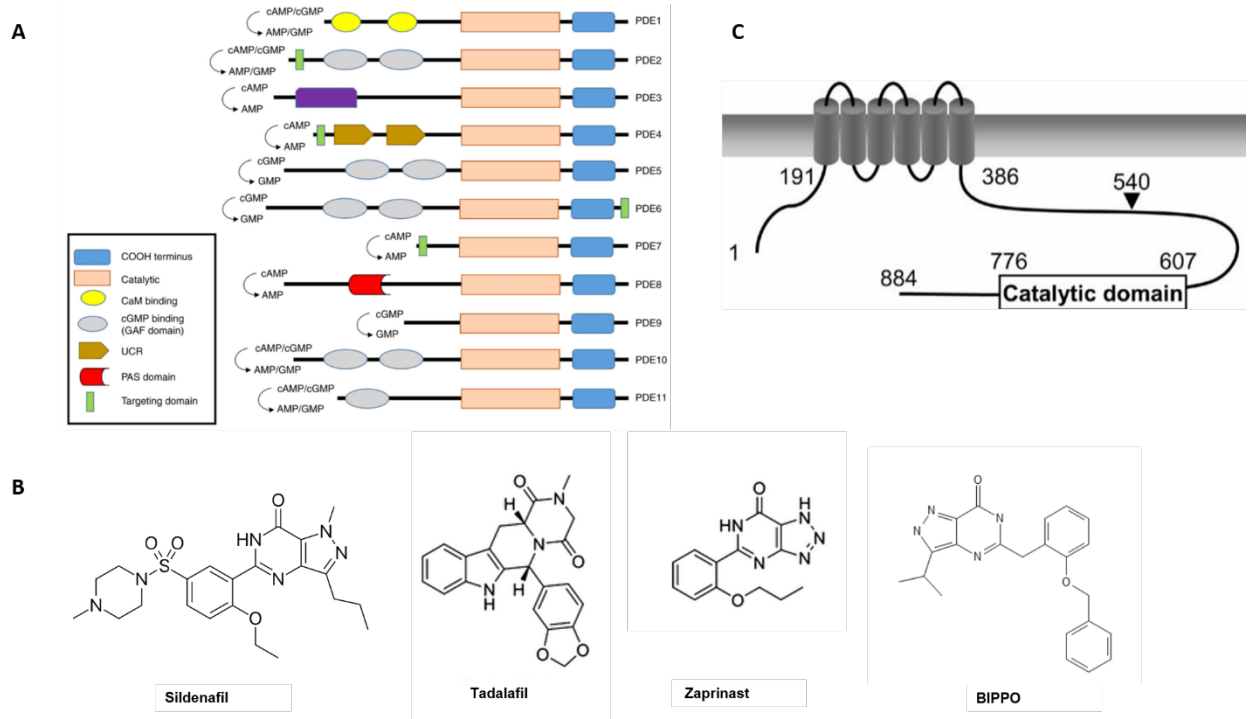

Fig. 28. Phosphodiesterases. A) Structure and functions of the human PDE family (Gyeyeong Kong *et al*, 2022)[207]. *h*PDEs play a crucial role in regulating the levels of cAMP and cGMP in the body. While all PDEs share a catalytic domain with a common COOH end, each family has distinct domains, including CaM, cGMP binding, UCR, PAS, and target domains. PDE, phosphodiesterase; CaM, calmodulin; PAS: Per-Arnt-Sim; UCR: upstream conserved region. **B)** Compounds inhibiting PDE activity. **C)** Schematic representation of *Pf*PDE1 (Keizo Yuasa *et al*, 2005)[208].

All *h*PDEs are soluble except for the *h*PDE-3 and *h*PDE-4 families which contain transmembrane helices[209,210]. The *h*PDEs play major roles in many physiological and pathophysiological processes including cellular growth, differentiation, proliferation, reproduction, cardiac function, vision, inflammation and tumor development[207]. The importance of *h*PDEs in pathophysiology made it an interesting drug target.

To date there are many *h*PDEs inhibitors used for the treatment of various diseases such as optic neuropathy, erectile dysfunction, certain cancers, heart failure[211,212,213,214]. We can cite two selective *human* PDE5 (*h*PDE5) inhibitors who are on the market: sildenafil better known as VIAGRA and tadalafil **(Fig. 28.B)**. These inhibitors are used for the treatment of erectile dysfunction [215–217]. The first one is a purine analogue and the last one is the first non-purine *h*PDE5 inhibitor on the market.

Plasmodium spp genome encodes for four PDEs: *Pf*PDE-α (PF3D7_1209500) which has two subtypes depending on the alternative splicing which leads to either *Pf*PDE-αA or *Pf*PDE-αB; *Pf*PDE-β (PF3D7_1321500); *Pf*PDE-γ (PF3D7_1321600) and *Pf*PDE-δ (PF3D7_1470500) [192]. They share a limited amount of sequence conservation among each other[218]. They are constituted of an N-terminal domain, this domain is variant in the four *Pf*PDE, a catalytic domain which shares a 40% amino acid identity between *Pf*PDEs and a C-terminal domain closely related to those of the 11 human PDE families[219]. The constitution of *Pf*PDEs are considered to be exceptions in the class I PDEs as they have four (PDE-αB) to six transmembrane helices (PDE-αA, PDE-γ and PDE-δ) **(Fig. 28.C)** whereas class I PDE usually are soluble[192].

It has been shown that *Pf*PDEα, and *Pf*PDE-γ are cGMP specific, whereas *Pf*PDEβ and *Pf*PDEδ are dual specific as they can also hydrolyze cAMP[220,221]. Each *Pf*PDE exhibits stage specific patterns of expression[192]. *Pf*PDEα and *Pf*PDEβ are predominantly expressed in the asexual blood cycle, while *Pf*PDEγ and *Pf*PDEδ are only present at very low levels **(Fig. 26)**[192]. The only reported essential *Pf*PDE for the blood stage is *Pf*PDEβ[192]. On the other hand, *Pf*PDEγ and *Pf*PDEδ are predominantly expressed in sporozoite and gametocyte stages, respectively **(Fig. 26)**[192].

The first parasite inhibitor was zaprinast **(Fig. 28.B)**, which is also a *h*PDE5 inhibitor. Treatment of *P. falciparum* and *T.gondii* with zaprinast induces a premature egress of both parasites[222]. However, this compound is a moderately potent inhibitor (ED_{50}=35µM)[208] and therefore has

been used to determine the role of PDEs in infection, and not for treatment. The 5-Benzyl-3-isopropyl-1*H*-pyrazolo[4,3-*d*]pyrimidin-7(6*H*)-one (BIPPO) has shown to be a better anti-parasitic than Zaprinast, with an ED_{50} of 0.4µM on *P. falciparum*[192]. It has been shown that *Pf*PDE inhibition causes a lethal effect on the asexual and sexual stages of the parasites which makes this protein a promising anti-malarial target[223].

C. The cGMP-Dependent Protein Kinase G

i. Human cGMP-Dependent Protein Kinase G

In human cells, the genes *prkg1* and *prkg2* are responsible for encoding two distinct types of PKGs: PKG-I (chromosome 10) and PKG-II (chromosome 4). In addition, PKG-I's first 100 amino acids can be spliced at 2 different regions, which results in the generation of two isoforms known as PKG-Iα and Iβ[224]. Among these isoforms, PKG-Iα exhibits a 10-fold higher sensitive to cGMP when compared to PKG-Iβ.

All of the *h*PKG isoforms have the same three functional domain organization, which includes an N-terminal domain, a regulatory domain and a C-terminal catalytic domain[224]. The N-terminal domain is comprised of a leucine zipper motif which mediate homodimer formation. Following the leucine zipper, there is an auto-inhibitory sequence (AIS) which serves to suppress the kinase activity. The regulatory domain contains two allosteric cyclic nucleotide binding domains (CNBs): cGMP-II and cGMP-I[225] **(Fig. 29.A)**. The CNB-I domain exhibits a higher affinity for cGMP compared to the CNB-II domain[224]. CNB-I plays an important role in controlling the auto-inhibitory segment, thereby influencing the cGMP-dependent activation of the *h*PKG enzyme[224].

In the case of PKG-I, differential splicing leads to variation in the leucine zipper motif and the AIS, while the CNBs and catalytic domains remain identical[224]. These differences in isoform structure contribute to variations in subcellular localization, tissue-specific expression, substrate specificity and kinase activity between these two isoforms[224].

It is noteworthy that PKG-I and PKG-II exhibit a sequence identity of 49-50%. The dissimilarity between these two PKGs primarily lies in the C-terminal region of their CNB-I domains, which serves as a linker connecting the regulatory and catalytic domains. This divergence in sequence further contributes to the functional diversity observed between PKG-I and PKG-II **(Fig. 29.A).**

Both PKG-I isozymes are soluble homodimer proteins, and are expressed in 24 different tissues including vascular smooth muscle cells, platelets, lung, certain endothelial cells, fibroblasts, heart, and the cerebellum[226]. PKG-I is required to accomplish diverse cell functions such as hypertrophy[227], apoptosis differentiation, neuronal plasticity, platelet aggregation, cell motility, cell migration, cell proliferation. In particular, the role of PKG-I is smooth muscle function has been extensively studied[228], and it was shown to play an important role in penile erection, cardiovascular physiology and pathophysiology[228]. PKG-I has other functions relatively less studied, including its involvement in long term sensitization of sensory neurons[229].

The PKG-II is a membrane bound monomer protein and is expressed in several brain nuclei, intestinal mucosa, kidney adrenal cortex, chondrocytes and lungs[230].

*h*PKG is an allosteric protein, the binding of cGMP to PKG-I and PKG-II results in the release of the AIS and leads to the phosphorylation of serine/threonine residues in target proteins[230] **(Fig. 29.B)**. In recent years, there have been advancements in the development of cGMP analogues. However, it is important to note that these cGMP analogues have not yet received approval for therapeutic use.

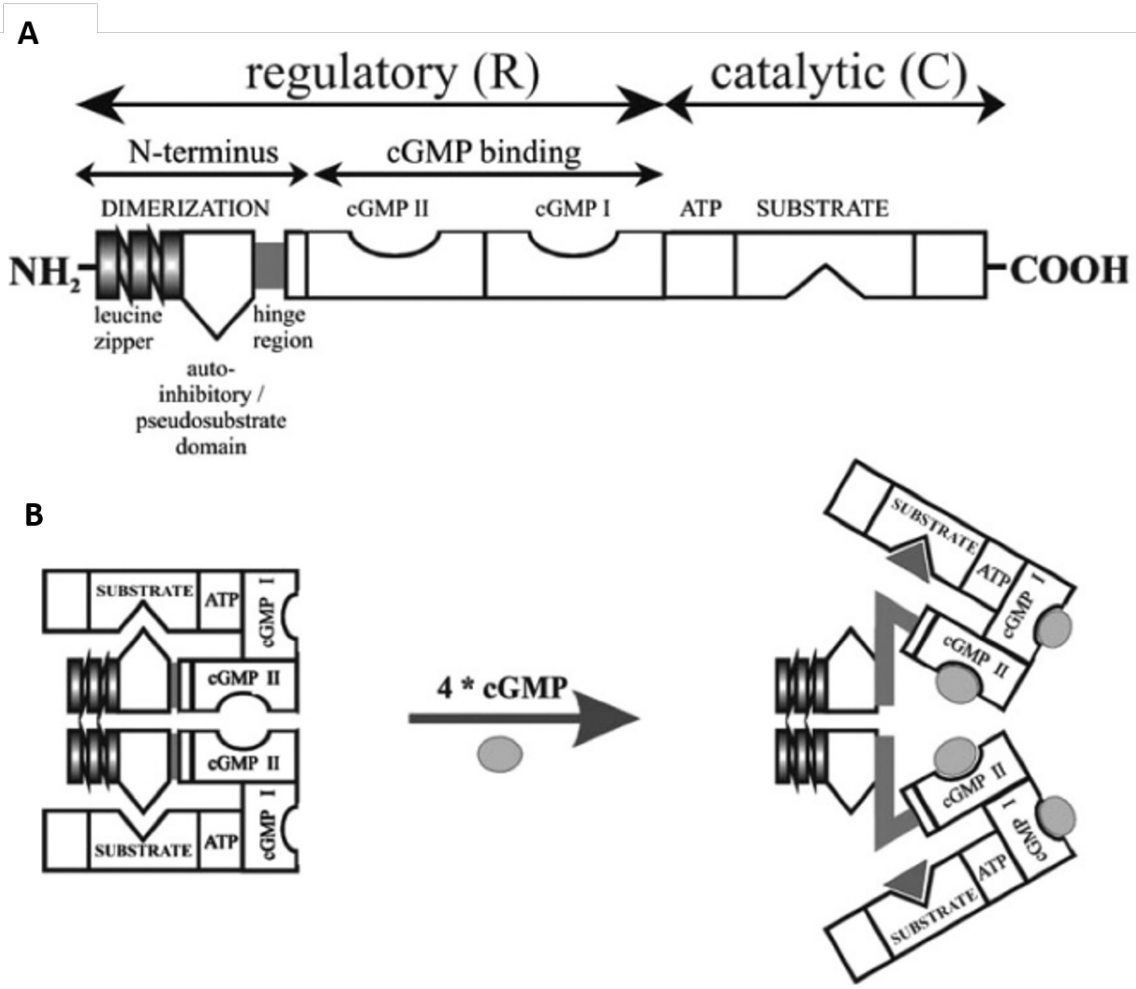

Fig. 29. Structure of the human Protein kinase G[230]. A) PKG- I and II feature a PKA-like catalytic domain. B) Human PKG activation requires the binding of cGMP to the CNB domains, causing a lift of the autoinhibition state and an allosteric activation of this kinase[230].

ii. *Plasmodium* cGMP-Dependent Protein Kinase G, and its Allosteric Activation

*Pf*PKG belongs to a distinct class of PKGs known as class III[231]. Unlike PKG class I and II, which have two cyclic binding domains, class III PKGs possess more than two cyclic binding domains[231].

P. falciparum PKG (*Pf*PKG) is recognized as the sole enzyme regulated by cGMP in the parasite[192].

*Pf*PKG is a monomeric allosteric protein consisting of 853 amino acids[231]. It is found in the cytosol of the parasite, and is composed of an N-terminal regulatory domain and a C-terminal catalytic domain[231]. The regulatory domain consists of an AIS and 4 CNB domains (CNB-A:32-

158 aa, CNB-B: 159-275 aa, CNB-C: 276-401 and CNB-D: 402-543) **(Fig. 30.A)**. Among the four domains CNB-A, CNB-B, and CNB-D bind cGMP, whereas CNB-C does not possess cGMP-binding capability[231]. The inability of CNB-C to bind cGMP is due to a degenerate cGMP binding site. The *Pf*PKG's CNB-D domain has a 55% sequence identity with the human PKG-Iβ CNB-I[231].*Pf*PKG full apo crystal structure is described as a pentagonal arrangement by the 4 CNBs, the N-lobe of the catalytic domain, and in the center is localized the C-lobe of the catalytic domain[231] **(Fig. 30.B)**.

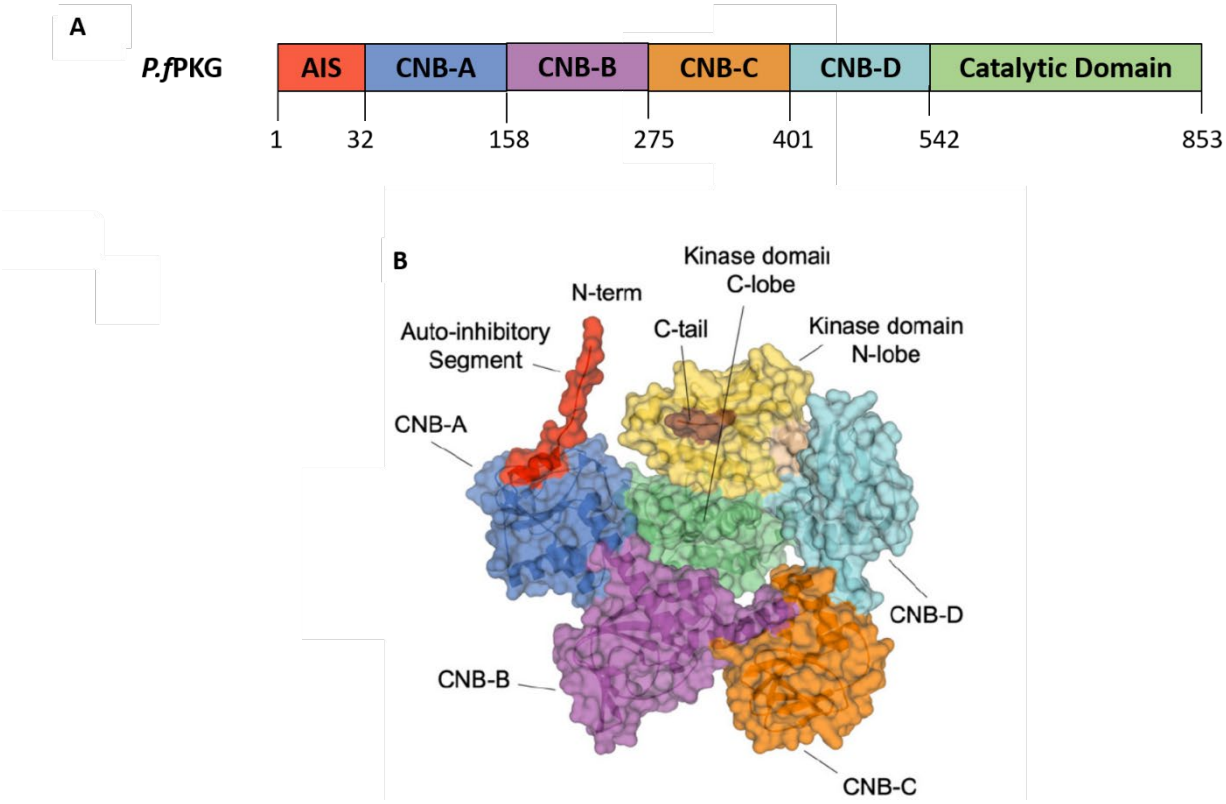

Fig. 30. *Plasmodium* protein kinase G (Majida El Bakkouri *et al*, 2019) [231]**. A)** *Pf*PKG consists of a regulatory domain containing an auto-inhibitory segment, and four integrated CNBs, one of which does not bind cGMP, CNB-C; and a catalytic domain. **B)** *Pf*PKG consists of a pentagonal structural comprising four CNBs and the N lobe kinase domain in the outer rim and the C lobe kinase domain locked in the middle. AIS: Auto-inhibitory segment, CNB: Cyclic Nucleotide Binding.

The characterization of the *Pf*CNB-D structure has been described in both apo (inactive state) and holo (cGMP-bound active state), and this characterization has provided valuable insights into CNB-D role in the activation of *Pf*PKG[187]. The binding of cGMP to the CNB-D is responsible for approximately 60% of the overall activity of the full length protein[187]. This indicates the significance of the CNB-D domain in mediating the allosteric regulation of *Pf*PKG upon cGMP

binding.

The affinities of each CNB domain for cAMP and cGMP were determined using a competition fluorescence polarization assay with recombinant PKG protein[187]. Among the CNB domains, the CNB-D exhibited the highest affinity for cGMP and displayed a significant selectivity for cGMP over cAMP, with a 190 nM fold preference for cGMP[187]. This finding suggests that this CNB domain plays a critical role in both *Pf*PKG autoinhibition and activation[187]. In contrast, the other two CNB domains demonstrated affinities for cGMP that were at least two orders of magnitude lower than that of CNB-D[187].

In the absence of cGMP, the protein is suggested to be auto-inhibited. The AIS functions intramolecularly to suppress kinase activity[231].

On the other hand, the allosteric activation of *Pf*PKG relies on a sequence of events, with *Pf*PKG going through different transition states. This transition starts with the binding of cGMP to the CNB-D domain, causing the gradual release of the AIS. The complete release of the AIS and the full activation of the protein require both CNB-A and CNB-B to bind cGMPs[232].

The first protozoa PKG inhibitors were generated to target *Eimeria* and *Toxoplasmas'* PKGs in an aim to understand the function of this protein[233]. The first family of inhibitors were tri-substituted pyrrole, 4-[2-(4-fluorphenyl)-5-(1-methylpiperidine-4-yl)-1*H* pyrrol-3-yl]pyridine (Compound 1: C1)[233] **(Fig. 31)**, and then a more specific PKG inhibitor was generated from the imidazopyridine family, (4-[7-[(dimethylamino)methyl]-2-(4-fluorophenyl)imidazo[1,2-*a*]pyridine-3-yl]pyrimidin-2-amine) (Compound 2: C2)[234] **(Fig. 31)**. Both of these compounds were shown to also target *Pf*PKG and therefore are effective in blocking the intraerythrocytic egress[186] and invasion[235] of the merozoites, as well as the inhibition of gametocyte activation[236]. In addition, the ability of C1 to inhibit sporozoites invasion of the hepatocytes was also described[237].

Since 2017, efforts have been made to develop new analogues of C2, with ML10 being the lead compound in this family **(Fig. 31)**. ML10 exhibited an impressive IC_{50} value of 160 pM on recombinant *Pf*PKG, significantly lower than the IC_{50} of C2 (3100 pM)[238]. *In vivo* studies using *P. berghei*-infected mouse model demonstrated that oral administration of C2 and ML10 at a dose of 25mg/kg twice a day for four days' lead to a reduction of parasitemia ranging from 52% to 60.4% compared to untreated mice[238]. These compounds also showed efficacy in blocking parasite transmission to mosquitoes.

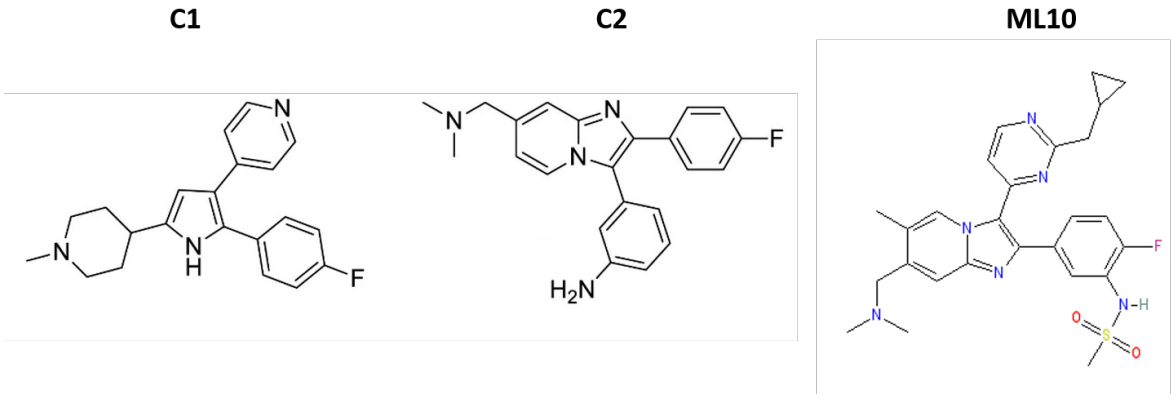

Fig. 31. *Plasmodium* PKG inhibitors.

Concerning the molecular mechanism of action of these compounds, it has been shown that they can block the access to the ATP-binding site causing inhibition of this protein. Indeed, they bind to an hydrophobic pocket, the so-called "gatekeeper pocket" which is adjacent to the ATP-binding pocket[239]. The amino acid T618 within the *Pf*PKG protein sequence, is known as the gatekeeper residue allowing ATP to enter its binding site. It plays a crucial role in the protein function[236]. Therefore, the presence of this small residue makes accessible the gatekeeper pocket. A mutation of the gatekeeper residue in *Plasmodium* to a bulkier residue such as Glutamine (T618Q) preventing the entry of the compounds into the gatekeeper pocket[186], causes a resistance to these compounds.

All of the known *Pf*PKG inhibitors to date target the gatekeeper pocket[240], as *h*PKG possesses a bulkier residue at this position, these inhibitors aren't able to enter the pocket and consequently renders the kinase insensitive to them. This selective inhibition of *Pf*PKG offers a promising approach to avoid toxicity and effectively combat *Plasmodium* infection.

Thesis Objectives

The absence of an effective malaria vaccine and the emergence of drug-resistant parasites and insecticide-resistant mosquitoes have posed significant challenges to malaria eradication efforts. Therefore, the search for new antimalarial drugs with novel mechanisms of action has become a priority.

The mechanism of action of a drug refers to how it affects specific targets within the parasite, such as enzymes or cell functions. It is crucial to find new targets to avoid the rapid emergence of resistance, as observed with the 4-aminoquinoline family of drugs, where resistance to one drug can confer resistance to others within the same family.

The promising results obtained with UA2239, an ANP, have created a potential avenue for the development of new antimalarial drugs. To date, no ANP has been approved by the FDA as an antimalarial. The literature has often linked the potential targets of ANPs in malaria to the inhibition of essential enzymes in the DNA synthesis pathway, which has not been targeted before. Inhibition of this pathway leads to the inhibition of DNA synthesis and parasite growth.

However, our investigation into the effect of UA2239 on malaria cultures revealed unexpected results. While we observed activity against both the asexual and sexual stages of the parasite, it did not align with our initial expectations. These preliminary finding described above prompted us to conduct a more in-depth investigation into the compound's mechanism of action.

The primary aim of this thesis is to decipher the mechanism of action of UA2239 as a potential new antimalarial drug. To achieve this aim, our first objective is to identify the target of UA2239 and validate it using molecular biology tools. Once the target is identified, it will enable us to uncover the pathways in which it is involved.

The second aim of this research is to characterize UA2239 as an antimalarial drug. This involves evaluating its efficacy against different parasite stages, assessing its pharmacokinetic and pharmacodynamic properties, and exploring its potential as a therapeutic agent.

By unraveling the mechanism of action and characterizing UA2239, we hope to contribute to the development of new and effective antimalarial drugs that can overcome drug resistance and help in the fight against malaria.

The Results

Chapter I: UA2239 Target Validation and Characterization

1. Introduction

Understanding the mechanism of action of a drug is of paramount importance in the field of pharmacology. It not only improves our understanding of how the drug works but also enables us to develop targeted and more specific interventions for particular cell types.

Our approach on this matter was to uncover the main target of UA2239 in *P. falciparum*, by doing so, we gain valuable information into the pathways it influences. This knowledge serves as a basis for formulating hypotheses, and designing experimental protocols.

2. Results

A. UA2239 does not Target *P. falciparum* DNA Synthesis

As an ANP, UA2239 was suspected to target DNA synthesis. However, as seen in the preliminary results in **Fig. 22**, the parasites seem able to replicate their DNA normally and mature until they reach the schizont stage. While a phenotypic drug discovery approach gives a hint sometimes to the pathways targeted by the drugs, we still need a more quantitative approach to validate this previous assumption. Therefore, we decided to quantify the DNA using flow cytometry of both treated and untreated cultures. Samples were collected at regular 6-hour intervals, they were subjected to fixation and were labeled with SYBR green for subsequent analysis by flow cytometry. The data obtained after the sorting were analyzed and the results are depicted in **Fig. 32.A-B**. The observed peak at 0 hpi, labeled 1N (N= DNA copy number), represents the haploid DNA content in rings. DNA replication starts around 24 hpi **(Fig. 4)**[20]. At 36 hpi, the peaks corresponding to 2N, 4N, 8N and 16 to 32N are observed, indicating the replication of DNA through the cycle **(Fig. 32.B)**. The graph demonstrates that the DNA content of both the control and treated samples follows a similar pattern and it reaches 16 to 32N, which corresponds to mature schizonts containing 16 to 32 merozoites. Leading us to conclude that UA2239 does not target the parasite DNA synthesis.

On the other hand, a notable difference was observed between the control and the treated cultures at 42 hpi. Indeed, the 1N peak representing the new rings is present in the control culture but absent in the UA2239 treated cultures **(Fig. 32.B)**. This suggests an impairment in the progression of the parasite's life cycle beyond the schizont stage.

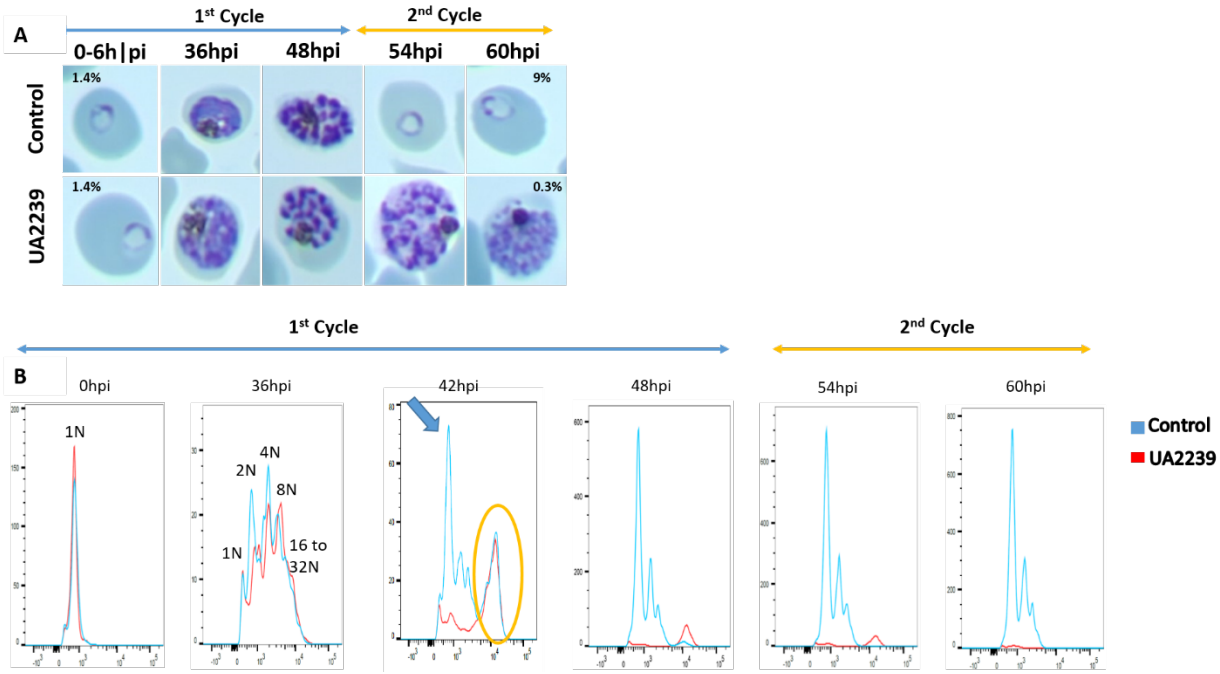

Fig. 32. UA2239 does not target DNA synthesis. A) Phenotypic follow up of the effect of UA2239 (2 µM) on *P. falciparum* parasite during 2 cycles. **B)** Control and UA2239 treated samples were fixed every 6h for 60 h for the follow up of DNA replication, N represents the DNA copy number. 1N represents the haploid rings. As the parasite starts transitioning to trophozoites and replicating its DNA, the DNA copy number will start varying going up till 16 to 32N representing the mature schizonts containing 32 merozoites. N=2. Hpi: Hours Post-Invasion.

B. Identification of UA2239 Target

After confirming that UA2239 doesn't target the DNA synthesis of the parasite, we aimed to identify the target of this compound in *P. falciparum*. A well-established approach known as resistant screening was followed[241]. This method involves culturing *P. falciparum* 3D7 strain continuously under pressure from UA2239 at a single concentration (10 x IC_{50}) or in a stepwise manner (3 x IC_{50} until 10 x IC_{50}), aiming to select the parasites resistant to the drug. For each assay three independent cultures were done, cumulating to six petri dishes **(Fig. 33)**. In addition, a parallel control culture consisting of untreated 3D7 was also continuously cultured in parallel. The drug sensitivity assay was used to determine the UA2239 IC_{50} values and monitor the resistance.

After subjecting the parasites to 7 months of drug pressure, resistant parasites emerged and were subsequently isolated and cloned. These UA2239-resistant clones presented 10 to 50

fold increase in their IC_{50} when compared to the IC_{50} of the 3D7 WT strain that was cultivated in parallel for 7 months.

In total, 14 clones including the 3D7 WT 7 months control underwent next-generation sequencing method using Illumina miniseq with 150 bp paired-end reads. The main objective of this whole genome sequencing (WGS) was to identify potential genetic variants associated with drug resistance. The analysis of the WGS data was conducted by Marc-Antoine Guery, in the team of Antoine Claessens at the LPHI.

The analysis revealed the presence of 41 non-synonymous mutations, including SNPs and micro insertions/ deletions (INDELS). Other mutations such as duplication, inversion and translocations were also reported. All of these previous mutations were exclusively present in the UA2239-resistant clones and were absent in the drug-sensitive strain. Out of all the mutations, the SNPs were considered directly associated with drug resistance. The rest of the mutations were not taken in consideration either due to their lack of relevance to cyclic nucleotide pathways or their presence in only a small number of drug-resistant clones.

Among the mutated proteins, one protein in particular caught our interest, the cGMP-dependent protein kinase G (PKG). Of the 13 clones subjected to the WGS, 12 exhibited independent amino acid substitution in *Pf*PKG. One clone had the *Pf*PKG R420I substitution, another clone had the *Pf*PKG H524N substitution, three clones had the *Pf*PKG H524Y substitution and finally seven clones had the *Pf*PKG D597Y substitution **(Fig. 33)**.

The remaining 13th clone exhibited an SNP in the *P. falciparum* phosphodiesterase-β (*Pf*PDEβ), resulting in a Y539D substitution **(Fig. 33)**. The PDE enzymes play a crucial role in regulating the concentrations of second messengers (cAMP and cGMP) through hydrolysis, making them an integral part of the enzymatic cascade involved in the egress pathway[220]. *Plasmodium* encodes four different PDEs, namely *Pf*PDEα, *Pf*PDEγ, *Pf*PDEδ, and *Pf*PDEβ. Studies have demonstrated that *Pf*PDEα, *Pf*PDEγ, and *Pf*PDEδ are not essential for the intraerythrocytic cycle, while *Pf*PDEβ was proven to have an essential role during the blood stage[220]. An inhibition of *Pf*PDEβ was shown not to affect the egress, but rather decreases the invasion rate, and interfere with early ring stage development[220]. This phenotype would be in contrast to what we saw on the smears where parasites egress was blocked.

These findings suggest that *Pf*PKG protein could be the main target of UA2239. Further validation will be required to determine the functional implications of these mutations and their contribution to drug resistance.

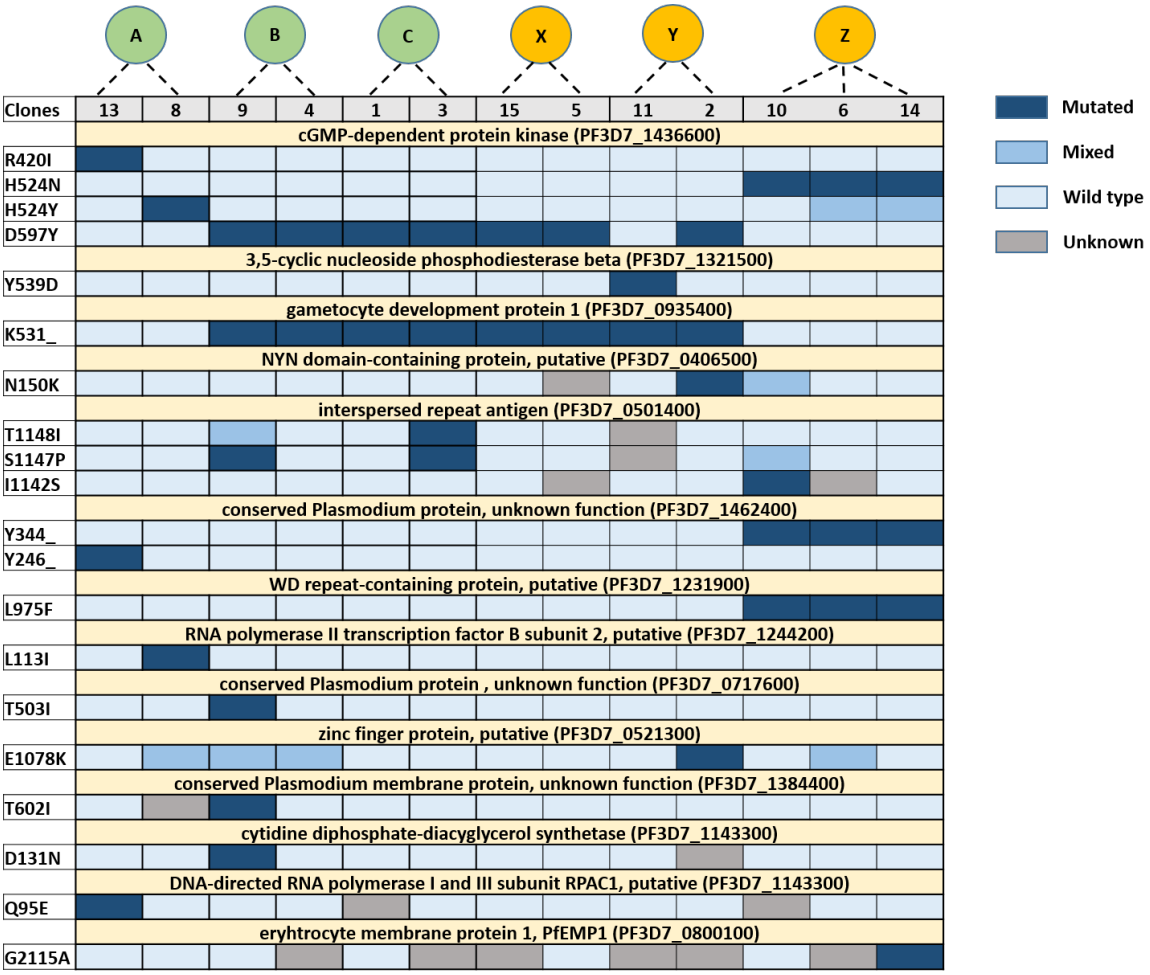

Fig. 33. The SNPs identified through WGS of the resistant strains. The petri dishes A, B and C represent the cultures cultivated under stepwise UA2239 pressure (from 3 x IC_{50} to 10 x IC_{50}). The rest of the petri dishes (X, Y and Z) represent the cultures cultivated under continuous UA2239 pressure (10 x IC_{50}). The culture in each petri dish was cloned, and 2 clones from each culture, except culture Z were three clones, had their DNA extracted and underwent WGS. Mixed represent a culture showing a mutation in one of the two alleles. Unknown represent the region a that had less than 10 reads.

C. Validation of PKG as the Target of UA2239

i. Generation of *Pf*ePKG Transgenic Parasites

The genome sequences of 12 of the 13 UA2239-resistant parasite clones code for a SNP non-synonymous mutation in *Pf*PKG protein **(Fig. 34.A)**. We therefore hypothesized that *Pf*PKG might be the main target of UA2239. In order to ascertain whether these mutations indeed confer resistance to UA2239 and to validate *Pf*PKG as a target, we aimed to introduce the SNPs identified above in a *P. falciparum* 3D7 WT.

The introduction of the SNPs was done using the CRISPR-Cas9 gene editing tool. In this study

the approach followed for the gene editing tool relied on the use of two plasmids. The first plasmid, pDC2-Cas9-sgRNA-*h*DHFR, contains the gRNA that guides the Cas9 protein to the target DNA site, where it will introduce double-strand breaks (DSB)[242]. The second plasmid, pBluescript, is used to repair the DSB by homologous recombination through HR1 and HR2. This recombination will introduce or not one of the 4 SNPs identified by WGS (*Pf*ePKG R420I, *Pf*ePKG H524 N/Y, and *Pf*ePKG D597Y) **(Fig. 34.B)**. We also generated a previously described mutation in *Pf*PKG T618Q conferring resistance to a well-studied inhibitor of *Pf*PKG, C2[238], for further investigation.

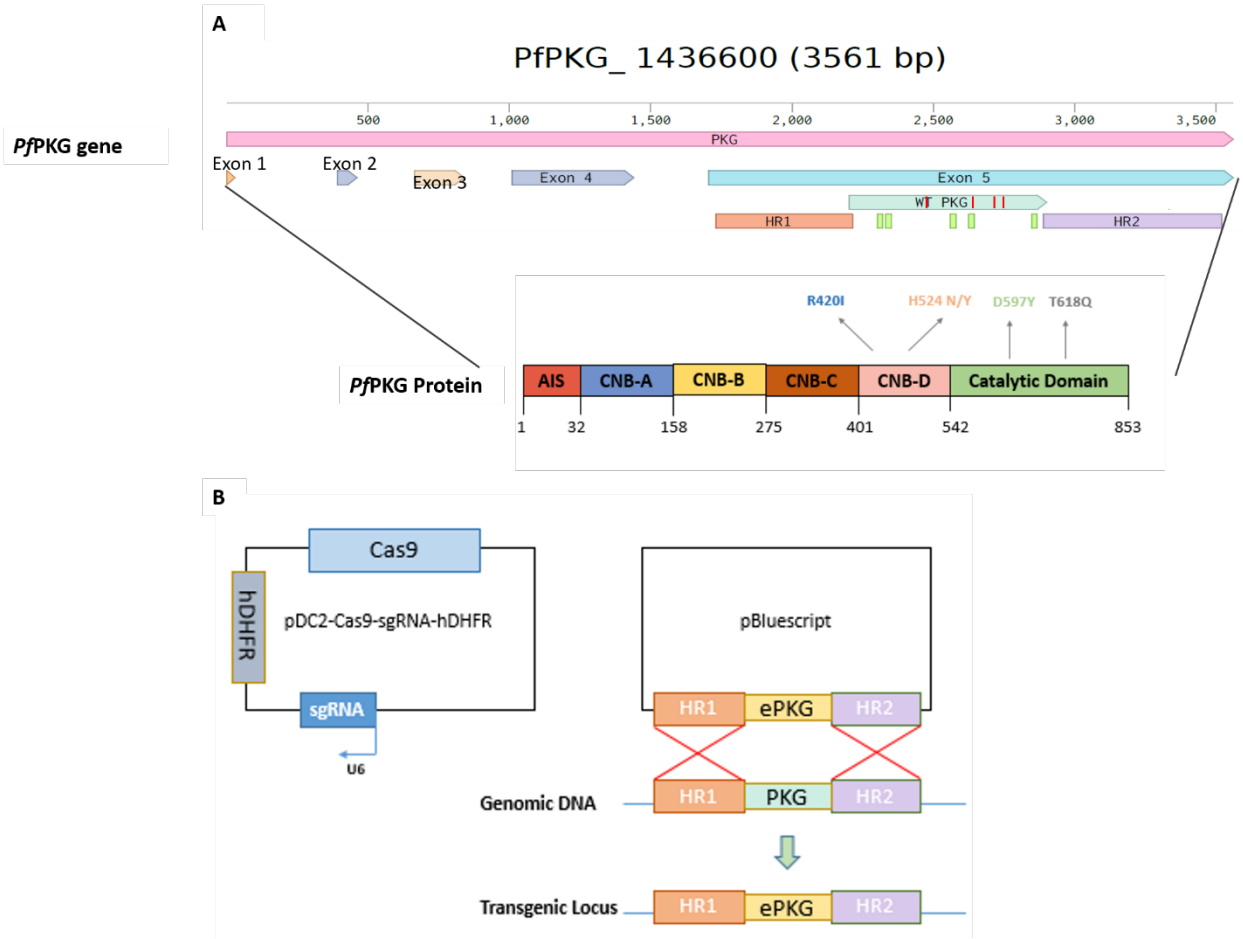

Fig. 34. Identification of UA2239 target in *P. falciparum*. A) The gene *Pf*PKG (PF3D7_1436600) is depicted in the upper part of the figure, consisting of exons indicated by numbered boxes. The encoded protein, WT PKG, is represented below the gene. The red lines within the WT PKG sequence represent the locations of single nucleotide polymorphisms (SNPs) associated with mutations in the protein. Specifically, the identified mutations in UA2239 resistant clones include R420I, H524 N/Y, and D597Y. Additionally, the T618Q mutation is observed in C2 resistant strains. **B)** Construct used for *Pf*PKG gene editing. pDC2-Cas9-sgRNA-*h*DHFR was designed to induce a double-strand break (DSB) near the 5' or 3' ends of WT PKG. The pBluescript contains the HR1, HR2 and the *E. coli* codonized sequence of interest, *Pf*ePKG, that will be inserted into the parasite genome through

homologous recombination. HR: homology region, ePKG optimized sequence using *E. coli* codon Protein Kinase G, PKG: Protein Kinase G.

Throughout the course of this thesis, several transfections were conducted using multiple gRNAs individually, and in desperate situations a mix of two gRNAs were employed. After transfection, the parasites were monitored by routine blood smears for 40 days' post-transfection. The presence of ring stage parasites served as an indication of a healthy transgenic culture. From which parasites were recovered, their genomic DNA was extracted and used for a diagnostic PCR analysis. A set of primers was designed to amplify the 5' and 3' integrations in order to evaluate the integration of the donor DNA into the targeted loci of the transgenic parasite. A positive integration was expected to yield fragments of 1125 bp (5' integration) and 1091 bp (3' integration) respectively **(Fig. 35.A-E)**.
The populations showing positive integration were cloned, and the resulting clones were employed for the further studies.

Notably, two interesting observations were made during this experiment. Firstly, it was observed that the same gRNA did not yield successful results in all transfections. Secondly, all the successful integrations were obtained from transfections involving one gRNA.

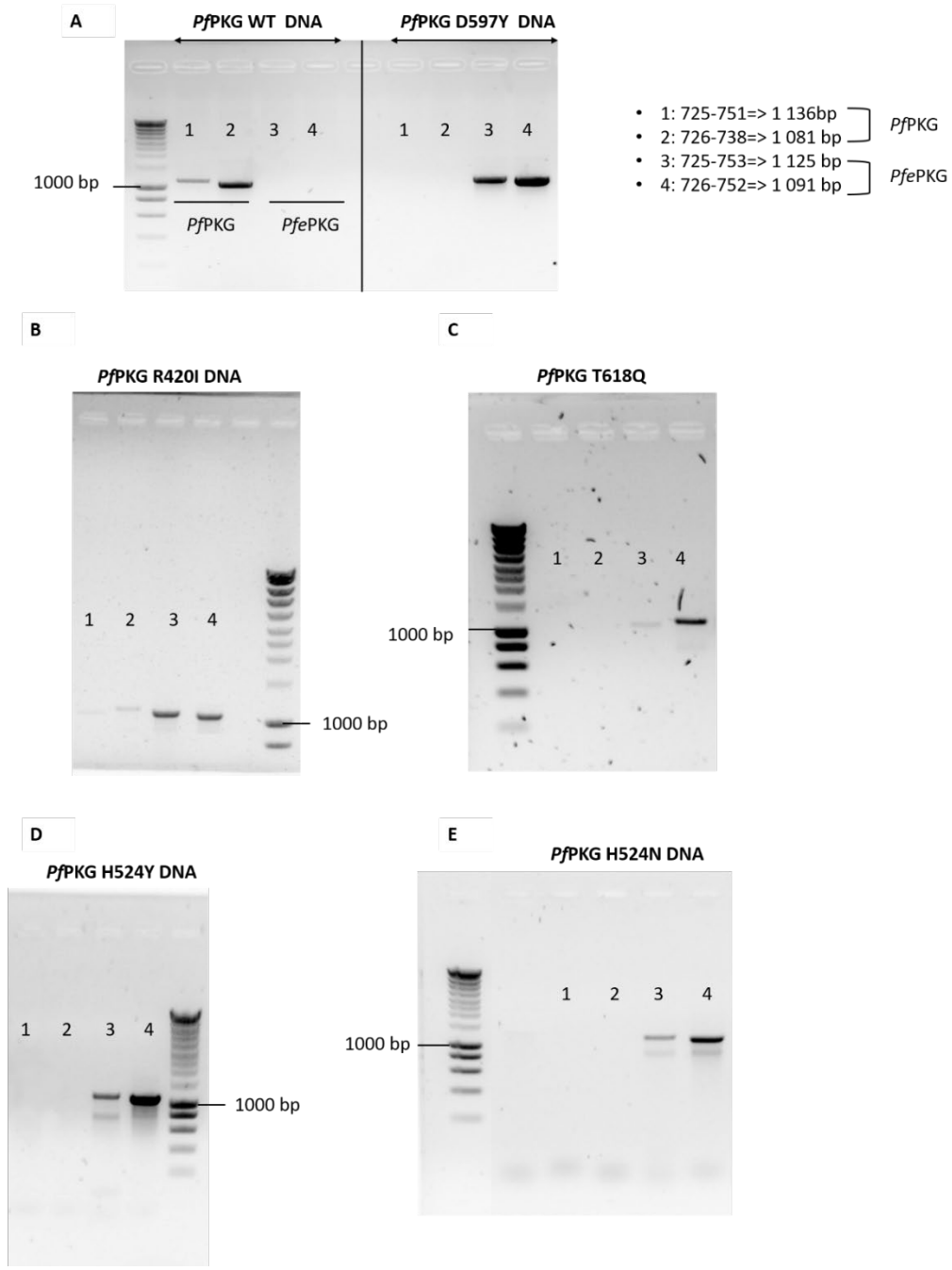

Fig. 35. Diagnostic PCRs for the transgenic population of *Pf*ePKG. A-E) Wells 1, 2, 3 and 4 were with different DNA samples, extracted from the transgenic that came back, and the same set of primers. Transfection were done separately, minimizing the possibility of strain mixing. Wells 1 and 2 were included as controls and utilized primers 725-751 and 726-738, which specifically target *Pf*PKG. Therefore, they are controls for the assessment of the presence or absence of 3D7 WT. Whereas wells 3 and 4 contain the primers 725-753 and 726-752, which recognize specifically *Pf*ePKG and will assess the presence or absence of the integration of the gene block (ePKG). The positive results are represented by the correspondent band size mentioned in this figure.

ii. Let's Talk Controls

The UA2239 resistant strains were cultured for several months and considering the reported mutation rate in vitro for *P. falciparum* as 1.0–9.7×10^{-9} mutations per base pair per generation[243], our objective was to determine if any of these naturally occurring mutations could affect the effectiveness of UA2239. We tested UA2239 susceptibility on a 3D7 WT that was cultured for 7 months, in parallel to the drug pressured cultures. The purpose of including this first control was to gain insights into the effects of long-term *in vitro* culture.

The comparison of the IC_{50} values of two strains was done using the two-tailed T-test. When the newly thawed 3D7 IC_{50} (IC_{50}= 83.43 ± 17.94 nM) was compared with the 7 months 3D7 strain IC_{50} (IC_{50}= 180 ± 50.4 nM), a significant difference was reported (p-value = 0.0167) **(Fig. 36)**. However, this increase is not an indication of resistance. The 3D7 WT 7 months was used as a control to follow the evolution of the resistance of the cultures under UA2239 pressure.

On the other hand, the validation of *Pf*PKG as the target of UA2239 involved assessing the IC_{50} of newly transfected strains in which the different mutations were introduced. The optimized *E. coli* codon construct, *Pf*epkg, represents a 699 bp long sequence, we wanted to control the effect of the synonymous mutations in this gene block on the susceptibility of UA2239. Therefore, we introduced this sequence containing only synonymous SNPs to generate a 3D7 *Pf*ePKG WT.

The comparison of the IC_{50} value of 3D7 WT with 3D7 *Pf*ePKG WT (IC_{50}= 120 ± 18.5 nM) showed no significant difference **(Fig. 36)**. This control ensures that the synonymous mutations are not influencing the response to UA2239.

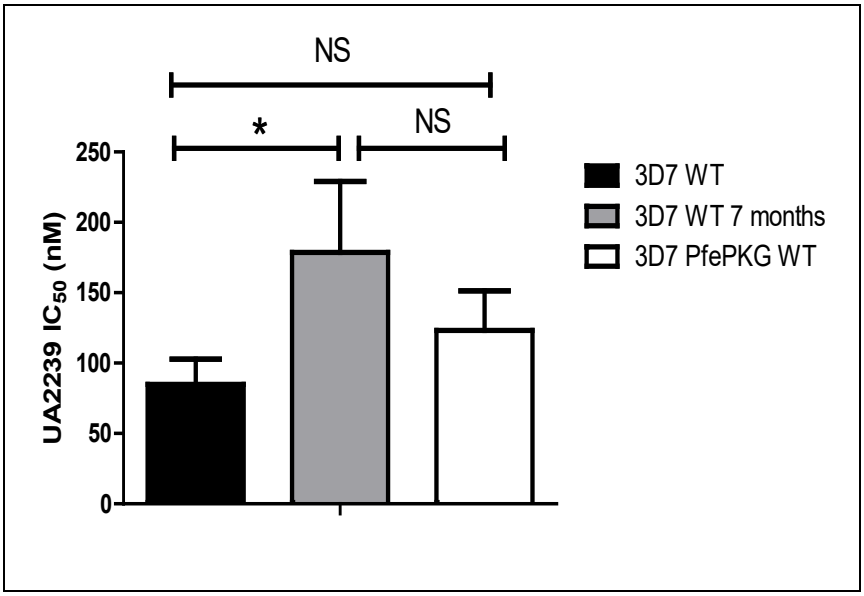

Fig. 36. *In vitro* UA2239 activity on the different control strains used in this study. 3D7 WT represent a newly thawed strain. 3D7 WT 7 months represent the strain that was cultured in parallel to the drug pressure strains. Finally, 3D7 *Pf*ePKG WT, represents the strain where we introduced the optimized *E. coli* codon constructs (*Pf*ePKG). Each bar represents the mean of 3 independent experiments (mean ± SD).

iii. Genetic Validation of *P. falciparum* as UA2239 Target

Once we ensured that the conditions and the synonymous mutations did not affect the efficiency of UA2239, we proceeded to validate *Pf*PKG as the target of UA2239.

Drug sensitivity assays were conducted separately for all of the transgenic clones, and their IC_{50} values were compared to *Pf*ePKG WT, which had an IC_{50} of 120 ± 18.5 nM **(Table 3)**.

The R420I mutated clones exhibited an IC_{50} of 598.1 ± 64 nM, which is 5 times higher than the IC_{50} of *Pf*ePKG WT. The remaining mutations (*Pf*ePKG H524N, *Pf*ePKG H524Y, and *Pf*ePKG D597Y) showed even higher IC_{50} values as shown in **Table 3**. This increase in the IC_{50} caused by a single SNP allows us to validate *Pf*PKG as being the main target of UA2239.

Interestingly, the resistant and the transgenic parasites with the same mutation do not have the same IC_{50} values, this can be caused by several factors, such as the long *in vitro* culture of the resistant strains (7 months) giving the parasites an opportunity to adapt and to overcome any fitness cost the mutations could have caused. Another possibility might be an epigenetic modification that cannot be identified through the method of sequencing used.

		IC_{50} UA2239 (µM)	
		3D7 WT 7 months	**3D7 WT < 1month**
Control	**Wild-type**	0.18 ± 0.05	0.08 ± 0.01
Mutated protein	***Pf*ePKG**	**Resistant**	**Transgenic**
***Pf*PKG**	**WT**	-	0.12 ± 0.01
	R420I	2.76 ± 0.66	0.57 ± 0.06
	H524N	4.10 ± 1.67	1.33 ± 0.98
	H524Y	2.91 ± 0.93	0.81 ± 0.17
	D597Y	3.92 ± 0.12	0.69 ± 0.12
***Pf*PDEβ**	**Wild-type**	-	0.11 ± 0.01
	Y539D	2.59 ± 0.81	0.58 ± 0.13

Table 3. *In vitro* antimalarial activity of UA2239 on resistant strains (Resistant) and *Pf*ePKG or *Pf*ePDEβ mutated strains (Transgenic). For the "resistants", one clone for each mutation was chosen among the 12 clones bearing a mutation in *Pf*pkg gene (N=3) plus the clone bearing a mutation in *Pf*pdeβ gene (N=3). They are compared with the 3D7 WT cultivated during 7 months in parallel of the parasites under UA2239 pressure. For the "transgenic", the four transgenic parasite strains mutated in *Pf*PKG were compared to wild type transgenic parasite strain (*Pf*ePKG WT). The transgenic parasite strain mutated in *Pf*PDEβ was compared to wild-type transgenic parasite strain (*Pf*ePDEβ WT). N=3; (mean **±** SD).

iv. Phenotypic Validation of UA2239 Target

*Pf*PKG plays a crucial role in the egress pathway of the malaria parasite[244,245,235]. During the final minutes before egress, *Pf*PKG is activated by cGMP, initiating the egress pathway[192]. Activation of *Pf*PKG leads to the poration and rupture of the parasitophorous vacuole membrane (PVM)[192] **(Fig. 37.A)**. The rupture of the PVM releases the merozoites into the cytoplasm of the RBCs. Their increased movements combined with the poration of the RBC membrane (RBCm), leads to the curling and buckling of the RBC[246]. Eventually, the RBCm ruptures, releasing the merozoites into the bloodstream, where they will invade other RBCs. The PVM poration and rupture can be blocked by inhibiting *Pf*PKG as it was shown with the imidazopyridine family, to which C2 belongs[14]. When treated with UA2239, the merozoites egress is blocked as seen in the Giemsa staining **(Fig. 37.A)**. Since UA2239 targets *Pf*PKG, this

compound is also supposed to inhibit the parasite PVM poration. Our previous Data have shown that UA2239 treated parasites developed normally until the segmented schizont stage[185] **(page 71)** and the parasites are blocked before the egress **(Fig. 32.A).** We therefore wanted to check the integrity of the PVM after UA2239 treatment. Immunofluorescence assays were performed using a 3D7 strain with a GFP-tagged parasitophorous vacuolar protein 1 (*Pf*PV1) strain. *Pf*PV1 is a protein present only in malaria parasite and is localized in the parasitophorous vacuole (PV)[247]. C2, which blocks the egress before the PVM ruptures[238] and E64, which blocks the egress after the PVM ruptures[186] , were used as controls **(Fig. 37.A)**. The results showed fluorescence of PV1 surrounding the merozoites of parasites treated with C2 and UA2239, indicating that the PVM was still present in both cases. On the other hand, the absence of fluorescence in E64-treated parasites indicates the disruption of the PVM **(Fig. 37.B)**.

Moreover, electron microscopy experiments showed a contrast between PV cytoplasm and RBC cytoplasm of the UA2239-treated iRBCs, suggesting an intact PVM (**Fig. 37.C)**. Indeed, in the literature, the PVM poration will cause an exchange between PV and RBC cytosols, resulting in non-distinguishable staining between RBC and PV cytoplasm[248]. It can be noted that, images also showed correctly formed merozoites, allowing us to cross out an inhibition of egress due to merozoites abnormality.

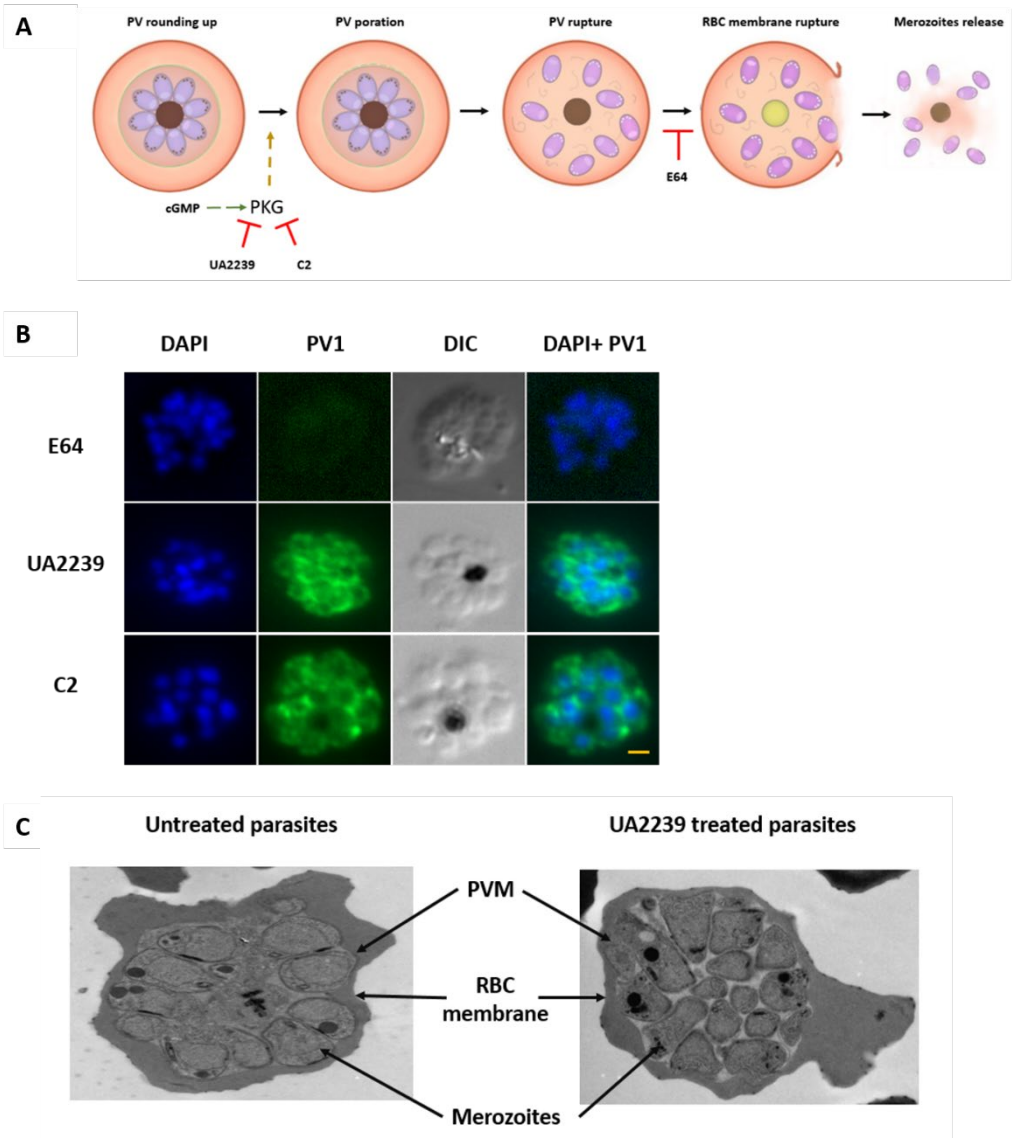

Fig. 37. Visualization of the parasitophorous vacuole membrane of *P. falciparum* schizonts. A) Schematic representation of the egress pathway and of the steps inhibited by UA2239, Compound 2 (C2) and E64. Immunofluorescence assay on PV1-GFP *P. falciparum strain.* iRBC at late schizont stage were incubated with UA2239 (750 nM), C2 (1.5 µM) or E64 (10 µM) for 4 h. The presence or absence of the PVM was assayed by immunofluorescence of the GFP-tagged protein PV1 (green). Nuclei was stained with Hoeschst (blue). E64 was used as a negative control, it blocks the parasite after the PVM rupture. C2 a known PKG inhibitor, was used as a positive control, it blocks the egress before the PVM rupture. Scale 1µm. N=3 **C)** Electron microscopy of untreated and UA2239 treated segmented schizonts. Parasites were treated or not with 2 µM UA2239 during 6 h. The difference in contrast between the RBCs cytoplasm and the PV cytoplasm is an indication of the presence of the PVM in both UA2239 treated or untreated parasites N=1. PV1: Parasitophorous vacuole protein 1; GFP: Green Fluorescence protein; iRBC: infected Red Blood Cells; PVM: Parasitophorous Vacuole Membrane; PV: Parasitophorous Vacuole.

D. Characterizing the Evolution of Resistance, the Fitness Toll

The challenging process of generating UA2239 site-directed mutations *in vitro* using CRISPR-Cas9 has shed light on a substantial fitness trade-off resulting from the acquisition of UA2239 resistance. Understanding the fitness toll imposed by these mutations is of paramount importance for several reasons. Firstly, it provides critical insights into the complex interplay between resistance development and the overall fitness landscape of the parasite. Secondly, it offers valuable information for the design of future therapeutic strategies that can exploit the vulnerabilities associated with resistance acquisition.

i. Surviving the Challenge: *Pf*ePKG D597Y

The *Pf*ePKG D597Y was the transfection the most difficult to obtain. After numerous trials, we finally got a positive integration but this strain was growing very slowly. Clones were obtained after 40 days of culture, while the other mutations came back between day 25-27 post cloning. The growth rate of the *Pf*ePKG D597Y culture was evaluated to assess its parasite multiplication rate. A growth curve experiment was performed, comparing the highly synchronized *Pf*ePKG D597Y parasites with the *Pf*PKG WT parasites over a period of 6 days, representing three replication cycles. Both cultures were maintained independently and under static conditions with an initial parasitemia of 0.25%. The results showed that *Pf*PKG WT parasites exhibited a 4-fold increase in growth with each replication cycle **(Fig. 38)**. In contrast, *Pf*ePKG D597Y culture displayed an average growth rate of approximately 1.75-fold, with the parasitemia reaching 0.9% on day 6 **(Fig. 38)**. This difference suggests that the D597 amino acid of *Pf*PKG plays a crucial role in *Pf*PKG function, and the mutation of this site is associated with a very high fitness cost, resulting in a reduced multiplication rate for *Pf*ePKG D597Y strain.

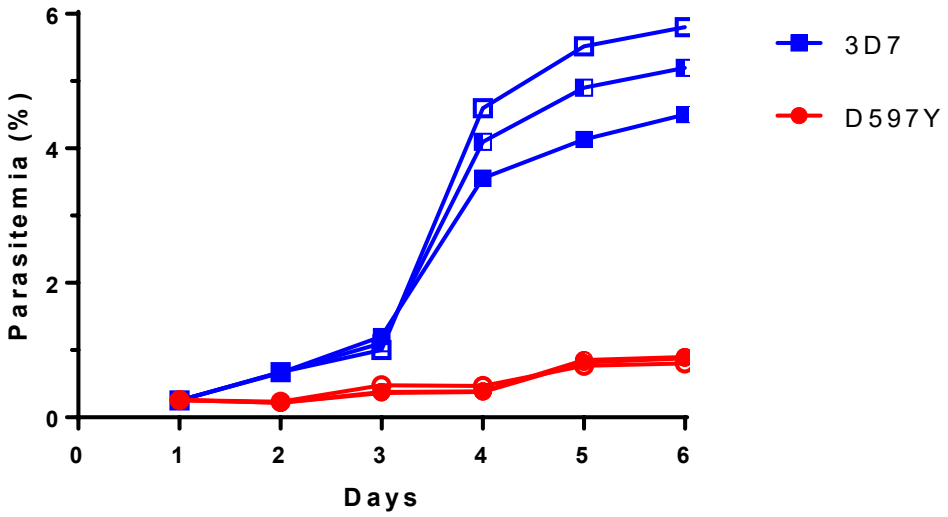

Fig. 38. *Pf*ePKG D597Y mutation causes a strong fitness cost for the parasite. Parasites were tightly synchronized with a 3h window. Parasitemia of 3D7 WT and *Pf*ePKG D597Y strains were followed for 6 days. 3D7 WT showed normal growth. However, the mutant was barely surviving along the cycles. Each curve represents a biological replicate (N=3).

ii. Uncovering the Subtle Fitness Toll

Contrary to what was observed with *Pf*ePKG D597Y strain, the *Pf*ePKG R420I, *Pf*ePKG H524N and *Pf*ePKG H524Y mutations did not show any significant fitness cost when cultured alone. To further assess their fitness, pairwise competitive growth assays were performed and followed by qPCR. Each mutated strain was mixed with an equal parasitemia of the 3D7 WT strain. The cultures were diluted and DNA samples were collected every cycle for a total of 20 parasite cycles for each competition test. Specific primers have been designed and tested to ensure accurate detection without cross-recognition.

To address potential role of the optimized *E. coli* codon construct, a pairwise competitive growth assay was also conducted with the *Pf*ePKG WT strain. The competition assay between 3D7 WT and 3D7 *Pf*ePKG WT strains demonstrated no significant difference in their ability to outcompete each other **(Fig. 39.A)**, indicating no fitness cost induced by the *E. coli* codonization of a part of this gene. Consequently, if a fitness cost is observed in the 3 mutated strains, it can only be attributed to the introduced *Pf*PKG mutation.

The *Pf*ePKG R420I, *Pf*ePKG H524N and *Pf*ePKG H524Y were all rapidly outcompeted by *Pf*PKG WT **(Fig. 39.B-D)**. This suggests that the site-directed mutations conferring resistance to UA2239 impose a fitness disadvantage on the parasites when compared to the WT strain.

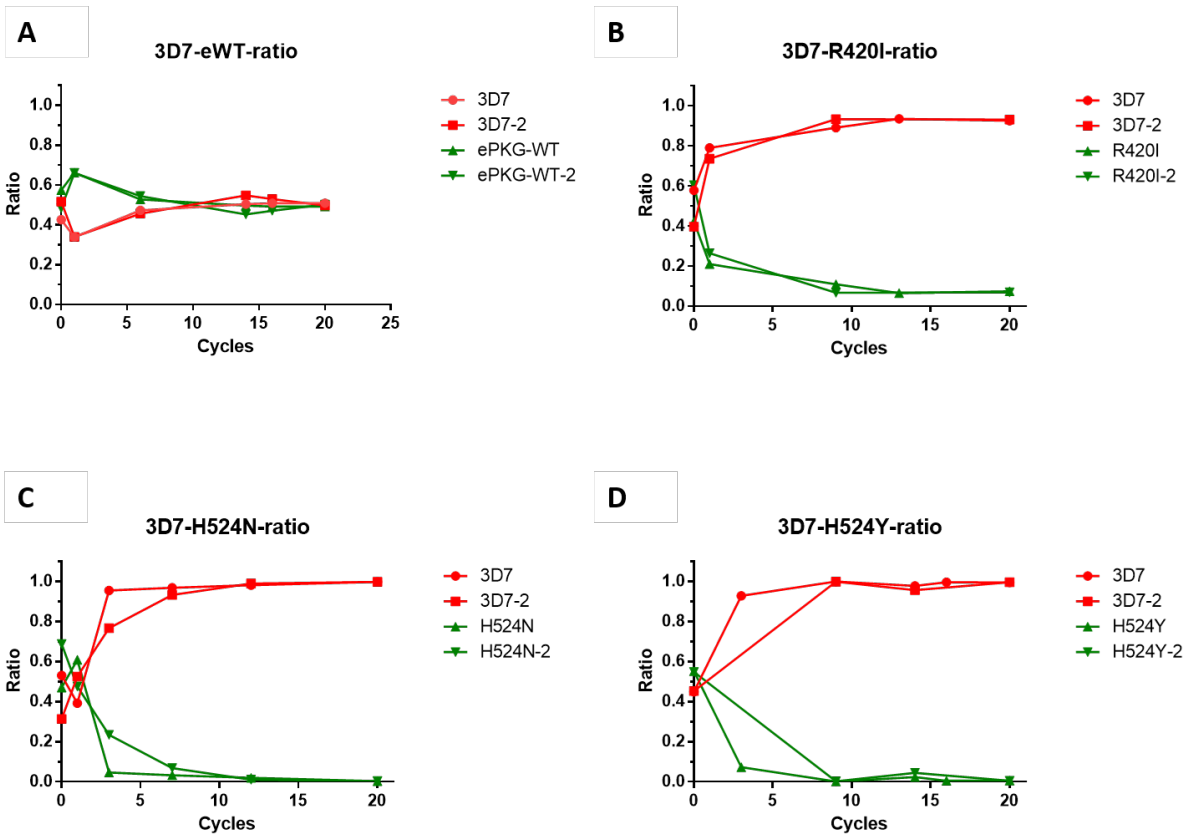

Fig. 39.The mutation conferring resistance to UA2239 cause a fitness cost. Pairwise competitive growth assays followed by qPCR were conducted for each mutated strain and for *Pf*ePKG WT (control) with 3D7 WT strain. Competition assays began with a parasite ratio of approximately 0.5 for each strain. **A)** Ratio between ***Pf*ePKG WT** strain and 3D7 WT strain. *Pf*ePKG WT strain contains a codonized part of the *Pf*pkg gene, into which the mutations have been inserted. **B-D)** Ratio between **R420I** (B), **H524N** (C) or **H524Y** (D) mutated strains and 3D7 WT. Red curves represent the 3D7 WT strain, and each curve is a biological replicate (N=2). The green curves represent the mutated 3D7, and each curve represent a biological replicate (N=2). The ratio of *Pf*PKG and *Pf*ePKG is represented in these graphs.

E. Assessing Antimalarial Drug's Efficacy on UA2239-Resistant Strains

We investigated the possible cross resistance of UA2239-resistant strains to other anti-malarial drugs. We first tested the sensitivity of UA2239-resistant strains and the transgenic strains to CQ. The result of this experiment showed that all of the strains had a similar IC_{50} values to the controls tested **(Table 4)**.

	CQ IC_{50} (nM)	
	3D7 WT 7 months	***Pf*ePKG WT< 1 month**
Control	14.3 ± 1.6	15.66 ± 0.4
***Pf*PKG**	**Resistant**	**Transgenic**
WT	-	13.4 ± 6.5
R420I	16.7 ± 7.2	12.0 ± 4.4
H524N	17.5 ± 3.4	21.0 ± 8.7
H524Y	12.3 ± 7.9	12.9 ± 3.2
D597Y	12.2 ± 1.6	8.2 ± 3.9

Table 4. Antimalarial activity of chloroquine on UA2239 resistant and transgenic strains. (mean ± SD, N=3)

Artemisinin resistance was observed to specifically affect the ring stage of the parasite, while other stages remain susceptible to the drug. Therefore, the assessment of artemisinin was conducted using the ring-stage survival assay (RSA). Parasitemia was determined on Giemsa-stained thin blood smears and the survival rates were calculated. A strain is considered resistant to artemisinin if its survival rate exceeds 1%.

The survival rates of different strains were assessed, including *Pf*PKG H524N (resistant (r) =0.21%, Transgenic (T)=0.22%), *Pf*PKG H524Y (r=0.52%, T=0.23%), and *Pf*PKG R420I (r=0.25%, T=0.28%). These strains exhibited survival rates below 1%, indicating that these mutations do not confer resistance to artemisinin **(Fig. 40.A)**.

Intriguingly, the resistant strain with the *Pf*PKG D597Y showed a low resistance to artemisinin, with a survival rate higher than 1% **(Fig. 40.B)**. Notably, this resistance was observed in all seven UA2239-resistant clones sequenced and carrying this mutation with their survival rates ranging between 1.5 and 3% **(Fig. 40.B)**. However, when the same mutation was introduced into the transfected parasites, resistance to artemisinin was not observed (*Pf*ePKG D597Y survival rate < 1%) **(Fig. 40.B**), suggesting that the D597Y mutation in the *Pf*pkg gene should not be responsible for DHA resistance.

Resistance to artemisinin is generally due to mutations in the Kelch13 gene. Interestingly, the WGS analysis of the 7 resistant clones revealed the absence of mutation in this gene. Further investigations are required to elucidate the underlying mechanisms of this resistance but it

could result from other mutations in the genome during long-lasting *in vitro* culture, or from epigenetic regulation. It can be noted that the seven *Pf*PKG D597Y resistant clones shared only one other common mutation in the gametocyte development 1 gene **(Fig. 33)**. The product of this gene is an upstream activator of sexual commitment. We can hypothesize that the regulation of this gene could be modified to counterbalance the perturbations caused by drug pressure or mutation.

These findings indicate that the mutations responsible for resistance to UA2239 do not confer resistance to CQ nor to DHA.

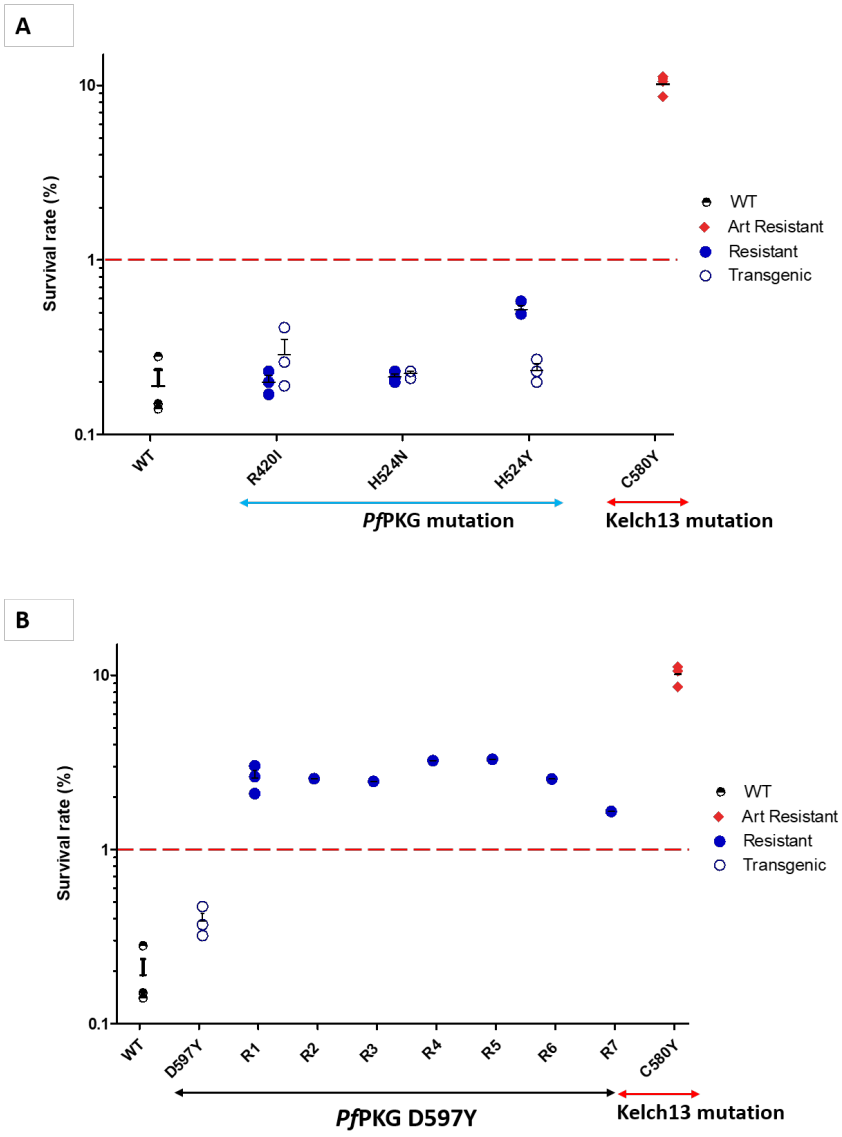

Fig. 40. Sensitivity of UA2239 resistant clones to dihydroartemisinin (DHA). The threshold for resistance of DHA is marked by the red line, which is a survival rate >1%. A survival rate <1% indicates sensitive strains to DHA. 3D7

WT strain is the sensitive control and the 3D7 Kelch 13 C583Y strain is the resistant control to DHA. Each point represents a biological replicate. **A)** Survival rates of the transgenic (open circle) and resistant (closed circle) strains containing R420I, H524N and H524Y mutations. **B)** Survival rates of the D597Y transgenic strain (open circle) and of the 7 resistant clones (closed circle, R1-R7) containing D597Y mutations.

F. *P. falciparum* Mechanism of Resistance Against UA2239

Among the 13 sequenced resistant clones, one had a non-synonymous SNP in the *Pf*PDEβ, resulting in Y539D substitution. The PDE enzymes play a crucial role in regulating the concentrations of second messengers (cAMP and cGMP) through hydrolysis, making them an integral part of the enzymatic cascade involved in the egress pathway[220] **(**see introduction**)**.

In order to assess the effect of this mutated protein on the activity of UA2239, we introduced the SNP in *Pf*pdeβ of *P. falciparum* 3D7 WT strain. The same procedure as the generation of the transgenic above was used here. In this case a positive integration was expected to yield fragments of 725 bp for the 5' integration and 934 bp for the 3' integration **(Fig. 41.A)**.

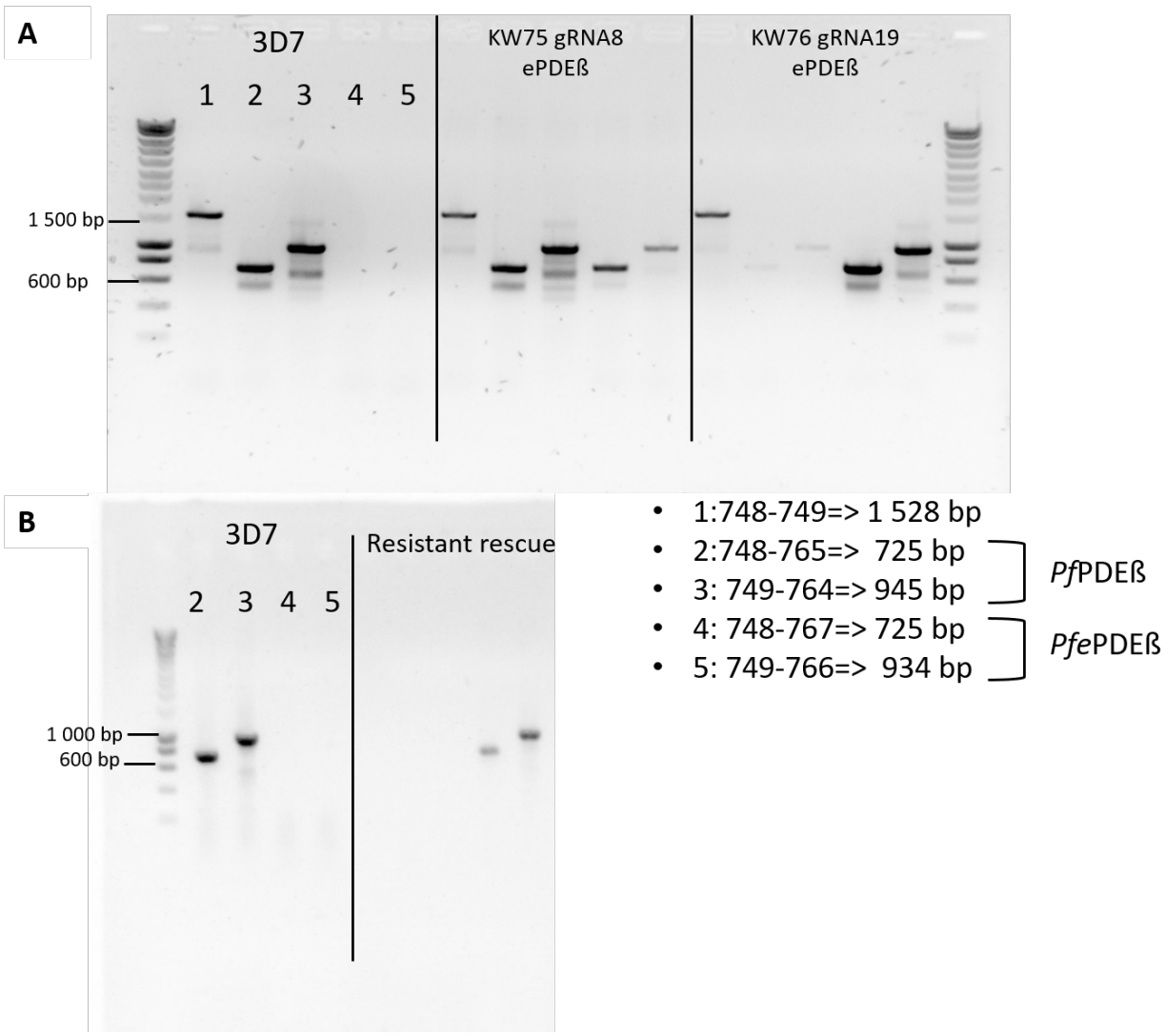

Fig. 41. Diagnostic PCRs for *Pfe*PDEβ integration. A) Genomic DNA were extracted from the transgenic that came back. 3D7 strain was used as a control of the specificity of the primers. KW75 and KW75 represent a population of transgenics that need to be cloned. **B) Diagnostic PCR of the rescue of the resistant strain with the *Pf*PDEβ mutation.** Due to difficulty cloning the transgenic, containing the *Pfe*PDEβ Y539D, we decided to rescue the resistant strain with the same mutation.

The populations showing positive integration were cloned. However, the cloning procedure of the mutated population resulted in either 3D7 WT alone, or all of the PCRs with the different set of primers were positive. In parallel to our efforts to obtain the clones of these transgenic, we decided to rescue the resistant clone containing the *Pf*PDEβ Y539D mutation, Y11 **(Fig. 33)**. The rescue included the insertion of the *Pfe*PDEβ WT sequence into the UA2239 resistant clone and test the sensitivity of UA2239 on this transgenic **(Fig. 41.B)**.

At the end, our efforts paid off and we were able to obtain the clones of both the mutated (*Pfe*PDEβ Y539D) and the rescue. The rescue strain showed a decrease of 5 folds in its IC_{50}

compared to the *Pf*PDEβ Y539D resistant strain. In addition, compared to the IC_{50} of 3D7 WT 7 months, the transgenic containing the *Pf*ePDEβ Y539D mutation showed a 7-fold increase **(Table 3)**.

3. Conclusion

In this chapter, our investigations have culminated in a remarkable revelation, starting with concrete proof that UA2239, an ANP, does not affect the parasite DNA synthesis. In our aim to identify the target of UA2239, we generated UA223-resistant strains and we were able to identify SNPs in *Pf*PKG. This discovery holds substantial logical merit, primarily owing to the structural resemblance between UA2239 and cGMP **(Fig. 24)**, the sole known *Pf*PKG activator[192] which lends a strong support to their interaction. *Pf*PKG plays a crucial role in the egress pathway, which explains the correlation between *Pf*PKG inhibition and the phenotypic response of the parasite to UA2239 has reinforced our suspicions.

To validate all of these findings, we deliberately introduced the SNPs into 3D7 WT strain, successfully generating resistant strains to UA2239. By pinpointing *Pf*PKG as the prime target of UA2239, we were able to reveal a previously unexplored mechanism of action for an ANP. This study demonstrates, for the first time, the activity of an ANP on a kinase enzyme. This breakthrough not only enhances our understanding on ANPs and *Pf*PKG but also paves the way for future investigations and the potential development of innovative therapeutic strategies.

In addition, we were able to show a fitness cost due to the mutations conferring resistance to UA2239. *Pf*ePKG D597Y mutation imposes a substantial fitness cost on the parasites, severely hindering their growth and survival. The other three SNPs associated with UA2239 resistance also exhibit fitness costs, albeit not as pronounced as the *Pf*ePKG D597Y mutation.

These findings underscore the delicate balance between drug resistance and fitness in the context of antimalarial interventions. While the parasites may acquire resistance to UA2239, their survival and growth are compromised, emphasizing the potential limitations of resistance as a long-term strategy for their survival.

Moreover, we were able to demonstrate the absence of cross resistance between the UA2239 resistant strains and two antimalarial drugs, CQ and ART.

Finally, we showed that a mutation in *Pf*PDEβ can also confer resistance to UA2239. However, *Pf*PDEβ is refuted as the target of UA2239 due to the unmatched phenotype. More studies regarding this mutation will need to be done so we can gain more insight into its direct effect of resistance against UA2239.

Chapter II: UA2239 Characteristic as an Antimalarial Drug

1. Introduction

In recent years, *Pf*PKG has been receiving a lot of attention as a drug target. *Pf*PKG was shown to be an essential protein during different stages of *Plasmodium* life cycle[240] **(Fig. 25)**. The lead *Pf*PKG inhibitor compound was C2, and most recently it is ML10 (an analogue of C2), they are members of the imidazopyridine family. These compounds target the gatekeeper pocket adjacent to the ATP binding site[240]. Resistance to all of the current *Pf*PKG inhibitors are linked to a T618Q substitution. Glutamine (Q) is a bulkier residue than threonine (T), therefore it prevents inhibitor access to the gatekeeper pocket and renders the kinase insensitive to the inhibitor[240]. UA2239 is unique as it is the first reported ANP to target *Pf*PKG. Resistance to UA2239, as seen in the chapter I of the results, is completely different from the previous reported *Pf*PKG inhibitors.

In addition, even though discovering the target of UA2239 has been a significant aid in unraveling its mechanism of action numerous questions still remain regarding this compound. One key question is the mode of entry of UA2239, a charged molecule, into iRBCs. We also wanted to discover whether UA2239 is effective against the different stages of the malaria intraerythrocytic cycle, including rings, trophozoites, and schizonts. Another important aspect to investigate is the minimum contact time required for UA2239 to exert its antimalarial effect. Determining the duration of exposure needed for the drug to exhibit its maximum efficacy can guide treatment strategies and dosage recommendations. In addition, as *Pf*PKG has been shown to be essential for gametocyte activation[236], we also wanted to explore the effect of UA2239 on the sexual forms of the parasite.

In this chapter, we aimed to address all of these questions, so we can further enhance our understanding of this compound and its potential as an antimalarial drug.

2. Results

A. Exploring Cross-Resistance to C2, a *Pf*PKG Inhibitor

To reach the aim of this chapter, first we generated the C2-resistant strain, *Pf*ePKG T618Q. This mutation caused at least 12-fold increase in C2 IC_{50} (IC_{50}=3511.7 ± 962 nM) compared to *Pf*ePKG WT's IC_{50} (IC_{50}= 254.1 ± 30.7 nM).

Interestingly, all the UA2239-resistant strains were as sensitive to C2 as the control **(Table 5)** and *Pf*ePKG T618Q was sensitive to UA2239 with an IC_{50} value of 145.8 ± 37.4 nM **(Table 5)**.

		IC_{50} (nM)	
		3D7 WT 7 months	***Pf*PKG WT< 1 month**
C2	**Control**	208.0 ± 14.3	284.2 ± 48.2
	***Pf*PKG**	**Resistant**	**Transgenic**
	WT	-	254.1 ± 30.7
	R420I	271.4 ± 57.4	282.8 ± 60.3
	H524N	128.9 ± 56.8	167.4 ± 37.5
	H524Y	116.9 ± 7.1	167.4 ± 38.5
	D597Y	128.9 ± 59..9	284.2 ± 6.5
	T618Q	-	3 511.7 ± 962.0
UA2239	**WT**	-	120.0 ± 18.5
	T618Q	-	145.8 ± 37.4

Table 5. Antimalarial activity of UA2239 and C2 on C2- and UA2239-resistant strains, respectively. N=3; mean ± SD.

B. Combining UA2239 with C2

We then assessed the interactions at pharmacological level between these two PKG inhibitors. By treating the parasites with different concentrations of both UA2239 and C2, we can determine how these compounds interact with each other, employing the concept of the isobologram assay.

Three possibilities can result from an isobologram: an antagonistic, additive or synergistic effect of the drug combination[249] **(Fig. 42.A)**. An antagonistic effect occurs when the combined effect of two substances is less than what would be expected based on their individual effects. In other words, the substances interfere with each other's actions, resulting in a decreased overall effect. Antagonistic effects can occur through various mechanisms, such as blocking the receptor sites or counteracting the pharmacological actions of one

another. Clinically, antagonistic effects may reduce the therapeutic efficacy of a drug combination or hinder its desired outcomes.

Additivity refers to a situation where the combined effect of two or more substances is equal to the sum of their individual effects. In other words, the substances act independently and contribute to the overall effect without influencing or interfering with each other. Additive effects are often desirable in drug combinations as they lead to a predictable and expected outcome. It allows for the use of lower doses of individual drugs while achieving the desired therapeutic effect.

Synergy occurs when the combined effect of two or more substances is greater than the sum of their individual effects. In synergy, the substances act together in a way that enhances their overall effect, producing a more potent or efficacious response. Synergistic effects can result from various mechanisms, such as enhancing the action of one substance by another, improving drug absorption or distribution, or targeting different enzyme of a same pathway or different pathways of a disease simultaneously. Clinically, synergistic effects can lead to improved therapeutic outcomes, increased efficacy, and reduced drug resistance.

We determine the antimalarial activity of UA2239 alone or in combination with C2 on 3D7 WT strain. The IC_{50} of the combined compounds were expressed as sums of the fraction of IC_{50} (FIC_{50}) of each added compound. In three independent experiments, we observed an additive effect C2 and UA2239 with a maximal sum of FIC_{50} of 1.07 **(Fig. 42.B)**.

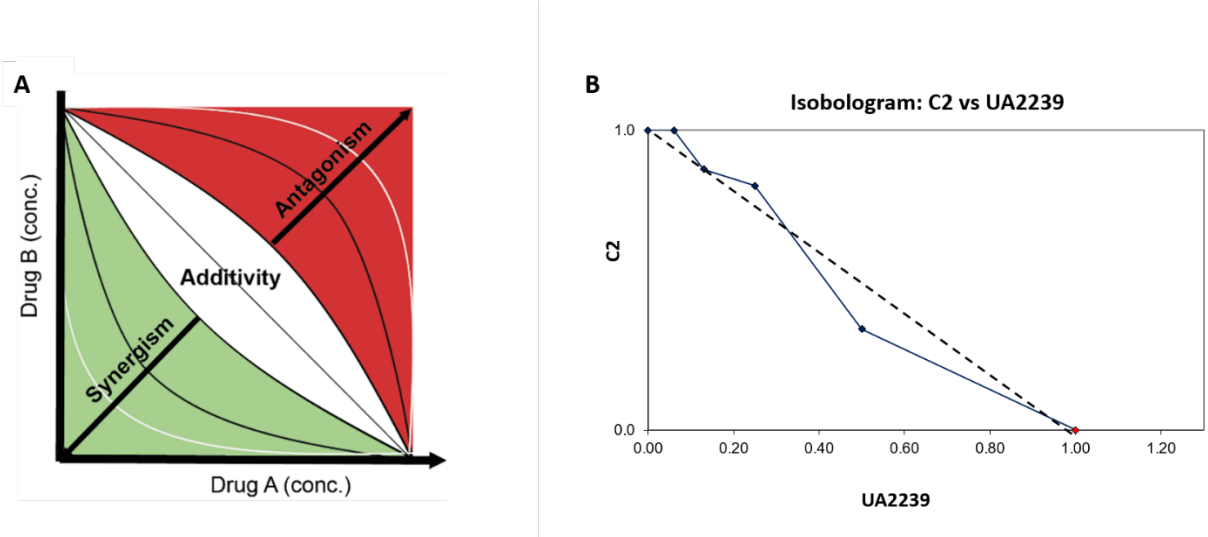

Fig. 42. *In vitro* interaction between UA2239 and C2, an inhibitor of *Pf*PKG. Effect of the combination of C2 and UA2239 is represented as isobole plot. Concentrations were expressed as a fraction of the IC_{50}s of the

compounds. These fractions were called fractional inhibitory concentrations (FIC_{50})[249]. For isobole plot, the sum of FIC_{50}s (ΣFIC_{50}) of UA2239 and C2 studied in combination for antimalarial activity are indicated. Additive effect: ΣFIC_{50} was ≥1 and <2; synergy: ΣFIC_{50} <1, slight antagonism: ΣFIC_{50} ≥2 and <4, marked antagonism: ΣFIC_{50} ≥4. Data presented are from one typical experiment, and experiment was conducted three times independently

C. Unveiling the Entry Mechanism of UA2239

Although UA2239 is a charged molecule, it has been observed in previous experiments that it enters the RBCs and reaches the parasite, despite the barrier of the RBC lipid bilayer membranes[250]. *Plasmodium* relies on specific channels known as new permeability pathways (NPPs) in the iRBC membrane to facilitate the uptake of nutrients and removal of waste products. These NPPs play a crucial role in the exchange of substances between the parasite and its external environment, including the exchange of charged molecules[251]. Based on this understanding, we hypothesized that UA2239 enters the iRBC through these NPPs. To investigate this hypothesis, we determined the effect of adding furosemide, a compound known to block the NPPs, on the antimalarial activity of UA2239.

The experiment was performed independently three times, each time, the appropriate concentration of furosemide was added to the culture and incubated for 20 min before the addition of serial dilutions of UA2239. The results showed an antagonistic effect of furosemide with a maximal sum of FIC_{50}s of 2.29 **(Fig. 43)**, suggesting that UA2239 enter the iRBCs via NPPs.

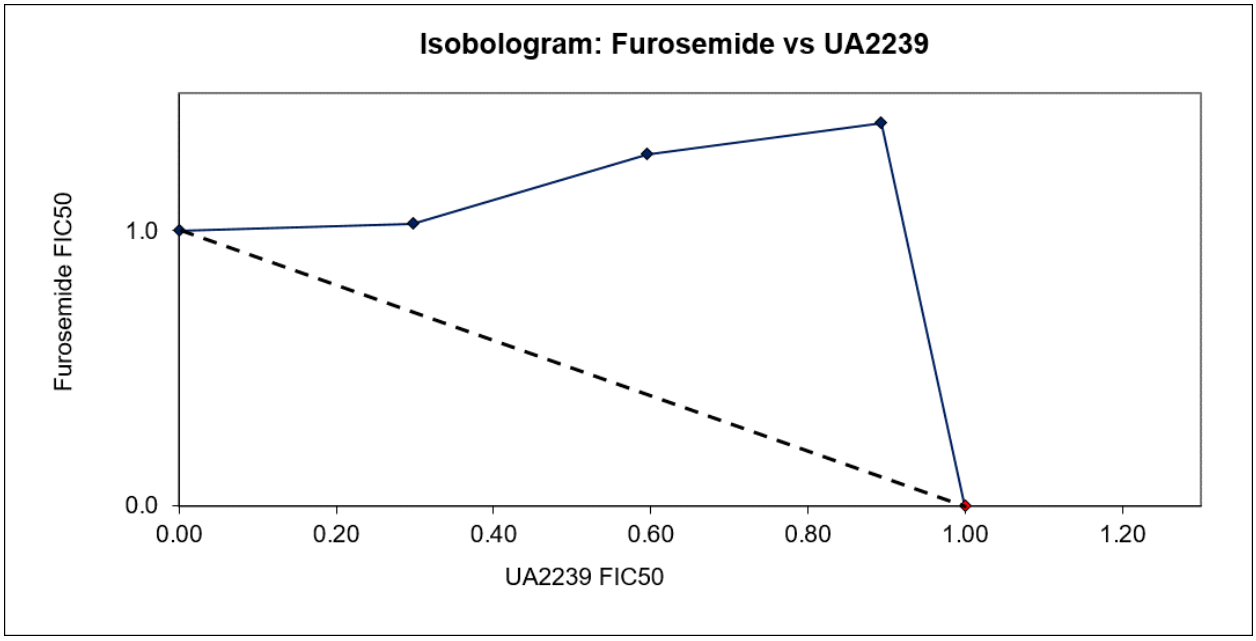

Fig. 43. *In vitro* interaction between UA2239 and Furosemide, a new permeability pathway (NPP) inhibitor. Effect of the combination of furosemide on UA2239 entry into iRBCs. N=3.

B. Assessment of UA2239 Efficacy Across Different Stages of the Malaria Parasite's Intraerythrocytic Cycle

To assess the efficacy of UA2239 at different stages of the malaria parasite's intraerythrocytic cycle, we conducted treatments on synchronized parasites at specific time points: ring (0-3 hpi), mature ring (12-18 hpi), trophozoite (24-27 hpi), and schizont (36-39 hpi) stages.

The compound was administered for a 6-hour period at each stage, followed by thorough washing and culturing again. At 48hpi, ^{3}H-hypoxanthine was added, and the culture was further incubated for 24 h **(Fig. 44.A)**. The IC_{50} values for trophozoites and schizonts were found to be 178 ± 15.7 nM and 142.8 ± 19.8 nM, respectively. These IC_{50} values were only about twice the IC_{50} obtained when UA2239 was added throughout the entire intraerythrocytic cycle (IC_{50}= 83.4 ± 17.9 nM), indicating an irreversible activity of UA2239 at the trophozoite and schizont stages. The compound was not active when used at the ring stage **(Table 6)**.

In contrast, the *Pf*PKG inhibitor C2, shows a reversible effect after 6-hours treatment followed by a washout, whatever the treated stage is **(Table 6)**. Antimalarial activity of C2 can be determined only after continuously exposition of the parasites to C2 for 48 h. In this case, its IC_{50} was 284.2 ± 62.3 nM **(Table 6)**.

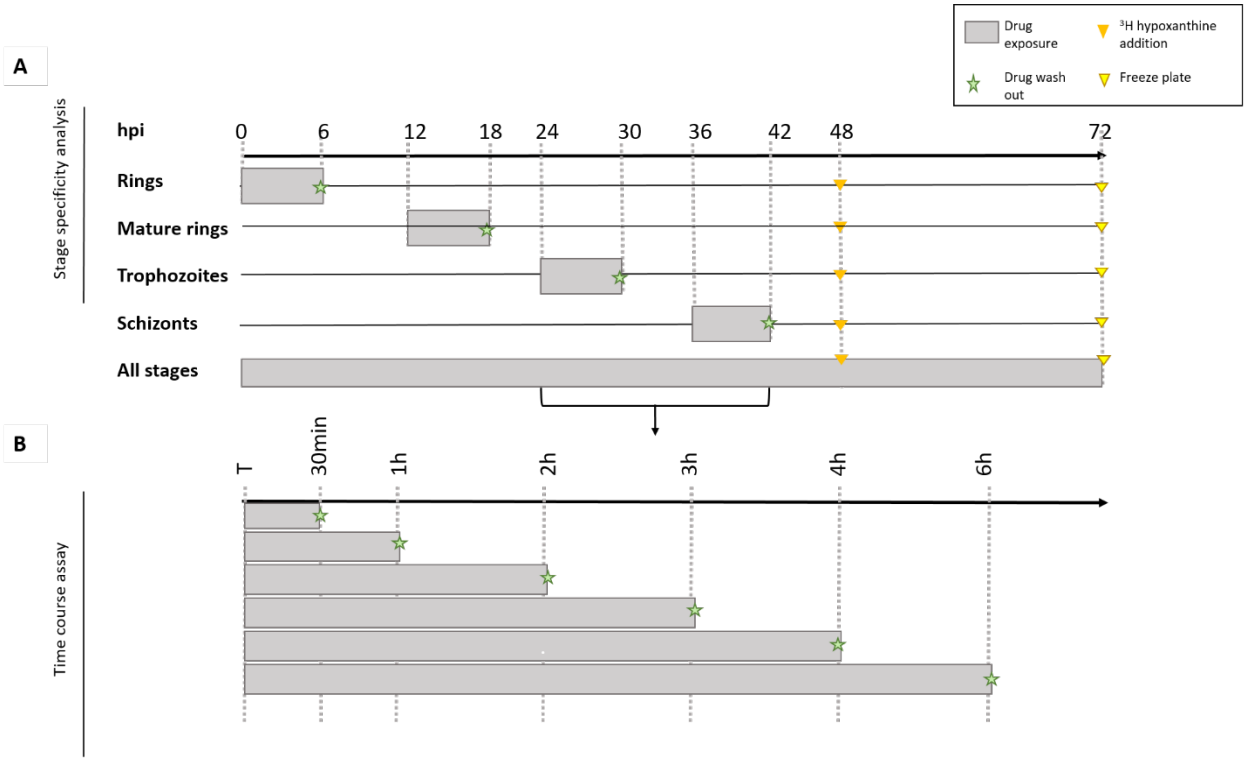

Fig. 44. Schematic representation of the methodology of two techniqures. A) the stage specificity. B) The time of contact assays.

IC_{50} (nM)	Rings	Trophozoites (24hpi)	Schizonts (36hpi)	Whole cycle
UA2239	≥20 000	178 ± 15.7	142.8 ± 19.8	83.4 ± 17.9
C2	≥10 000	≥10 000	≥10 000	284.2 ± 62.3

Table 6. *In vitro* stage-dependent susceptibility of *P. falciparum* (3D7) to UA2239. For rings, trophozoites and schizonts, cells were incubated with UA2239 or C2 for 6h, then washed and resuspended in fresh complete medium before addition of 3H-hypoxanthine at 48hpi. For whole cycle, cells were incubated continuously with the drug until 48hpi and addition of the ^{3}H-hypoxanthine.

We then treated trophozoite (24-30 hpi) and schizont (36-42 hpi) stages with 750 nM of UA2239 for 30 min, 1, 2, 3, 4, and 6 h **(Fig. 44.B)**. After incubation for the indicated time, cells were washed and resuspended in fresh media. Parasite viability was monitored by adding ^{3}H-hypoxanthine at 52 h until 72 h. At the schizont stage, 2-h treatment resulted in a reduction

of 74.6% in parasite growth and an additional hour of incubation resulted in 90% inhibition of the parasite growth **(Fig. 45)**. At the trophozoite stage, a 6-h incubation with the compound was required to achieve 75% of growth inhibition **(Fig. 45)**. As the quantification of ^{3}H-hypoxanthine incorporation is not a direct determination of parasitemia, we have checked parasitemia and parasite health on thin blood smears after 6 h of treatment, where residual incorporation of hypoxanthine was 7% and 23%. Upon microscopic examination of blood smears, the residual incorporation was attributed to the presence of picnocytes **(Fig. 45)**. These findings suggest that UA2239 exerts a rapid and irreversible cytotoxic effect on schizonts, while its impact on trophozoites is relatively slower, yet still significant.

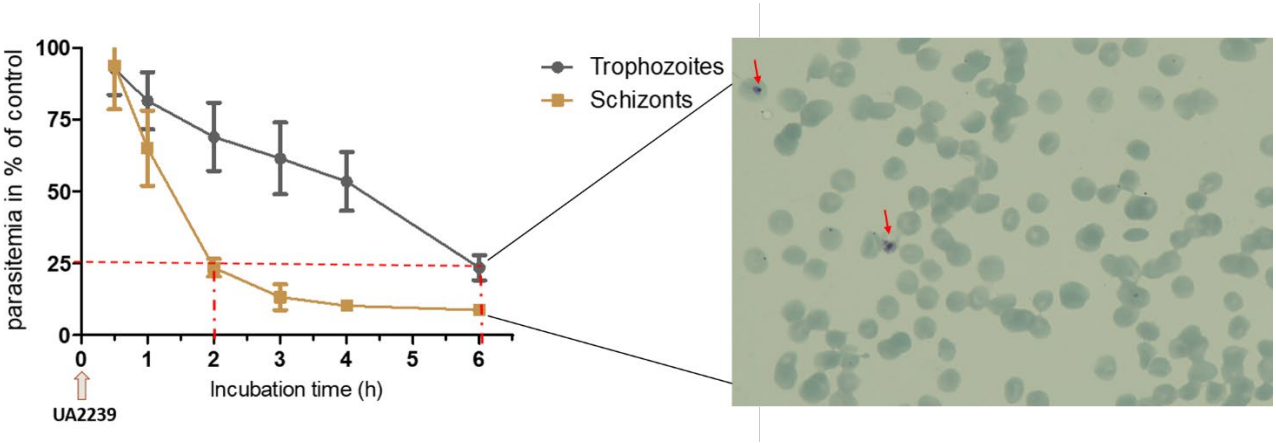

Fig. 45. Time course of *P. falciparum* growth inhibition. *P. falciparum* 3D7 culture was tightly synchronized within a 3h window. Trophozoites (24 hpi) and schizonts (30 hpi) were treated with 750 nM of UA2239 for 30 min, 1, 2, 3, 4 and 6 h. After incubation for the indicated time cells were washed and resuspended in fresh media. Parasite viability was monitored by adding ^{3}H-hypoxanthine at 52 h until 76 h. N=3.

C. UA2239 Effect on *P. berghei* Gametocytes

*Pf*PKG has been demonstrated to play a crucial role in the activation of gametocytes. Inhibition of this protein has been shown to result in the inhibition of gametocyte exflagellation[236] **(Fig. 25)**. To investigate the effect of UA2239, we tested UA2239 effect on *P. berghei* gametocytes exflagellation. The results revealed that UA2239 has the ability to inhibit the exflagellation of male gametocytes, with an ED_{50} value of 0.1 mg/kg through intraperitoneal administration **(Fig. 46)**. This new finding suggests that UA2239 can effectively block the sexual reproduction of gametocytes in mosquitoes, thereby inhibiting transmission of the parasite.

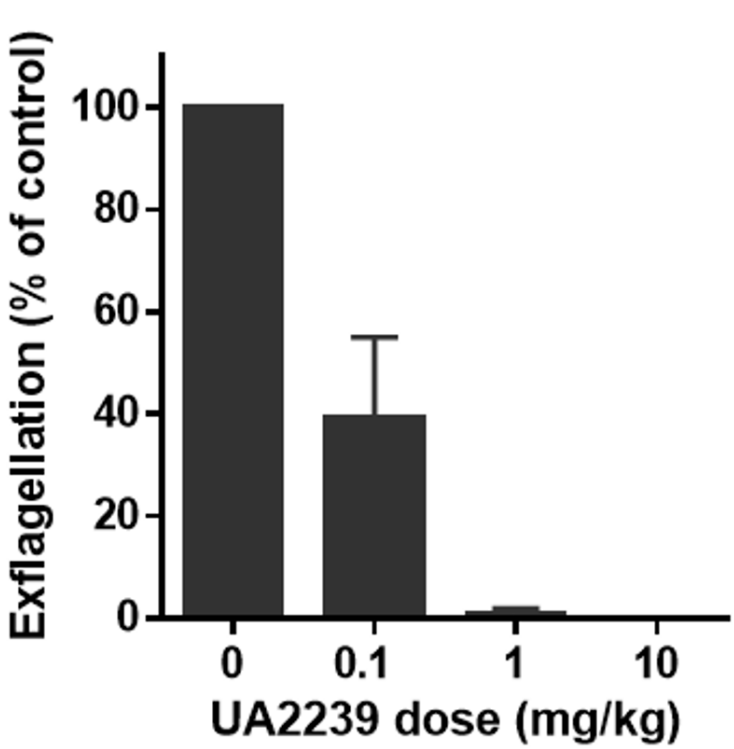

Fig. 46. Impact of UA2239 on *P. berghei* gametocyte exflagellation after intraperitoneal (i.p) administration. To quantify gametocyte exflagellation, the number of exflagellation centers was counted 12-15 mins after a drop of blood from *P. berghei* – infected mouse was placed at 19°C. Then, the mouse was treated with UA2239 via i.p administration. A drop of blood was collected 30 min after UA2239 treatment and the number of exflagellation centers was quantified.

3. Conclusion

All these observations provide valuable insights into the mechanism of action of UA2239. The absence of cross-resistance between UA2239 and C2 highlights the fact that UA2239 and C2, while sharing the same target, they have distinct binding site on the enzyme. C2 binds to the ATP-binding site in the *Pf*PKG catalytic domain[240], while UA2239, which is a GMP analogue, could prevent cGMP binding to CNB domains (regulatory domains) and thereby impedes activation of *Pf*PKG.

This chapter has also provided us with a wealth of information regarding the unique characteristics of UA2239. We have shown that UA2239 enters iRBCs through NPPs. NPPs are established at the iRBC membrane from 15 hpi and reach a plateau after 36 hpi[16]. Unlike other *Pf*PKG inhibitors, this compound exhibits irreversible activity requiring a minimum contact time of 6 hours for trophozoites and 4 hours for schizonts, to inhibit respectively 75% and 90% of parasite growth. However, the compound is not active when added at ring stage. The

inactivity on the rings (0-6 hpi) can be explained by the fact that the NPPs, which represent the mode of entry of UA2239, are not present before 15hpi. UA2239 also exhibited an effect of *P. berghei* gametocyte exflagellation. Gametocytes iRBCs were shown to also have the NPPs[252], which explains the activity of UA2239 on inhibiting their activation.

The ability of UA2239 to be active on both the asexual and sexual stages makes it even more interesting to be developed as an antimalarial drug.

Interestingly, while *Pf*PKG is known to be required and expressed at the end of the intraerythrocytic life cycle[14], our observations showed that even trophozoites that do not express *Pf*PKG were affected by UA2239. This can be explained by the possibility that UA2239 enters the iRBCs then the parasite but is unable to exit. Then, once *Pf*PKG is expressed at the schizont stage, UA2239 exerts its effect by binding to *Pf*PKG and inhibiting its activation.

All these results are included in a manuscript to be submitted for publication.

Material & Methods

Cell Biological Methods

1. Thawing of *P. falciparum* Parasites

The cryotube containing the culture is thawed rapidly in a water bath at 37°C, and the culture transferred to a 15 mL falcon tube. For 1 ml of culture, 200 µL of sterile 12% NaCl is added and the tube is swirled gently and incubated for 5 min at room temperature. Afterwards, 9 mL of sterile 1.6% NaCl is added drop by drop while swirling. The culture is incubated for an additional 5 min and then centrifuged (1 200 g for 5 min). The supernatant is discarded and the pellet is resuspended in 12 mL of complete media containing 600 µL of packed cell volume (PCV) of RBCs and transferred into a petri dish for cultivation. The parasitemia is followed on a daily basis through blood smears.

2. Freezing of *P. falciparum* Parasites

To store *P. falciparum* cultures, a culture containing mainly ring stages with a parasitemia of at least 1% for transfected strains, and 5% for normal strains is transferred into a 15 mL falcon tube. The culture is then centrifuged (1 200 rpm for 5 min) and the supernatant is discarded. For each 1 mL of PCV, first 400 µL, then 1.2 mL and finally 2.4 mL of freezing solution (6.2 M Glycerol, 0.14 M sodium lactate, 0.5 mM KCl in PBS) is added drop by drop while gently swirling the tube, and each time the mixed solution is incubated for 5 min at room temperature. Subsequently, 1mL of the prepared culture is transferred into cryotubes, which are stored at -80°C or in liquid nitrogen.

3. *P. falciparum* Culture

The blood stages of *Plasmodium falciparum* 3D7 (MRA-102 from MR4, BEI Resources), and generated transgenic lines are cultured in human RBCs (*h*RBCs) at 5% hematocrit. The complete culture medium is constituted of RPMI 1640 containing HEPES and Glutamine (Gibco Life Technologies, #52400), supplemented with 10% of human serum and 25µg/mL of gentamicin (Sigma). Cultures are maintained at 37°C under a controlled tri-gas atmosphere: 5%O_2, 5%CO_2 and 90% N_2. Parasitemia is determined after Giemsa staining of thin blood smears. Cultures are generally diluted twice a week. Total human blood is obtained from the local blood bank (Etablissement Français du Sang, approval number 21PLER2016-0103). The *h*RBCs are washed RPMI three times before use.

4. *P. falciparum* Synchronization

i. 70%-Percoll Synchronization

Mixed stage cultures of at least 5% parasitemia are collected by centrifugation (1 200 rpm, 5 min). The supernatant is discarded and the cells resuspended in 5 mL of media, which are then used to carefully drop by drop overlay a cushion of 5 mL of 70%-percoll. The gradient is then centrifuged at 2 600 rpm for 11 min with low acceleration and low brake. The schizonts have a lower density then the less mature parasites due to hemoglobin digestion[253]. As a result, after centrifugation schizonts will remain on the surface of the percoll solution whereas all the other stages and uninfected RBCs are in the pellet. The ring formed at the boundary between the RPMI and Percoll containing the mature forms is collected, washed once with RPMI, and returned to culture with 12mL of complete media and 600 µL of PCV.

ii. 5%-Sorbitol Synchronization

Sorbitol synchronization takes advantage of the fact that *Plasmodium* establishes the NPPs in the infected erythrocyte. These channels allow the import of various low-molecular-weight metabolites, including sorbitol. Treatment of the culture with sorbitol induces selective osmotic lysis of stages that possess these NPPs (starting from the trophozoite stage), while younger stages (rings) and uninfected RBCs are not affected[254]. To perform sorbitol synchronization, the culture is resuspended, and transferred to a 15 mL falcon tube. The culture is centrifuged at 1 200 rpm for 5 min. The supernatant is discarded, and the pellet is resuspended in 10 ml of 5% sorbitol solution in H_2O. The mixture is incubated for 10 min at 37°C. Then, cells are collected by centrifugation (1200 rpm, 5 min), washed once in complete medium, before being resuspended in complete medium and returned to culture. For achieving a tight synchronization window of 3 hours, late stage parasites are first isolated by Percoll synchronization, allowed to reinvade RBCs over the next 3 hours, before remaining late stage parasites are removed by sorbitol synchronization.

5. Ring-Stage Survival Assay

Artemisinin (ART) resistance is characterized by its selective effect on the ring stage. The measurement of ART resistance *in vitro* is done through the ring-stage survival assay (RSA)[255]. Parasites were synchronized using 70%-percoll, and cultured for 3 h with fresh erythrocytes.

Then, cultures were treated with 5%-sorbitol to eliminate remaining schizonts and only keep 0-3 hpi rings. Cultures were diluted to 0.5 to 1% parasitemia and 2% hematocrit. Parasites were exposed to 0.01% of DMSO (control) or to 700 nM DHA for 6h in 24-well plate, with two technical duplicates for each condition. At the end of the incubation period, the supernatant was removed, the cultures were washed twice with 9 mL of RPMI and finally they were resuspended in 2mL of fresh media in a newly 24 well plate at 37°C in a tri-gas atmosphere. Culture medium was changed every day and blood smears were realized 66 h after drug removal. Parasitemia was determined by microscopy and at least 10000 cells were counted. The percentage of survival is calculated using the following equation:

$$\%\ of\ survival = \left(\frac{DHA}{UT}\right) x\ 100$$

DHA: Parasitemia of the treated culture at 72 h.

NE: Parasitemia of the untreated culture at 72 h.

If the % of survival is above 1%, the strain is considered resistant, whereas a percentage of survival below 1% is an indication of sensitivity to ART.

The positive strain used during this assay was generously given to us by Jose-Juan Lopez Rubio. It presents an NF54 *P. falciparum* with the C580Y substitution in the kelch 13 gene. The rest if the strains are all 3D7.

6. Flow Cytometry

Flow cytometry was used to analyze the DNA content during the cell cycle of both the UA2239-treated and untreated synchronized cultures. Before conducting the flow cytometry experiment, the parasites underwent tight synchronization with a 2 h re-invasion window. The parasites were then either treated with 2 µM of UA2239 or left untreated as a control. At intervals of 6 h over a period of 72 h, infected erythrocytes from both the treated and untreated cultures, were transferred into a 1.5 mL Eppendorf tube and fixed in 4% paraformaldehyde (PFA) for 4 hours at room temperature. The fixed cultures were then stored at 4°C until all the desired time points were collected. Once all the time points were obtained, the fixed cells were washed twice with phosphate-buffered saline (PBS) and stained with 3.3X SYBR Green (Invitrogen) for 30 minutes.

After staining, the tubes were centrifuged, and the supernatant was discarded. The pellet containing the stained cells was resuspended in 900 µL of 1X PBS. The analysis of the samples was performed using Becton Dickinson canto 1, with the Diva software. SYBR Green, which was excited by a blue laser at 488 nm, emitted fluorescence that was detected using a 530/30 nm filter.

7. Immunofluorescence Assay

Immunofluorescence assays (IFAs) were performed on smears of infected RBCs. The smears were fixed with 4% PAF/PBS for 30 min, followed by 4 min of quenching with 0.1 M of glycine/PBS. Cells were then permeabilized with 0.1% Triton/PBS for 5 min. Following this, slides were incubated for 30 min with 1.5% of bovine serum albumin (BSA)/PBS solution to block unspecific binding. Afterwards the primary anti-bodies were added and the slide was incubated for an hour. In case the antibodies were not conjugated, the slide was washed 3 times with 1X PBS, and a secondary antibody (Alexa-488 conjugated secondary antibodies) was added and incubated for an additional hour. Nuclei were stained with Hoechst (1/ 10000). Images were taken on the Leica Thunder microscope at the Montpellier MRI imaging facility. Images were processed by Fiji software for sectioning and contrast adjustment.

8. Transfection

Identified SNPs in *Pf*PKG found in the resistant strain through WGS, were introduced into the sequence of 3D7 *Pf*PKG WT, a strain that was never in contact with UA2239. Two different approaches for transfection were employed.

A. Transfection by Direct Electroporation.

Transfection by direct electroporation was performed as previously described[256]. Briefly, 75 µg each of pBluescript and pDC2-cas9-sgRNA-*h*DHFR DNA were precipitated with ethanol and were resuspended in 30 µL of TE buffer (10 mM Tris pH 8, 1mM EDTA). Cultures containing 5-10% ring stages were centrifuged and 100µL of packed cells were used per transfection. The cells were resuspended with the DNA mix and 270 µL of cytomix (120 mM KCl, 0.2 mM $CaCl_2$, 2 mM EGTA, 10 mM $MgCl_2$, 25 mM HEPES, 5 mM K_2HPO_4, 5 mM KH_2PO_4; pH 7.6). The cells were transferred into a 2mm electroporation cuvettes (Bio-rad) and electroporated using the GENEPULSER XCELL from Bio-rad (0.31 kV and 0.950 µF). Transfected parasites were selected with WR99210 used at 2.5 nM starting 5 h after the transfection. Media and drugs were

renewed every 24h for the first 5 days, thereafter drug selection was stopped and media was renewed 3 times a week. The transgenic parasites were grown in agitation until parasites were detected by a smear.

B. Transfection by Invasion of DNA-Loaded Erythrocytes.

We attempted to introduce the *Pf*PKG D597Y mutation using the above described transfection method but we were unsuccessful. As an alternative approach, we applied the transfection method of parasite invasion of DNA-loaded erythrocytes[257]. In this method, uninfected RBCs (150 µL) were washed with RPMI and mixed with the DNA preparation in TE buffer (30 µL) and cytomix solution (270 µL). 100 µg of each plasmid, pDC2-cas9-sgRNA-*h*DHFR and pBluescript, was used. The mixture was then electroporated using a Bio-Rad Gene Pulser using the same parameters as the previous transfection (310 V, 950 µF). After electroporation, the solution was washed once with complete media. The transfected erythrocytes were subsequently resuspended with schizonts in sort to have a final parasitemia of 0.5%, at 5% hematocrit. The parasites were maintained on the shaker. Drug pressure was applied 36 h post-transfection. The media with 2.5nM of WE99210 was changed daily for the first 5 days of culture. Afterwards, the drug selection was stopped and media was changed three times a week.

9. *In vitro* Drug Sensitivity Assay

These assay were based on a modified Desjardins tested[258]. The assay allows us to determine the IC_{50}, which is the concentration of the drug required to inhibit 50% of parasite growth by quantifying the incorporation of radioactive hypoxanthine (^{3}H-hypoxanthine) into the parasite nucleic acids. The assay was conducted in a 96 well plate. Wells in the columns 1, 6 and 11 served as negative controls and did not contain any drugs, while wells in column 12 served as a background noise and contained only RBCs. The assay was performed using a mixed culture of *P. falciparum* with a parasitemia of 0.6% and a hematocrit of 2.5%. A volume of 150 µL of the *P. falciparum* culture was added to each well containing 50 µl of serial dilutions of the drugs (1/3 dilution). The parasites were then incubated with the drugs for 48 h, after which ^{3}H-hypoxanthine (0.5 µCi per well) was added to the wells for an additional 24 hours.

Subsequently, the plates were frozen at -80°C to stop the integration of radioactive hypoxanthine. Cells were lysed by thawing and the DNA of the parasite was recovered by

harvesting the lysate on glass-fiber filter plates (Unifilter 96 GF/C; Perkin-Elmer) using a FilterMate cell harvester (Packard Instruments), and the radioactivity was counted on a microplate scintillation counter (Microbeta 2, Perkin Elmer).

10. Isobologram

An isobologram assay is a pharmacological method used to assess the interaction between two or more drugs or compounds when administrated together. It can determine whether the combined effect the drugs is synergistic, additive, or antagonistic (more information are found in the result section)..

For this purpose, the antimalarial activity of UA2239 was determined in the presence of various compounds added at concentrations lower than their IC_{50}. The IC_{50} of each compound alone is also determined. In these experiments, compound concentrations were expressed as a fraction of the IC_{50}s of the compounds alone. These fractions were called fractional 50% inhibitory concentrations (FIC_{50}). The sum of FIC_{50}s drug A and drug B were noted as (ΣFIC_{50}). Isobolograms were constructed from the FIC_{50}s of drug A and drug B at the tested fixed concentration ratios, for which a straight line represents additivity ($\Sigma FIC_{50} = 1$), a concave line denotes a trend toward synergy ($\Sigma FIC_{50} < 1$) or synergy ($\Sigma FIC_{50} \leq 0.5$), and a convex curve represents independence or a trend toward antagonism ($\Sigma FIC_{50} > 1$ and <2) or antagonism ($\Sigma FIC_{50} \geq 2$)[249]. In all experiments, UA2239 had always been serial diluted (1/3 dilution) and the other compounds were added at several fixed concentrations.

11. Stage Specificity Assay

In order to assess the effect of UA2239 on the different blood stages of *P. falciparum*, the drug was added at various concentrations to a tightly synchronized culture (0-3 h window) at 0.6% parasitemia and 2% hematocrit, at ring (6 h), trophozoite (24 h) and schizont (36 h) stages. After 6 h of incubation, cells were washed twice to remove the drug and resuspended in fresh culture medium. At 52 h, radioactive hypoxanthine was added, and the cultures were further incubated for 24 h. The IC_{50} value was determined following the same procedure as in the drug sensitivity assay.

12.Time Course Assay

The time course assay assists in determining the minimum duration of drug exposure necessary to achieve the desired therapeutic outcome. For this assay, UA2239 was added at

750 nM to 0-3 h synchronized cultures at the trophozoite (24 h), or schizont (36 h) stages. After incubation of each parasite stage for various time periods (30 min, 1h, 2h, 3h, 4h and 6h), cells were washed twice and resuspended in fresh complete medium. To assess the impact of the drug on parasite viability, ^{3}H-hypoxanthine was added at 52 h and incubated for an additional 24h. Cell viability was assessed following the procedure for the drug sensitivity assay.

13. Activity of *Plasmodium berghei* on Male Gametocyte Exflagellation

The activity of UA2239 on male gametocyte exflagellation of was performed on female NMRI mice infected with *P. berghei* at a parasitemia of 15 - 30%. A drop of blood was taken from the tip of the mouse tail and put between a slide and a coverslip. After 10 min at 20°C, exflagellation centers were counted under microscope and the number of exflagellations per 10000 cells were determined as a control. This is repeated at least twice. Then, the mouse was treated with a dose of UA2239 by intraperitoneal administration. After 30 min., one drop of blood was taken from the tip of the mouse tail and put between slide and coverslip and exflagellation centers were counted after 10 min at 20°C. Activity of UA2239 is expressed as the number of exflagellation centers/10,000 cells as a percentage of control.

Molecular Biology

1. Insertion of the Sequence of Interest into pBluescript

A. *P. falciparum* cGMP-dependent Protein Kinase G

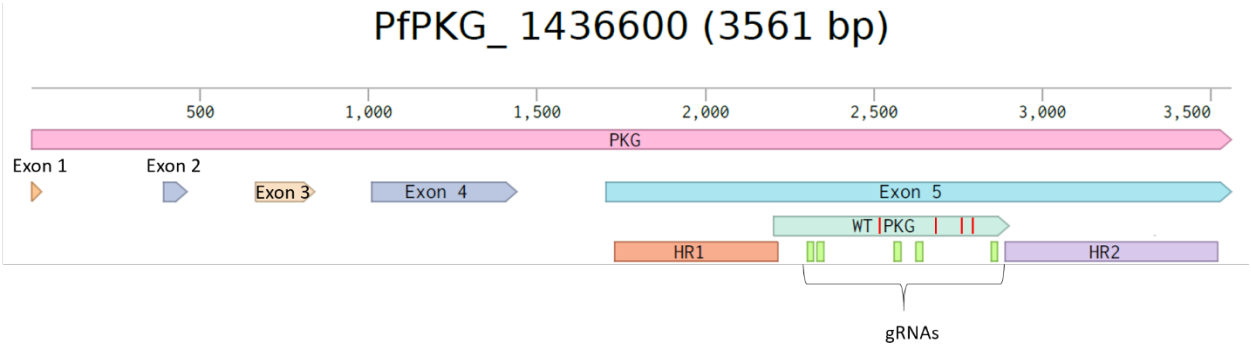

Fig. 47. The genomic locus of the *P. falciparum* 3D7 PKG. *Pf*PKG_1436600 represents the gene ID of *Pf*PKG as found in PlasmoDB (https://plasmodb.org/plasmo/app). *Pf*PKG is a 3561 bp sequence, consisting of 5 exons. All identified mutations in the *Pf*PKG UA2239 resistant clones are located in Exon 5. The CRISPR-Cas9 tool construct consisted of two homology regions HR1 (510 bp) and HR2 (658 bp); and the gene of interest, WT PKG. the sequence of the WT PKG will be re-codonized using *E. coli,* to create the sequences of interest. The red lines located in the WT PKG sequence represent the SNPs responsible for the mutations in the protein sequence: R420I, H524 N/ Y, D597Y and T618Q. The last mutation was reported to cause resistance to C2, a PKG inhibitor[238]. The green rectangles underneath the WT PKG sequence represents the location of the gRNA obtained from Chopchop (https://chopchop.cbu.uib.no/).

The *Pf*3D7 PKG locus consists of 5 exons and 4 introns, spanning a region of 3561 base pairs (bp) and encodes for a 853 amino acid (aa) long protein. The mutations identified in the resistant strains by the WGS are all located in exon 5. For the construction of the pBluescript plasmid, the homology region 1 (HR1) spanning from base 1705 to 2214. HR1 was amplified using the following primers:

- 721: tatagggcgaattggagctc ACTGTATGATGAACCAAGAAGTGC
- 722: taattttctgat ATCAATAGATGCATCAATATTATTATTTCC.

The lowercase letters in the primers represent the overlap with the plasmid (primer 721) and with the homology region 2 (HR2) (primer 722).

HR2 spanned from base 2887 to 3544. The primers to amplify HR2 were:

- 723: gcatctattgat atcAGAAAATTAGGTTTATTATCTAAATCACAAGC
- 724: agggaacaaaagctggtacc CCTCATCATCCTCAGCATCC.

In this case the lowercases letters represent an overlap with HR1 (primer 723), and with the pBluescript plasmid (primer 724).

The pBluescript plasmid was digested and linearized using KpnI-HF and SacI-HF restriction enzymes. An In-fusion kit was then used to fuse the linearized pBluescript with HR1 and HR2 **(Fig. 48.A)**. The fusion of HR1 and HR2 created an EcoRV restriction site, which was used to linearize the pBluescript and fuse the different optimized *E. coli* codon of *Pf*pkg construct, *Pf*ePKG, through another In-fusion reaction **(Fig. 48.B)**.

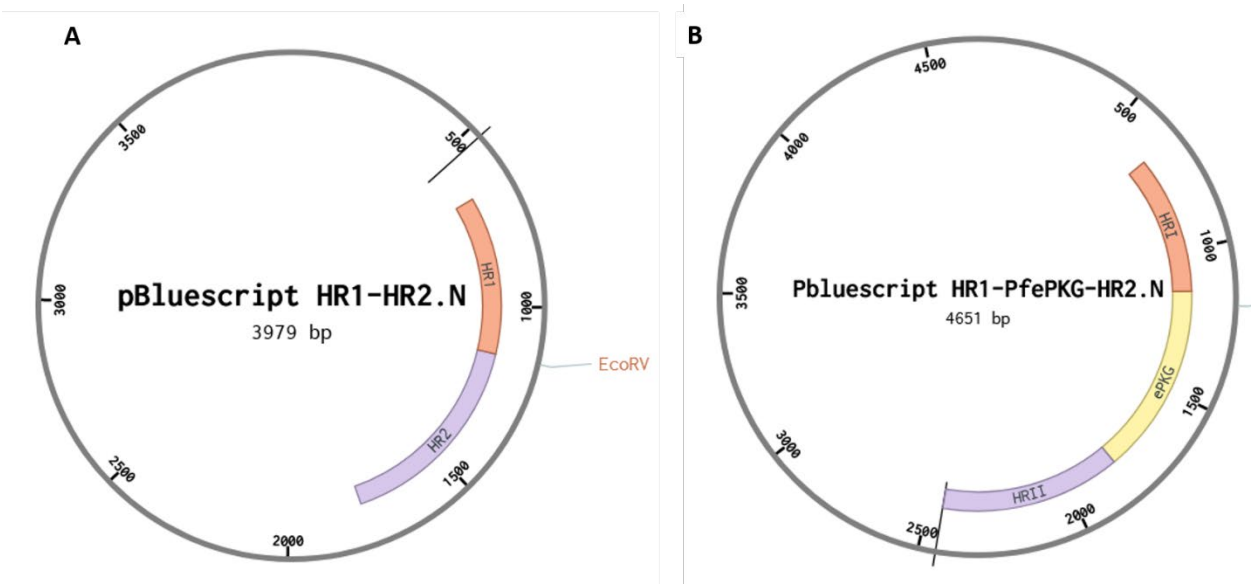

Fig. 48. Preparing the pBluescript containing the donor *Pf*PKG DNA. A) Schematic representation of the pBluescript plasmid containing *Pf*PKG HR1, HR2, and EcoRV restriction site that was used for the cloning of the *Pf*PKG constructs. **B)** Schematic representation of the pBluescript plasmid containing HR1-*Pf*ePKG-HR2.

The *E. coli* codonized sequence of interest of *Pf*PKG (*Pf*ePKG) is 672 bp long. It is important to note that between the original genomic sequence of *Pf*PKG-WT and *Pf*ePKG-WT, many synonymous mutations were inserted **(Fig. 49)**. This was done to facilitate the generation of the 6 transgenic parasite lines by using the same donor-DNA construct that varies only in the one codon position that generates (or not) the desired point mutation. In addition, it provides a large number of potential guide RNA sequences. The construct termed *Pf*ePKG-WT thus encodes exactly the same amino acid sequence as the genomic *Pf*pkg gene but varies in the codon usage of the 672 bp region in exon 5 covering the identified mutations in *Pf*PKG. This transgenic line was used as a control for several experiments alongside *Pf*3D7 wild-type strain. The sequences for the different constructs can be found in the annex.

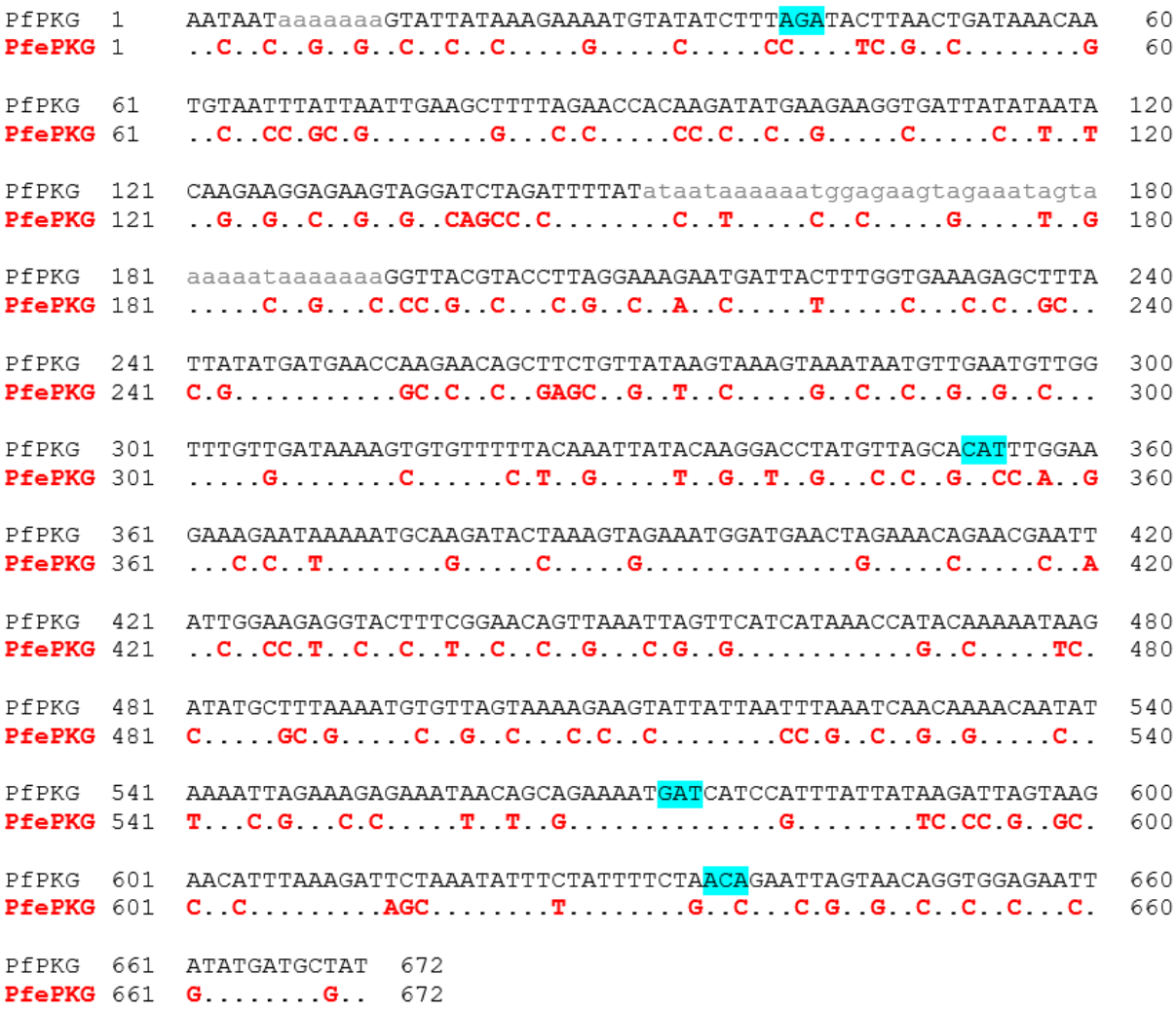

Fig. 49. Alignment of *Pf*PKG and *Pf*ePKG wild type sequences aligned. The red bases in *Pf*ePKG represent the synonymous mutation we introduced into this sequence of interest. The blue highlighted bases represent the location of the non-synonymous mutation found through the WGS.

B. *P. falciparum* Phosphodiesterase-β into pBluescript

The genomic DNA of the *Pf*3D7 PDE locus is 4677 bp long and consists of 9 exons and 8 introns and encodes for a 1139 aa long protein. The mutation identified the 13th clone is located in exon 1. For the construction of the pBluescript plasmid, HR1 spanned from base 958 to 1512, was amplified using the following primers:

- 760: tatagggcgaattggagctcCGTTCATCTAGAAAATCATTAGG
- 761: aaagaatatgtcGACCATTAAAGAGAAAAGTACATAAGAC.

The lowercase letters in the primers represent acyclic nucleosides that overlap with the plasmid (primer 760) and with the HR2 (primer 761).

HR2 spanned from base 1163 to 2165, and the primers used to amplify HR2 were:

- 762: tctttaatggtcGACATATTCTTTCCCTCACGG
- 763: agggaacaaaagctggtaccctacAAGTAAATTATAAAAAACATAACG

In this case the lowercases letters represent an overlap with HR1 (primer 762), and with the pBluescript plasmid (primer 763).

The pBluescript plasmid was digested and linearized using KpnI-HF and SacI-HF restriction enzymes. An In-fusion kit was then used to fuse the linearized pBluescript with HR1 and HR2 **(Fig. 50.A)**. The fusion of HR1 and HR2 created an HincII restriction site, which was used to linearize the pBluescript and fuse the gene sequence of interest (150 bp) through another In-fusion reaction **(Fig. 50.B)**. The sequences for these constructs can be found in the annex.

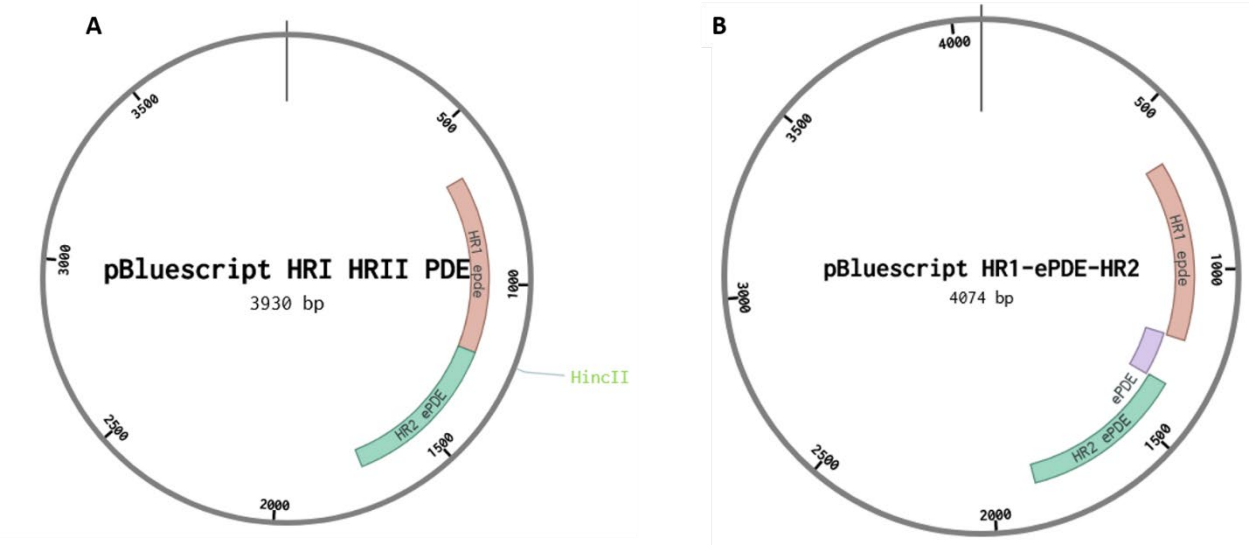

Fig. 50. Preparing the pBluescript containing the donor DNA for *Pf*ePDEß. A) Schematic representation of the pBluescript plasmid containing *Pf*PDE HR1, HR2, and HincII restriction site that was used for the cloning of the *Pf*ePDE constructs. **B)** Schematic representation of the pBluescript plasmid containing HR1-*Pf*ePKG-HR2.

To increase the number of gRNA's we followed the same procedure as the *Pf*ePKG. The *Pf*ePDE sequence of interest consisted of 150 bp that was *E. coli* codonized **(Fig. 51)**.

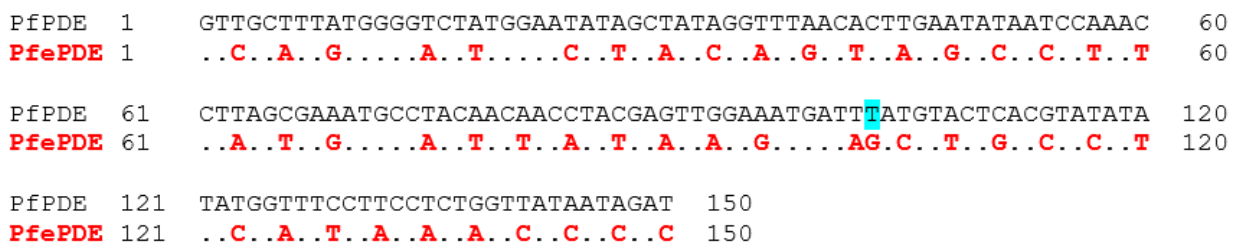

Fig. 51. Alignment of *Pf*PPDEß and *Pf*ePDEß wild type sequences aligned. The red bases in *Pf*ePDE represent the synonymous mutation we introduced into this sequence of interest. The blue highlighted base represent the location of the non-synonymous mutation found through the WGS.

2. Insertion of the Guide RNA in the pDC2-cas9-sgRNA-*h*DHFR Plasmid

This plasmid contains three key components: the Cas9 enzyme driven by the calmodulin promoter, the single guide RNA (sgRNA) insertion site, and the selectable marker human dihydrofolate reductase (*h*DHFR) conferring resistance to WR99210[257] **(Fig. 52.A)**. In an aim to insert the gRNA, the plasmid was digested with the restriction enzyme BbsI, which cuts in two restriction sites, and allows a traceless cloning. This digestion generated overhangs that would be complementary to the gRNA sequence.

The gRNA primers that were chosen from CHOPCHOP site, consisted of a forward and a complementary strand, that were annealed together. The annealing solution had a final volume of 10 µL. It contained 1 µL of both the forward and reverse primers at 100 µM, 1 µL of 10X Ligation Buffer (NEB), 0.5 µL of T4 PNK (NEB) and 6.5 µL of distilled water. The overhangs of the primers allow the that overlap with the digested pDC2. The annealing of the gRNA to the digested plasmid, involved pre-warming the solution at 37°C for 30 min, followed up by heating it up to 95°C for 5 min and then slowly cooling it down (5°C/min) until it reached 25°C. Once they were ready the gRNA primers were ligated using the T4 ligase enzyme. The gRNA expression was driven by the U6 RNA polymerase III promoter. The resulting construct was transformed into DH5α bacteria, which were then spread on LB agar plates containing ampicillin for selection. Colony PCRs were conducted using the forward primer of the gRNAs and PG51. Positive colonies had their plasmid extracted and sent to make sure of their sequence **(Fig. 52.B)**. The plasmids with no mutations were used for transfection.

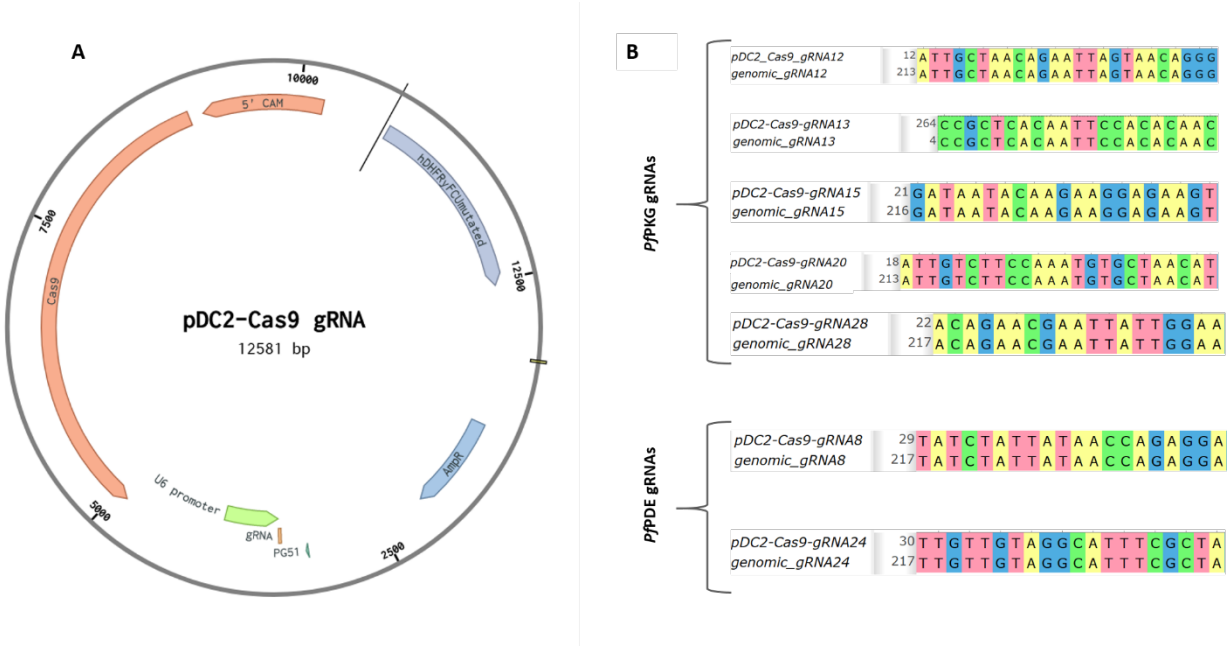

Fig. 52. Constructing the pDC2-Cas9-gRNA plasmid for *Pf*PKG. A) Schematic representation of the pDC2-Cas9-gRNA plasmid. **B)** Alignment of the sequence of genomic gRNAs picked from CHOPCOP with their sequenced gRNA inserted into the pDC2 plasmid using Unipro.

C. Colony Screening- PCR1

In an aim to make sure of the integration of the DNA sequence of interest, after every bacterial transformation, colonies were tested by PCR and the positive colonies were sent to validate their sequence through sequencing.

In fact, single colonies that grew over night were picked with a tip and cloned into another petri dish. The tip was then added to a PCR tube containing 20 µL of distilled water. The tube was heated up to 95ºC for 2 min. This will cause the lysis of the bacteria cell walls and the release of the DNA. From the previous solution 2 µL were taken and added to 10 µL of GoTaq 2x master mix, containing the specific primers. The plasmids were used once we made sure of the absence of undesired mutations in their sequence.

D. Analysis of Transgenic Parasites- PCR2

The genomic DNAs were isolated from 200 µL of PCV using the QIAamp DNA blood kits (Qiagen). These genomic DNA were used for genotyping to evaluate the incorporation of the gene bloc into the target locus. Based on the CRISPR-Cas9 system, after the site specific DNA was cleaved by Cas9 endonuclease, the cleaved target locus was then repaired by homology recombination through HR1 and HR2 flanking the gene bloc, causing its integration.

Therefore, the primer for the diagnostic PCR of the 5' and 3' integrations were generated by designing the outer primers as being only in genomic DNA specific without including any of the HR sequence to avoid amplifying the plasmid. The inner primers were in the *E. coli* codonized construct. Ideally, the diagnostic primers are expected to amplify only the integrated mutant-specific sequences, whereas the WT parasites and the episomal mutant parasites are expected to produce no product. A control using specific primers for the WT was also done.

For genotyping, the PCR reactions were performed in a 20 µL mixture reaction, containing 5 – 10 ng of DNA, 10 pmol/ µL of forward and reverse primers, 10 µL of GoTaq 2x master mix and the final volume was adjusted with sterile water. The PCR reaction was performed for 30 cycles.

E. Quantitative PCR

DNA extraction was performed using the DNA blood extraction kit (know the mark of the kit). The primers designed for this experiment were carefully checked to ensure their specificity and to avoid any cross-reactivity between the two strains. Primers 849-752 were specific for *Pf*ePKG, and 852-854 were specific for *Pf*PKG.

For quantifying *Pf*PKG WT and *Pfe*PKGs, the LightCycler 480 Sybr Green I system (Roche) was employed. In order to determine the precise amplification efficiency for each gene, standard curves were generated. The lightCycler 480 Software, Version 1.5 was used for "absolute fit point" data analysis.

NB: A list containing all the primers used during this thesis can be found in the annex.

Conclusion & Discussion

1. Exploring the Mechanism of Action of UA2239

The major part of this thesis manuscript presented a comprehensive understanding of the mechanism of action and resistance patterns associated with UA2239. Deciphering the mechanism of action of a drug helps us identify the specific target that UA2239 interacts with in *Plasmodium*. In pursuit of this aim, we were also able to understand the resistance patterns associated with UA2239, which led us to gain insights into the mechanisms that allow parasites to evade the drug's effect. This knowledge can inform the development of strategies to overcome or prevent resistance.

In order to advance towards these objectives, our primary aim was to determine the target of UA2239. This involved a systematic approach, beginning with the generation of resistant strains to the drug. Subsequently, we performed whole-genome sequencing on these strains and carefully analyzed the resulting mutations. The analysis of the mutations revealed that 12 out of the 13 sequenced clones exhibited a SNP in *Pf*PKG. Each clone presented an individual SNP in their *Pf*pkg sequence causing one of these 4 following mutations: R420I, H524N/Y and D597Y. The structural similarity between UA2239 and cGMP, the sole known activator of *Pf*PKG, provides strong support for the interaction between this compound and *Pf*PKG. Moreover, considering the critical role played by *Pf*PKG in the egress pathway, the correlation between *Pf*PKG inhibition and the observed phenotypic response to UA2239 was reinforced.

To validate this discovery, our next step was to deliberately introduce the specific individual mutations into the *Pf*pkg sequence of a 3D7 WT strain to check if these mutations can generate UA2239-transgenic resistant strains. Once transgenic strains were obtained, they were cloned and their sensitivity towards UA2239 was checked. All transgenic strains carrying the individual mutations exhibited at least a five-fold increase in the IC_{50} compared to the wild-type strain. The successful generation of UA2239-resistant strains through site-directed mutagenesis further confirms the role of *Pf*PKG as the primary target of UA2239.

The discovery of UA2239's activity on a kinase enzyme represents a breakthrough in our understanding of ANPs. Traditionally, ANPs were primarily described as targeting the DNA synthesis pathway[259–261]. However, this study demonstrates, for the first time, the activity of an ANP on a kinase.

In addition, the genetic manipulation employed in this study proved to be a valuable tool for investigating the relationship between *Pf*PKG and UA2239 resistance, enabling more focused exploration of the underlying molecular mechanisms. The current hypothesis regarding the molecular mechanism of action suggests that UA2239 functions as an antagonist of cGMP. It is worth noting that the mutations responsible for conferring resistance to UA2239 are not located in the region where cGMP binds to *Pf*PKG's CNB-D domain. Indeed, the binding of cGMP to the CNB-D domain involves a triad of amino acids: R484, Q532, and D533 in *Pf*PKG[231]. Mutations of any of these residues can therefore alter the affinity for cGMP, potentially leading to detrimental effects on the parasite.

Following the previous statement, Henry David Thoreau*,* a well-known philosopher described the rule of the world as "*You never gain something but that you lose something*". This principle holds true in the microbial world as well. In the case of resistance to UA2239, the parasite may have gained resistance but at the cost of its fitness. The identified SNPs in UA2239-resistant strains, particularly the D597Y mutation, have shown significant implications. Although this mutation does not confer the highest or lowest resistance, it imposes a substantial fitness cost on the parasites, severely impairing their growth. The transgenic parasites carrying this mutation exhibited an abnormal replication rate, which was approximately fourfold lower compared to normal replication rates.

On the other hand, the impact of the other mutations on the fitness cost, albeit not as pronounced as the D597Y was confirmed through growth competition assays. These assays provided direct evidence that the 3D7 WT outcompete the UA2239-resistant strains. This again highlights the delicate balance between drug resistance and overall fitness of the parasites[262,263]. While the parasites may acquire resistance to UA2239, their survival and growth are compromised, emphasizing the potential limitations of resistance to UA2239 as a long-term survival strategy for the parasites.

The fitness cost due to the mutations of these three residues can be linked to their importance in the protein conformational stability. The x-ray 3D structure of *Pf*PKG shows that the three amino acids which were mutated and conferred resistance to UA2239 are located at the interface between the CNB-D domain and the catalytic domain **(Fig. 53.A-B)**.

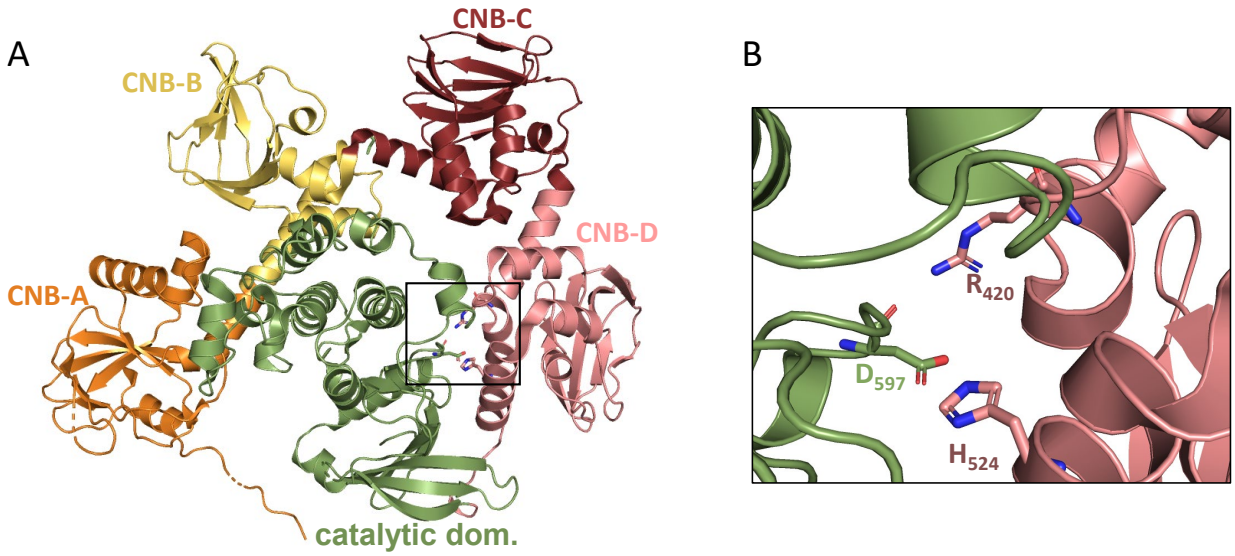

Fig. 53. X-ray 3D structure of *Pf*PKG (M El Bakkouri *et al*, 2019)[231]. A) 3D structure of the full length *mor*PKG with, from the N-terminal to the C-terminal ends of the protein: the four regulatory domain, CNB-A, CNB-B, CNB-C, CNB-D (pink) and the catalytic domain (green). **B)** Close view of the interface between the CNB-D and the catalytic domain showing the amino acids mutated in the resistant strains.

*Pf*PKG CNB-D has been shown in previous studies to have the strongest influence on the protein activation[187]. The latter domain makes multiple contacts with the catalytic domain of *Pf*PKG. In the apo-state of the protein, two intramolecular interactions caught our attention. The first one is a salt bridge between R528 and **D597**[264]. The second interaction is π-stacking between **H524** and R809[264]. These bonds have been described to play crucial role in the conformational stability of the inactivated protein state[264].

Binding of cGMP to *Pf*PKG CNB-D causes conformational changes, where R528 switches to interacting with Y480, causing the stabilization of the protein in the activated state[264] **(Fig. 54).**

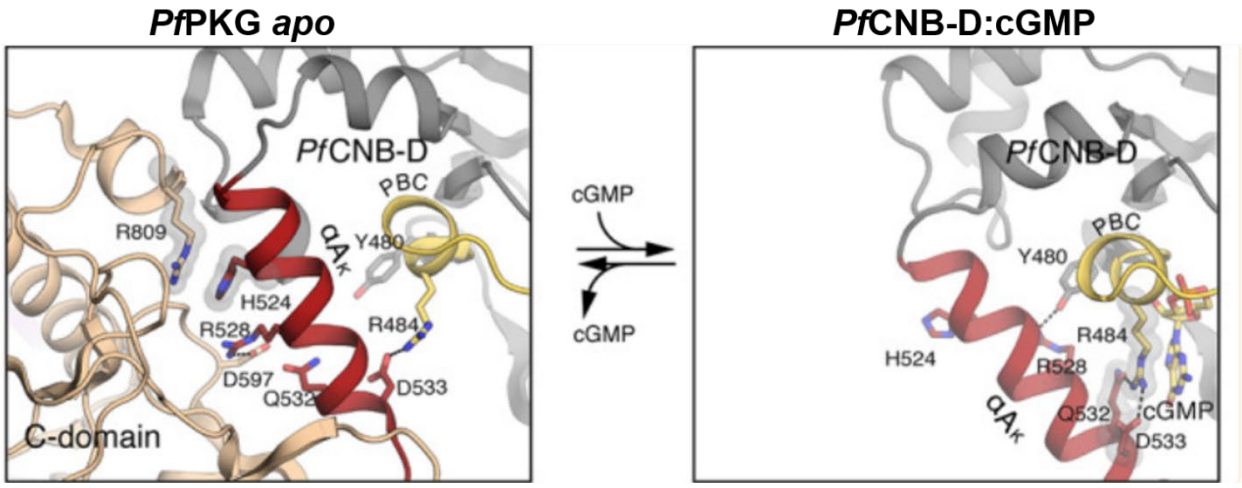

Fig. 54. *Pf*PKG conformational changes upon cGMP binding in the CNB-D domain of *Pf*PKG (Choel Kim *et al* 2021)[265].

To investigate the impact of *Pf*PKG D597 residue, a previous study introduced the D597N mutation into *Pf*PKG recombinant protein. While this mutation didn't show any binding effect on cGMP affinity, nor on its activity, it resulted in a 3 fold decrease in the activation constant[264], indicating that mutating this amino acid causes a destabilization of the inactivated state of *Pf*PKG. Similarly, *Pf*PKG H524A mutation was generated, this mutation also caused a destabilization in the protein[231]. We hypothesize that the mutations obtained in the resistant strains, cause the same significant destabilization of inactivated form of *Pf*PKG, rendering the kinase "more sensitive to activation". To validate this hypothesis, current work on the recombinant protein is being investigated. Recently, we obtained a recombinant protein encompassing the CNB-D domain and the catalytic domain of *Pf*PKG and showed that this construct is active and inhibited by UA2239. Future work will aim at deciphering the mechanism of action of the drug at the molecular level by solving the 3D structures of the WT *Pf*PKG and mutated *Pf*PKG in presence of UA2239.

We investigated the presence of these mutations in the reported sequences of published WGS field parasites, and they were absent in all of them. Highlighting that these mutations do not easily happen, and a resistance to UA2239 in the future human trials would not be as easy as the *in vitro* generation of resistance.

The 13th UA2239 resistant clone, lacked a mutation in its *Pf*pkg sequence. Nevertheless, we identified a mutation in *Pf*pdeβ. This protein, as shown before, is important in the

Plasmodium enzyme cascade pathway during egress. Indeed, *Pf*PDE plays a role in the regulation of the cGMP concentration in the parasite by hydrolyzing cGMP into GMP. The implication of *Pf*PDEβ in resistance to UA2239 adds an additional layer of complexity to the resistance mechanisms. However, it is important to note that *Pf*PDEβ is not considered as the primary target of UA2239, because it does not match the phenotype observed. In fact, an inhibition of *Pf*PDEβ affects the invasion rate and interferes with early ring stage development[220], which contrasts with the observed blockage of parasite egress. Here, we could hypothesize that the *Pf*PDE mutation obtained in the resistant parasite will render the protein less active and thus, result in an increase in cGMP concentration. Further studies are required to gain a deeper understanding of the direct effect of this mutation on resistance against UA2239 and its implications for the overall resistance landscape.

2. Pharmacological Properties of UA2239

Compound UA2239 exhibited interesting phenotypic properties. An interesting property of UA2239 is despite being a charged compound, it is able to enter cells and inhibit egress. The general expectation for such compounds is low membrane permeability[266]. This observation led us to speculate that UA2239 enters the iRBCs through the NPPs. Our suspicions were confirmed when we demonstrated that inhibiting the NPPs resulted in antagonistic effect for UA2239 activity. The entry of antimalarial compounds through the NPPs has been previously reported in the asexual intraerythrocytic cycle[267] and more recently in the sexual intraerythrocytic stages[252]. This finding provides an explanation for the efficacy of UA2239 on *P. berghei* gametocytes. The entry of the compounds through the NPPs enhances the specificity towards iRBCs, therefore minimizing the possible toxic effects.

UA2239 treated parasites develop normally until the schizont stages, then the cycle stops. UA2239 showed similar effect on both trophozoites and schizonts stages of the intraerythrocytic cycle within a similar range of IC_{50}. This compound has also been shown to inhibit the male gametocyte activation of *P. berghei* enabling by this, *Plasmodium* transmission. In addition, *Pf*PKG has been shown to be essential for sporozoites motility and invasion of the hepatocytes, it is also essential for the merozoites egress from the hepatocytes[245], consequently it is suspected that UA2239, is also probably effective on the hepatic stages[240]. A collaboration with Dominique Mazier and Valérie Soulard group at the

CIMI, is currently on-going to assess this previous statement.

The profile of UA2239 makes it highly desirable for the development of new antimalarial drugs, as it mainly targets *Pf*PKG, a protein essential during all the parasite life cycle. If UA2239 is also effective against hepatocytic stages, it would possess all of the promising properties of *Pf*PKG inhibitors described previously[235,238,240,268], along with additional advantages. Unlike other *Pf*PKG inhibitors that primarily target schizonts, and show a reversible effect[238], UA2239 demonstrates its irreversible effect on both trophozoites and schizonts. Indeed, incubating the culture with 750 nM of UA2239 for 6 and 2 h at trophozoite and schizont stage, respectively, blocks the parasite at egress step thereby disrupting the parasite's life cycle. This is attributed to UA2239 remaining within the iRBCs.

On the other hand, a particular interest in drug development is assessing the sensitivity of resistant strains to other compounds. In this study, we tested the effect of a *Pf*PKG inhibitor, C2, on UA2239 resistant strains. Additionally, we examined the effect of UA2239 on C2 resistant strains. Interestingly, both compounds showed to be effective in inhibiting the egress pathway. This emphasizes the distinct molecular mechanisms of action of these compounds and underscore once again the uniqueness of UA2239.

In addition, we assessed the sensitivity of ART and CQ on the transgenic and UA2239 resistant strains. The transgenic clones, which carried the introduced mutations, remained sensitive to both ART and CQ. However, an unexpected discovery emerged when we examined the sensitivity of these two antimalarial drugs on the UA2239 resistant clones (cultivated for 7 months). While the mutated resistant clones, *Pf*PKG R420I and *Pf*PKG H524N/Y showed no cross resistance to ART or CQ, a turn of event was reported with the *Pf*PKG D597Y clones. These clones displayed sensitivity to CQ but showed a resistance to artemisinin. Notably, the absence of resistance observed in transgenic parasites suggests that the mutation in *Pf*pkg alone is not solely responsible for artemisinin resistance. The mutations found in the *Pf*Kelch13 protein described to confer ART resistance were not found in our UA2239-resistant strains. This indicates the involvement of additional factors or mutations contributing to artemisinin resistance, emphasizing the complexity of this phenomenon.

Another mutation found in the *Pf*PKG D597Y clones was identified in the gene sequence of *P. falciparum* gametocyte development protein 1 (*Pf*gdv1) (PF3D7_0935400). The *Pf*gdv1 gene encodes a peri-nuclear protein that plays a crucial role in the regulatory network governing

gametocytogenesis in *P. falciparum*[269]. Previous studies have reported that a *Pf*gdv1 mutated gene results in a gametocyte-deficient laboratory parasite[270]. Although this gene has never been associated with ART resistance, our study suggests that it may unexpectedly contribute to the generation of ART resistant parasites. It will therefore be interesting to study the *Pf*PKG D597Y clone in greater depth to explain its resistance to ART.

Finally, UA2239 effects on both *in vitro* and *in vivo* (intraperitoneal administration), its ability to be active on the asexual and probably the sexual stages of the parasite led us to believe that UA2239 have the potential to become a new and effective antimalarial with a novel mechanism of action. However, one initial step back was reported concerning UA2239 ineffectiveness *in vivo* through oral administration[185]. To address this challenge, a solution was proposed to develop prodrugs, which are modified forms of a compound that can enhance its bioavailability[271,272]. The Suzanne Peyrottes Team, our collaborating group, has been working on developing UA2239 as a prodrug. Encouragingly, they have recently achieved success in generating a prodrug that showed promising results when administrated orally. Taking all of these results together, they provide optimism for UA2239 potential advancement into preclinical trials.

Annexes

Table containing all the primers used for this study

Primer's name	Sequence
721-PKG-HR1-F	tatagggcgaattggagctc ACTGTATGATGAACCAAGAAGTGC
722-PKG-HR1-R	taatttttctgat ATCAATAGATGCATCAATATTATTATTTCC
723-PKG-HR2-F	gcatctattgat atcAGAAAATTAGGTTTATTATCTAAATCACAAGC
724-PKG-HR2-R	agggaacaaaagctggtacc CCTCATCATCCTCAGCATCC
725-PKG-intF	TCCTATTTTGGGGAAAGAGC
726-PKG-intR	AGTTGTCTTCATCGTTCAATGG
727-gRNA#12F	attg CTAACAGAATTAGTAACAGG
728-gRNA#12R	aaac CCTGTTACTAATTCTGTTAG
729-gRNA#13F	attg AGAACCACAAGATATGAAGA
730-gRNA#13R	aaac TCTTCATATCTTGTGGTTCT
731-gRNA#20F	attg TCTTCCAAATGTGCTAACAT
732-gRNA#20R	aaac ATGTTAGCACATTTGGAAGA
733-PKG-ID-F	AATCAGAAACAACCATTTAAGC
734-PKG-ID-R	TTGGCACAACCAAAATCG
739-gRNA#15F	attgATAATACAAGAAGGAGAAGT
740-gRNA#15R	aaacACTTCTCCTTCTTGTATTAT
741-gRNA#28F	attgACAGAACGAATTATTGGAAG
742-gRNA#28R	aaacCTTCCAATAATTCGTTCTGT
743-gRNA#30F	attgAAGTAAATAATGTTGAATGT
744-gRNA#30R	aaacACATTCAACATTATTTACTT
752-epkg-wt-F	GCTACTGTATGATGAACCGC
753-epkg-wt-R	GCTATCTTTAAAGGTGCGC
PG51	GTTGTGTGGAATTGTGAGC
754-gRNA#8F	attgTATCTATTATAACCAGAGGA

755-gRNA#8R	aaacTCCTCTGGTTATAATAGATA
756-gRNA#19F	attgGGTCTATGGAATATAGCTAT
757-gRNA#19R	aaacATAGCTATATTCCATAGACC
758-gRNA#24F	attgTTGTTGTAGGCATTTCGCTA
759-gRNA#24R	aaacTAGCGAAATGCCTACAACAA
760-PDE-HR1-F	TATAGGGCGAATTGGAGCTCCGTTCATCTAGAAAATCATTAGG
761-PDE-HR1-R	AAAGAATATGTCGACCATTAAAGAGAAAAGTACATAAGAC
762-PDE-HR2-F	TCTTTAATGGTCGACATATTCTTTCCCTCACGG
763-PDE-HR2-R	AGGGAACAAAAGCTGGTACCCTTACAAGTAAATTATAAAAAACATAACG
764-PfPDE-F	TGCTTTATGGGGTCTATGG
765-PfPDE-R	TATAACCAGAGGAAGGAAACC
766-ePDE-F	GACTTTGGAACATTGCAATC
767-ePDE-R	GATGACTAGTGGTAGAAATCCG
M13-Forward	gtaaaacgacggccag
M13-Reverse	caggaaacagctatgac
849-qPCR-ePKG-F	AGGTGCCACGGCCGATTATGC
852-qPCR-PKG-F03	CAAGGACCTATGTTAGCACATTTG
854-qPCR-PKG-R01	CTAATTTAACTGTTCCGAAAGTACCTCTT

The Different *E. coli* Codonized *Pf*pkg (699bp) Sequences

a. Protein kinase g: *Pf*ePKG-WT:

GCATCTATTGATTACAACAACAAGAAGAGCATCATCAAGAAGATGTACATCTTCCGATATCT
GACCGATAAACAGTGCAACCTGCTGATTGAAGCGTTTCGCACCACCCGCTACGAGGAAGGCG
ATTACATTATTCAGGAGGGCGAGGTGGGCAGCCGCTTTTATATCATTAAAAACGGCGAAGTG
GAAATTGTGAAAAACAAGAAACGCCTGCGCACCCTGGGCAAAAACGATTATTTTGGCGAACG
CGCGCTACTGTATGATGAACCGCGCACCGCGAGCGTGATTAGCAAAGTGAACAACGTGGAGT
GCTGGTTTGTGGATAAAAGCGTGTTTCTTCAGATTATTCAGGGTCCGATGCTCGCGCACCTA
GAGGAACGCATTAAAATGCAGGATACCAAAGTGGAAATGGATGAACTGGAAACCGAACGCAT
AATCGGCCGTGGCACCTTTGGCACCGTGAAACTGGTGCATCATAAACCGACCAAAATTCGCT
ATGCGCTGAAATGCGTGAGCAAACGCAGCATTATTAACCTGAACCAGCAGAACAACATTAAA
CTGGAACGCGAAATTACTGCGGAAAATGATCATCCGTTTATTATTCGCCTGGTGCGCACCTT
TAAAGATAGCAAATATTTTTATTTTCTGACCGAACTGGTGACCGGCGGCGAACTGTATGATG
CGATCAGAAAATTAGGT

b. *Pf*ePKG-R420I

GCATCTATTGATTACAACAACAAGAAGAGCATCATCAAGAAGATGTACATCTTCATCTATCT
GACCGATAAACAGTGCAACCTGCTGATTGAAGCGTTTCGCACCACCCGCTACGAGGAAGGCG
ATTACATTATTCAGGAGGGCGAGGTGGGCAGCCGCTTTTATATCATTAAAAACGGCGAAGTG
GAAATTGTGAAAAACAAGAAACGCCTGCGCACCCTGGGCAAAAACGATTATTTTGGCGAACG
CGCGCTACTGTATGATGAACCGCGCACCGCGAGCGTGATTAGCAAAGTGAACAACGTGGAGT
GCTGGTTTGTGGATAAAAGCGTGTTTCTTCAGATTATTCAGGGTCCGATGCTCGCGCACCTA
GAGGAACGCATTAAAATGCAGGATACCAAAGTGGAAATGGATGAACTGGAAACCGAACGCAT
AATCGGCCGTGGCACCTTTGGCACCGTGAAACTGGTGCATCATAAACCGACCAAAATTCGCT
ATGCGCTGAAATGCGTGAGCAAACGCAGCATTATTAACCTGAACCAGCAGAACAACATTAAA
CTGGAACGCGAAATTACTGCGGAAAATGATCATCCGTTTATTATTCGCCTGGTGCGCACCTT
TAAAGATAGCAAATATTTTTATTTTCTGACCGAACTGGTGACCGGCGGCGAACTGTATGATG
CGATCAGAAAATTAGGT

c. *Pf*ePKG-H524Y

GCATCTATTGATTACAACAACAAGAAGAGCATCATCAAGAAGATGTACATCTTCCGATATCT
GACCGATAAACAGTGCAACCTGCTGATTGAAGCGTTTCGCACCACCCGCTACGAGGAAGGCG
ATTACATTATTCAGGAGGGCGAGGTGGGCAGCCGCTTTTATATCATTAAAAACGGCGAAGTG
GAAATTGTGAAAAACAAGAAACGCCTGCGCACCCTGGGCAAAAACGATTATTTTGGCGAACG
CGCGCTACTGTATGATGAACCGCGCACCGCGAGCGTGATTAGCAAAGTGAACAACGTGGAGT
GCTGGTTTGTGGATAAAAGCGTGTTTCTTCAGATTATTCAGGGTCCGATGCTCGCGTATCTA
GAGGAACGCATTAAAATGCAGGATACCAAAGTGGAAATGGATGAACTGGAAACCGAACGCAT
AATCGGCCGTGGCACCTTTGGCACCGTGAAACTGGTGCATCATAAACCGACCAAAATTCGCT
ATGCGCTGAAATGCGTGAGCAAACGCAGCATTATTAACCTGAACCAGCAGAACAACATTAAA
CTGGAACGCGAAATTACTGCGGAAAATGATCATCCGTTTATTATTCGCCTGGTGCGCACCTT
TAAAGATAGCAAATATTTTTATTTTCTGACCGAACTGGTGACCGGCGGCGAACTGTATGATG
CGATCAGAAAATTAGGT

d. *Pf*ePKG-H524N

GCATCTATTGATTACAACAACAAGAAGAGCATCATCAAGAAGATGTACATCTTCCGATATCT
GACCGATAAACAGTGCAACCTGCTGATTGAAGCGTTTCGCACCACCCGCTACGAGGAAGGCG
ATTACATTATTCAGGAGGGCGAGGTGGGCAGCCGCTTTTATATCATTAAAAACGGCGAAGTG
GAAATTGTGAAAAACAAGAAACGCCTGCGCACCCTGGGCAAAAACGATTATTTTGGCGAACG
CGCGCTACTGTATGATGAACCGCGCACCGCGAGCGTGATTAGCAAAGTGAACAACGTGGAGT
GCTGGTTTGTGGATAAAAGCGTGTTTCTTCAGATTATTCAGGGTCCGATGCTCGCGAACCTA
GAGGAACGCATTAAAATGCAGGATACCAAAGTGGAAATGGATGAACTGGAAACCGAACGCAT
AATCGGCCGTGGCACCTTTGGCACCGTGAAACTGGTGCATCATAAACCGACCAAAATTCGCT
ATGCGCTGAAATGCGTGAGCAAACGCAGCATTATTAACCTGAACCAGCAGAACAACATTAAA
CTGGAACGCGAAATTACTGCGGAAAATGATCATCCGTTTATTATTCGCCTGGTGCGCACCTT
TAAAGATAGCAAATATTTTTATTTTCTGACCGAACTGGTGACCGGCGGCGAACTGTATGATG
CGATCAGAAAATTAGGT

e. *Pf*ePKG-D597Y

GCATCTATTGATTACAACAACAAGAAGAGCATCATCAAGAAGATGTACATCTTCCGATATCT
GACCGATAAACAGTGCAACCTGCTGATTGAAGCGTTTCGCACCACCCGCTACGAGGAAGGCG
ATTACATTATTCAGGAGGGCGAGGTGGGCAGCCGCTTTTATATCATTAAAAACGGCGAAGTG
GAAATTGTGAAAAACAAGAAACGCCTGCGCACCCTGGGCAAAAACGATTATTTTGGCGAACG
CGCGCTACTGTATGATGAACCGCGCACCGCGAGCGTGATTAGCAAAGTGAACAACGTGGAGT
GCTGGTTTGTGGATAAAAGCGTGTTTCTTCAGATTATTCAGGGTCCGATGCTCGCGCACCTA
GAGGAACGCATTAAAATGCAGGATACCAAAGTGGAAATGGATGAACTGGAAACCGAACGCAT
AATCGGCCGTGGCACCTTTGGCACCGTGAAACTGGTGCATCATAAACCGACCAAAATTCGCT
ATGCGCTGAAATGCGTGAGCAAACGCAGCATTATTAACCTGAACCAGCAGAACAACATTAAA
CTGGAACGCGAAATTACTGCGGAAAATTACCATCCGTTTATTATTCGCCTGGTGCGCACCTT
TAAAGATAGCAAATATTTTTATTTTCTGACCGAACTGGTGACCGGCGGCGAACTGTATGATG
CGATCAGAAAATTAGGT

f. *Pf*ePKG-T618Q

GCATCTATTGATTACAACAACAAGAAGAGCATCATCAAGAAGATGTACATCTTCCGATATCT
GACCGATAAACAGTGCAACCTGCTGATTGAAGCGTTTCGCACCACCCGCTACGAGGAAGGCG
ATTACATTATTCAGGAGGGCGAGGTGGGCAGCCGCTTTTATATCATTAAAAACGGCGAAGTG
GAAATTGTGAAAAACAAGAAACGCCTGCGCACCCTGGGCAAAAACGATTATTTTGGCGAACG
CGCGCTACTGTATGATGAACCGCGCACCGCGAGCGTGATTAGCAAAGTGAACAACGTGGAGT
GCTGGTTTGTGGATAAAAGCGTGTTTCTTCAGATTATTCAGGGTCCGATGCTCGCGCACCTA
GAGGAACGCATTAAAATGCAGGATACCAAAGTGGAAATGGATGAACTGGAAACCGAACGCAT
AATCGGCCGTGGCACCTTTGGCACCGTGAAACTGGTGCATCATAAACCGACCAAAATTCGCT
ATGCGCTGAAATGCGTGAGCAAACGCAGCATTATTAACCTGAACCAGCAGAACAACATTAAA
CTGGAACGCGAAATTACTGCGGAAAATGATCATCCGTTTATTATTCGCCTGGTGCGCACCTT
TAAAGATAGCAAATATTTTTATTTTCTGCAGGAACTGGTGACCGGCGGCGAACTGTATGATG
CGATCAGAAAATTAGGT

The Different *E. coli* Codonized *Pf*pdeβ (150bp) Sequences

a. *Pf*ePDEβ-WT:

TACTTTTCTCTTTAATGGTCGCATTGTGGGGACTTTGGAACATTGCAATCGGATTGACTCTA
GAGTACAACCCTAATCTAAGTGAGATGCCAACTACTACATATGAATTAGAGATGATATACGT
TCTGACCTACATTTACGGATTTCTACCACTAGTCATCATCGACATATTCTTTCCCTCACG

b. *Pf*ePDEβ-Y539D:

TACTTTTCTCTTTAATGGTCGCATTGTGGGGACTTTGGAACATTGCAATCGGATTGACTCTA
GAGTACAACCCTAATCTAAGTGAGATGCCAACTACTACATATGAATTAGAGATGATAGACGT
TCTGACCTACATTTACGGATTTCTACCACTAGTCATCATCGACATATTCTTTCCCTCACG

The red and underlined sequences on the extremities represent overlaps with HR1 and HR2. In addition, the yellow highlighted bases represent the location of the non-synonymous mutation that was identified through the WGS.

References

1. Drugs, I. of M. (US) C. on the E. of A., Arrow, K. J., Panosian, C. & Gelband, H. A Brief History of Malaria. (2004).

2. Votýpka, J., Modrý, D., Obornik, M., Šlapeta, J. & Lukeš, J. Apicomplexa. *Handb. Protists Second Ed.* 567–624 (2017) doi:10.1007/978-3-319-28149-0_20/COVER.

3. Sato, S. Plasmodium—a brief introduction to the parasites causing human malaria and their basic biology. *J. Physiol. Anthropol.* **40**, (2021).

4. Thieleke-Matos, C. *et al.* Host cell autophagy contributes to Plasmodium liver development. *Cell. Microbiol.* **18**, 437–450 (2016).

5. Vaughan, A. M. & Kappe, S. H. I. Malaria Parasite Liver Infection and Exoerythrocytic Biology. *Cold Spring Harb. Perspect. Med.* **7**, (2017).

6. Waller, R. F. & McFadden, G. I. The Apicoplast: A Review of the Derived Plastid of Apicomplexan Parasites. *Curr. Issues Mol. Biol. 2005, Vol. 7, Pages 57-80* **7**, 57–80 (2004).

7. Seeber, F. & Soldati-Favre, D. Metabolic pathways in the apicoplast of apicomplexa. *Int. Rev. Cell Mol. Biol.* **281**, 161–228 (2010).

8. Yeh, E. & DeRisi, J. L. Chemical Rescue of Malaria Parasites Lacking an Apicoplast Defines Organelle Function in Blood-Stage Plasmodium falciparum. *PLoS Biol.* **9**, 1001138 (2011).

9. Okamoto, N. & Keeling, P. J. The 3D Structure of the Apical Complex and Association with the Flagellar Apparatus Revealed by Serial TEM Tomography in Psammosa pacifica, a Distant Relative of the Apicomplexa. *PLoS One* **9**, 84653 (2014).

10. Gubbels, M. J. & Duraisingh, M. T. Evolution of apicomplexan secretory organelles. *Int. J. Parasitol.* **42**, 1071 (2012).

11. Yeoh, S. *et al.* Subcellular Discharge of a Serine Protease Mediates Release of Invasive Malaria Parasites from Host Erythrocytes. *Cell* **131**, 1072–1083 (2007).

12. Tawk, L. *et al.* A Key Role for Plasmodium Subtilisin-like SUB1 Protease in Egress of Malaria Parasites from Host Hepatocytes. *J. Biol. Chem.* **288**, 33336 (2013).

13. Yeoh, S. *et al.* Subcellular Discharge of a Serine Protease Mediates Release of Invasive Malaria Parasites from Host Erythrocytes. *Cell* **131**, 1072–1083 (2007).

14. Thomas, J. A. *et al.* A protease cascade regulates release of the human malaria parasite Plasmodium falciparum from host red blood cells. *Nat. Microbiol.* **3**, (2018).

15. Wunderlich, J., Rohrbach, P. & Dalton, J. P. The malaria digestive vacuole. *Front. Biosci. - Sch.* **4 S**, 1424–1448 (2012).

16. Counihan, N. A., Modak, J. K. & de Koning-Ward, T. F. How Malaria Parasites Acquire Nutrients From Their Host. *Front. Cell Dev. Biol.* **9**, (2021).

17. Prevention, C.-C. for D. C. and. CDC - Malaria - About Malaria - Biology.

18. Escobar, D., Ascencio, K., Ortiz, A., Palma, A. & Fontecha, G. Distribution and phylogenetic diversity of Anopheles species in malaria endemic areas of Honduras in

an elimination setting. *Parasites and Vectors* **13**, 1–12 (2020).

19. Lindh, J. M., Terenius, O. & Faye, I. 16S rRNA Gene-Based Identification of Midgut Bacteria from Field-Caught Anopheles gambiae Sensu Lato and A. funestus Mosquitoes Reveals New Species Related to Known Insect Symbionts. *Appl. Environ. Microbiol.* **71**, 7217 (2005).

20. Lee, A. H., Symington, L. S. & Fidock, D. A. DNA Repair Mechanisms and Their Biological Roles in the Malaria Parasite Plasmodium falciparum. *Microbiol. Mol. Biol. Rev.* **78**, 469–486 (2014).

21. Garcia, J. E., Puentes, A. & Patarroyo, M. E. Developmental Biology of Sporozoite-Host Interactions in Plasmodium falciparum Malaria: Implications for Vaccine Design. *Clin. Microbiol. Rev.* **19**, 686 (2006).

22. Amino, R. *et al.* Quantitative imaging of Plasmodium transmission from mosquito to mammal. *Nat. Med. 2006 122* **12**, 220–224 (2006).

23. Rosenberg, R., Burge, R. & Schneider, I. An estimation of the number of malaria sporozoites ejected by a feeding mosquito. *Trans. R. Soc. Trop. Med. Hyg.* **84**, 209–212 (1990).

24. Ying, P. *et al.* The malaria circumsporozoite protein: interaction of the conserved regions I and II-plus with heparin-like oligosaccharides in heparan sulfate. *Exp. Parasitol.* **85**, 168–182 (1997).

25. Sinnis, P., Willnow, T. E., Briones, M. R. S., Herz, J. & Nussenzweig, V. Remnant lipoproteins inhibit malaria sporozoite invasion of hepatocytes. *J. Exp. Med.* **184**, 945–954 (1996).

26. Shakibaei, M. & Frevert, U. Dual interaction of the malaria circumsporozoite protein with the low density lipoprotein receptor-related protein (LRP) and heparan sulfate proteoglycans. *J. Exp. Med.* **184**, 1699–1711 (1996).

27. Vaughan, A. M. & Kappe, S. H. I. Malaria Parasite Liver Infection and Exoerythrocytic Biology. *Cold Spring Harb. Perspect. Med.* **7**, (2017).

28. Kaushansky, A. *et al.* Malaria parasite liver stages render host hepatocytes susceptible to mitochondria-initiated apoptosis. *Cell Death Dis. 2013 48* **4**, e762–e762 (2013).

29. Sinnis, P. & Sim, B. K. L. Cell invasion by the vertebrate stages of Plasmodium. *Trends Microbiol.* **5**, 52 (1997).

30. Shears, M. J. *et al.* Proteomic Analysis of Plasmodium Merosomes: The Link between Liver and Blood Stages in Malaria. *J. Proteome Res.* **18**, 3404–3418 (2019).

31. Mo, A. X. & McGugan, G. Understanding the Liver-Stage Biology of Malaria Parasites: Insights to Enable and Accelerate the Development of a Highly Efficacious Vaccine. *Am. J. Trop. Med. Hyg.* **99**, 827 (2018).

32. Geoghegan, N. D. *et al.* 4D analysis of malaria parasite invasion offers insights into erythrocyte membrane remodeling and parasitophorous vacuole formation. *Nat. Commun. 2021 121* **12**, 1–16 (2021).

33. Rug, M. *et al.* Export of virulence proteins by malaria-infected erythrocytes involves remodeling of host actin cytoskeleton. *Blood* **124**, 3459–3468 (2014).

34. Olivier, M., Van Den Ham, K., Shio, M. T., Kassa, F. A. & Fougeray, S. Malarial Pigment Hemozoin and the Innate Inflammatory Response. *Front. Immunol.* **5**, (2014).

35. Liu, Z., Miao, J. & Cui, L. Gametocytogenesis in malaria parasite: commitment, development and regulation. *Future Microbiol.* **6**, 1351 (2011).

36. Josling, G. A. & Llinás, M. Sexual development in Plasmodium parasites: knowing when it's time to commit. *Nat. Rev. Microbiol. 2015 139* **13**, 573–587 (2015).

37. Brochet, M. & Billker, O. Calcium signalling in malaria parasites. *Mol. Microbiol.* **100**, 397–408 (2016).

38. Brochet, M. *et al.* Phosphoinositide metabolism links cGMP-dependent protein kinase G to essential Ca^{2+} signals at key decision points in the life cycle of malaria parasites. *PLoS Biol.* **12**, (2014).

39. Bansal, A. *et al.* Characterization of plasmodium falciparum calcium-dependent protein kinase 1 (PFCDPK1) and its role in microneme secretion during erythrocyte invasion. *J. Biol. Chem.* **288**, 1590–1602 (2013).

40. More, K. R. *et al.* Phosphorylation-Dependent Assembly of a 14-3-3 Mediated Signaling Complex during Red Blood Cell Invasion by Plasmodium falciparum Merozoites. *MBio* **11**, 1–17 (2020).

41. Sharma, M. *et al.* CDPKs: The critical decoders of calcium signal at various stages of malaria parasite development. *Comput. Struct. Biotechnol. J.* **19**, 5092–5107 (2021).

42. Paul, A. S. *et al.* Co-option of Plasmodium falciparum PP1 for egress from host erythrocytes. *Nat. Commun.* **11**, (2020).

43. Dvorin, J. D. *et al.* A plant-like kinase in plasmodium falciparum regulates parasite egress from erythrocytes. *Science (80-.).* **328**, 910–912 (2010).

44. Glushakova, S. *et al.* Cytoplasmic free Ca2+ is essential for multiple steps in malaria parasite egress from infected erythrocytes. *Malar. J.* **12**, 41 (2013).

45. Yeoh, S. *et al.* Subcellular discharge of a serine protease mediates release of invasive malaria parasites from host erythrocytes. *Cell* **131**, 1072–1083 (2007).

46. Withers-Martinez, C. *et al.* The malaria parasite egress protease SUB1 is a calcium-dependent redox switch subtilisin. *Nat. Commun.* **5**, (2014).

47. Fierro, M. A. *et al.* An Endoplasmic Reticulum CREC Family Protein Regulates the Egress Proteolytic Cascade in Malaria Parasites. *MBio* **11**, (2020).

48. Das, S. *et al.* Processing of Plasmodium falciparum Merozoite Surface Protein MSP1 Activates a Spectrin-Binding Function Enabling Parasite Egress from RBCs. *Cell Host Microbe* **18**, 433–444 (2015).

49. Tan, M. S. Y. *et al.* Autocatalytic activation of a malarial egress protease is druggable and requires a protein cofactor. *EMBO J.* **40**, e107226 (2021).

50. Koussis, K. *et al.* A multifunctional serine protease primes the malaria parasite for red blood cell invasion. **28**, 725–735 (2009).

51. Yeoh, S. *et al.* Subcellular Discharge of a Serine Protease Mediates Release of Invasive Malaria Parasites from Host Erythrocytes. *Cell* **131**, 1072–1083 (2007).

52. Bennink, S., Kiesow, M. J. & Pradel, G. The development of malaria parasites in the mosquito midgut. *Cell. Microbiol.* **18**, 905 (2016).

53. Olivieri, A. *et al.* Distinct properties of the egress-related osmiophilic bodies in male and female gametocytes of the rodent malaria parasite Plasmodium berghei. *Cell. Microbiol.* **17**, 355–368 (2015).

54. Yahiya, S. *et al.* Live-cell fluorescence imaging of microgametogenesis in the human malaria parasite Plasmodium falciparum. *PLoS Pathog.* **18**, (2022).

55. Kuehn, A. & Pradel, G. The coming-out of malaria gametocytes. *J. Biomed. Biotechnol.* **2010**, (2010).

56. Sinden, R. E. Malaria, sexual development and transmission: retrospect and prospect. *Parasitology* **136**, 1427–1434 (2009).

57. Angrisano, F., Tan, Y. H., Sturm, A., McFadden, G. I. & Baum, J. Malaria parasite colonisation of the mosquito midgut – Placing the Plasmodium ookinete centre stage. *Int. J. Parasitol.* **42**, 519–527 (2012).

58. Smith, R. C. & Barillas-Mury, C. Plasmodium Oocysts: Overlooked Targets of Mosquito Immunity. *Trends Parasitol.* **32**, 979–990 (2016).

59. Olivier, M., Van Den Ham, K., Shio, M. T., Kassa, F. A. & Fougeray, S. Malarial pigment hemozoin and the innate inflammatory response. *Front. Immunol.* **5**, 25 (2014).

60. Doolan, D. L., Dobaño, C. & Baird, J. K. Acquired Immunity to Malaria. *Clin. Microbiol. Rev.* **22**, 13 (2009).

61. Howard, R. J., Barnwell, J. W. & Kao, V. Antigenic variation of Plasmodium knowlesi malaria: identification of the variant antigen on infected erythrocytes. *Proc. Natl. Acad. Sci. U. S. A.* **80**, 4129–4133 (1983).

62. Van Schravendijk, M. R. *et al.* Characterization and localization of Plasmodium falciparum surface antigens on infected erythrocytes from west African patients. *Blood* **78**, 226–236 (1991).

63. Jensen, A. R., Adams, Y. & Hviid, L. Cerebral Plasmodium falciparum malaria: The role of PfEMP1 in its pathogenesis and immunity, and PfEMP1-based vaccines to prevent it. *Immunol. Rev.* **293**, 230 (2020).

64. Burrack, K. S., Hart, G. T. & Hamilton, S. E. Contributions of natural killer cells to the immune response against Plasmodium. *Malar. J.* **18**, 1–9 (2019).

65. Feleke, D. G. *et al.* Asymptomatic malaria infection among pregnant women attending antenatal care in malaria endemic areas of North-Shoa, Ethiopia: A cross-sectional study. *Malar. J.* **19**, 1–6 (2020).

66. Prevention, C.-C. for D. C. and. CDC - Malaria - About Malaria - Disease. (2022).

67. Angchaisuksiri, P. Coagulopathy in malaria. *Thromb. Res.* **133**, 5–9 (2014).

68. Sasi, P. *et al.* Metabolic Acidosis and Other Determinants of Hemoglobin-Oxygen Dissociation in Severe Childhood Plasmodium falciparum Malaria. *Am. J. Trop. Med. Hyg.* **77**, 256–260 (2007).

69. Gupta, S. *et al.* Malaria and the Heart: JACC State-of-the-Art Review. *J. Am. Coll. Cardiol.* **77**, 1110–1121 (2021).

70. Brown, D. D., Solomon, S., Lerner, D. & Del Rio, M. Malaria and acute kidney injury. *Pediatr. Nephrol.* **35**, 603–608 (2020).

71. Ponsford, M. J. *et al.* Sequestration and Microvascular Congestion Are Associated With Coma in Human Cerebral Malaria. *J. Infect. Dis.* **205**, 663 (2012).

72. Roberson, M. T. & Smith, A. T. Cerebral Malaria in a Patient with Recent Travel to the Congo Presenting with Delirium: A Case Report. *Clin. Pract. Cases Emerg. Med.* **4**, 533 (2020).

73. Idro, R., Marsh, K., John, C. C. & Newton, C. R. J. Cerebral Malaria; Mechanisms Of Brain Injury And Strategies For Improved Neuro-Cognitive Outcome. *Pediatr. Res.* **68**, 267 (2010).

74. World malaria report 2022. https://www.who.int/teams/global-malaria-programme/reports/world-malaria-report-2022.

75. Sholapurkar, S. L., Gupta, A. N. & Mahajan, R. C. Clinical course of malaria in pregnancy — a prospective controlled study from India. *Trans. R. Soc. Trop. Med. Hyg.* **82**, 376–379 (1988).

76. Chua, C. L. L. *et al.* Malaria in Pregnancy: From Placental Infection to Its Abnormal Development and Damage. *Front. Microbiol.* **12**, 3452 (2021).

77. Balcha, F., Menna, T. & Lombamo, F. Prevalence of asymptomatic malaria and associated factors among pregnant women at Boset District in East Shoa Zone, Oromia Region, Ethiopia: a cross-sectional study. *Malar. J.* **22**, 1–9 (2023).

78. Whitfield, J. Portrait of a serial killer. *Nature* (2002) doi:10.1038/NEWS021001-6.

79. Rafiee Parhizgar, A. & Tahghighi, A. Introducing New Antimalarial Analogues of Chloroquine and Amodiaquine: A Narrative Review. *Iran. J. Med. Sci.* **42**, 115–128 (2017).

80. Gething, P. W. *et al.* A Long Neglected World Malaria Map: Plasmodium vivax Endemicity in 2010. *PLoS Negl. Trop. Dis.* **6**, e1814 (2012).

81. World malaria report 2022. https://www.who.int/publications/i/item/9789240064898.

82. WHO and partners launch new country-led response to put stalled malaria control efforts back on track. https://www.who.int/news/item/19-11-2018-who-and-partners-launch-new-country-led-response-to-put-stalled-malaria-control-efforts-

back-on-track.

83. Questions & answers on the World malaria report 2022. https://www.who.int/teams/global-malaria-programme/reports/world-malaria-report-2022/questions-and-answers.

84. Laurens, M. B. RTS,S/AS01 vaccine (Mosquirix™): an overview. *Hum. Vaccin. Immunother.* **16**, 480 (2020).

85. RBM Partnership to End Malaria Overview | RBM Partnership to End Malaria. https://endmalaria.org/about-us/overview.

86. Phillips, M. A. *et al. Malaria*. *Nature Reviews Disease Primers* vol. 3 17050 (Nature Publishing Group, 2017).

87. Musiime, A. K. *et al.* Impact of vector control interventions on malaria transmission intensity, outdoor vector biting rates and Anopheles mosquito species composition in Tororo, Uganda. *Malar. J.* **18**, 1–9 (2019).

88. Global Malaria Programme. https://www.who.int/teams/global-malaria-programme/prevention/vector-control/insecticide-resistance.

89. Van Den Berg, H. Global Status of DDT and Its Alternatives for Use in Vector Control to Prevent Disease. *Environ. Health Perspect.* **117**, 1656 (2009).

90. Fillinger, U. & Lindsay, S. W. Larval source management for malaria control in Africa: myths and reality. *Malar. J.* **10**, (2011).

91. Watson, O. J. *et al.* False-negative malaria rapid diagnostic test results and their impact on community-based malaria surveys in sub-Saharan Africa. *BMJ Glob. Heal.* **4**, e001582 (2019).

92. Hosch, S. *et al.* Analysis of nucleic acids extracted from rapid diagnostic tests reveals a significant proportion of false positive test results associated with recent malaria treatment. *Malar. J.* **21**, 1–12 (2022).

93. Mfuh, K. O. *et al.* A comparison of thick-film microscopy, rapid diagnostic test, and polymerase chain reaction for accurate diagnosis of Plasmodium falciparum malaria. *Malar. J.* **18**, 1–8 (2019).

94. Govella, N. J. & Ferguson, H. Why Use of Interventions Targeting Outdoor Biting Mosquitoes will be Necessary to Achieve Malaria Elimination. *Front. Physiol.* **3**, (2012).

95. RTS, S. C. T. P. Efficacy and safety of RTS,S/AS01 malaria vaccine with or without abooster dose in infants and children in Africa: final results of a phase 3,individually randomised, controlled trial. *Lancet (London, England)* **386**, 31 (2015).

96. Arora, N., Anbalagan, L. C. & Pannu, A. K. Towards Eradication of Malaria: Is the WHO's RTS,S/AS01 Vaccination Effective Enough? *Risk Manag. Healthc. Policy* **14**, 1033 (2021).

97. Moorthy, V. & Binka, F. R21/Matrix-M: a second malaria vaccine? *Lancet* **397**, 1782–1783 (2021).

98. Datoo, M. S. *et al.* Efficacy and immunogenicity of R21/Matrix-M vaccine against clinical malaria after 2 years' follow-up in children in Burkina Faso: a phase 1/2b randomised controlled trial. *Lancet Infect. Dis.* **22**, 1728–1736 (2022).

99. Mordmüller, B. *et al.* Sterile protection against human malaria by chemoattenuated PfSPZ vaccine. *Nature* **542**, 445–449 (2017).

100. Sissoko, M. S. *et al.* Safety and efficacy of PfSPZ Vaccine against Plasmodium falciparum via direct venous inoculation in healthy malaria-exposed adults in Mali: a randomised, double-blind phase 1 trial. *Lancet. Infect. Dis.* **17**, 498–509 (2017).

101. Payne, R. O. *et al.* Human vaccination against RH5 induces neutralizing antimalarial antibodies that inhibit RH5 invasion complex interactions. *JCI Insight* **2**, (2017).

102. WHO Model Lists of Essential Medicines. https://www.who.int/groups/expert-committee-on-selection-and-use-of-essential-medicines/essential-medicines-lists.

103. Cheviet, T., Lefebvre-Tournier, I., Wein, S. & Peyrottes, S. Plasmodium Purine Metabolism and Its Inhibition by Nucleoside and Nucleotide Analogues. *J. Med. Chem.* **62**, 8365–8391 (2019).

104. Encyclopedia of Family Health - David B. Jacoby, R. M. Youngson - Google Livres. https://books.google.fr/books?hl=fr&lr=&id=VUA8DQCONgUC&oi=fnd&pg=PA1296&ots=6EcKVVE6rt&sig=U00QYENGHtdqDSEACM3UvBPaIKw&redir_esc=y#v=onepage&q&f=false.

105. Achan, J. *et al.* Quinine, an old anti-malarial drug in a modern world: Role in the treatment of malaria. *Malar. J.* **10**, 1–12 (2011).

106. Howard, M. A. *et al.* Quinine allergy causing acute severe systemic illness: report of 4 patients manifesting multiple hematologic, renal, and hepatic abnormalities. *Proc. (Bayl. Univ. Med. Cent).* **16**, 21–26 (2003).

107. Okitolonda, W., Delacollette, C., Malengreau, M. & Henquin, J. C. High incidence of hypoglycaemia in African patients treated with intravenous quinine for severe malaria. *Br Med J (Clin Res Ed)* **295**, 716–718 (1987).

108. F. David Winter, J. Immune thrombocytopenia associated with consumption of tonic water. *Proc. (Bayl. Univ. Med. Cent).* **28**, 213 (2015).

109. QuiNINE Monograph for Professionals - Drugs.com. https://www.drugs.com/monograph/quinine.html.

110. Peters, W. Antimalarial drug resistance: an increasing problem. *Br. Med. Bull.* **38**, 187–192 (1982).

111. Monlun, E. *et al.* Cardiac complications of halofantrine: a prospective study of 20 patients. *Trans. R. Soc. Trop. Med. Hyg.* **89**, 430–433 (1995).

112. WHO model list of essential medicines - 22nd list, 2021. https://www.who.int/publications/i/item/WHO-MHP-HPS-EML-2021.02.

113. Wong, W. *et al.* The antimalarial Mefloquine targets the Plasmodium falciparum 80S ribosome to inhibit protein synthesis. *Nat. Microbiol.* **2**, 17031 (2017).

114. Mefloquine (Lariam®) - Public Health. https://www.publichealth.va.gov/exposures/mefloquine-lariam.asp.

115. González, R. *et al.* Mefloquine for preventing malaria in pregnant women. *Cochrane Database Syst. Rev.* **2018**, (2018).

116. Achan, J. *et al.* Quinine, an old anti-malarial drug in a modern world: role in the treatment of malaria. *Malar. J.* **10**, 144 (2011).

117. Ciak, J. & Hahn, F. E. Chloroquine: mode of action. *Science* **151**, 347–349 (1966).

118. Pussard, E. & Verdier, F. Antimalarial 4-aminoquinolines: mode of action and pharmacokinetics. *Fundam. Clin. Pharmacol.* **8**, 1–17 (1994).

119. Singh Sidhu, A. B., Verdier-Pinard, D. & Fidock, D. A. Chloroquine Resistance in Plasmodium falciparum Malaria Parasites Conferred by pfcrt Mutations. *Science* **298**, 210 (2002).

120. Fidock, D. A. *et al.* Mutations in the P. falciparum Digestive Vacuole Transmembrane Protein PfCRT and Evidence for Their Role in Chloroquine Resistance. **6**, (2000).

121. Duraisingh, M. T. & Cowman, A. F. Contribution of the pfmdr1 gene to antimalarial drug-resistance. *Acta Trop.* **94**, 181–190 (2005).

122. Andersson, N. W., Skov, L. & Andersen, J. T. Fetal safety of chloroquine and hydroxychloroquine use during pregnancy: a nationwide cohort study. *Rheumatology* **60**, 2317–2326 (2021).

123. Chang, C., Lin-Hua, T. & Jantanavivat, C. Studies on a new antimalarial compound: Pyronaridine. *Trans. R. Soc. Trop. Med. Hyg.* **86**, 7–10 (1992).

124. Ringwald, P., Bickii, J. & Basco, L. Randomised trial of pyronaridine versus chloroquine for acute uncomplicated falciparum malaria in Africa. *Lancet* **347**, 24–28 (1996).

125. Chaires, J. B. & Travers, A. Pyronaridine: An update of its pharmacological activities and mechanisms of action. *Biopolymers* **112**, e23398 (2021).

126. Sullivan, D. J. Quinolines block every step of malaria heme crystal growth. *Proc. Natl. Acad. Sci. U. S. A.* **114**, 7483–7485 (2017).

127. Clark, R. L. Animal Embryotoxicity Studies of Key Non-Artemisinin Antimalarials and Use in Women in the First Trimester. *Birth Defects Res.* **109**, 1075–1126 (2017).

128. Kincaid, J. R. A. *et al.* Environmentally Responsible and Cost-Effective Synthesis of the Antimalarial Drug Pyronaridine. *Org. Lett.* (2022) doi:10.1021/ACS.ORGLETT.2C00944/SUPPL_FILE/OL2C00944_SI_001.PDF.

129. Ashley, E. A., Recht, J. & White, N. J. Primaquine: The risks and the benefits. *Malar. J.* **13**, 1–7 (2014).

130. Sutanto, I. *et al.* The effect of primaquine on gametocyte development and clearance in the treatment of uncomplicated falciparum malaria with dihydroartemisinin-piperaquine in South sumatra, Western indonesia: an open-label, randomized, controlled trial. *Clin. Infect. Dis.* **56**, 685–693 (2013).

131. Camarda, G. *et al.* Antimalarial activity of primaquine operates via a two-step biochemical relay. *Nat. Commun. 2019 101* **10**, 1–9 (2019).

132. Watson, J., Taylor, W. R. J., Menard, D., Kheng, S. & White, N. J. Modelling primaquine-induced haemolysis in G6PD deficiency. *Elife* **6**, (2017).

133. Lu, K. Y. & Derbyshire, E. R. Tafenoquine: A Step toward Malaria Elimination. *Biochemistry* **59**, 911 (2020).

134. McIntosh, H. & Olliaro, P. Artemisinin derivatives for treating severe malaria. *Cochrane Database Syst. Rev.* **1998**, (1998).

135. De Vries, P. J. & Dien, T. K. Clinical pharmacology and therapeutic potential of artemisinin and its derivatives in the treatment of malaria. *Drugs* **52**, 818–836 (1996).

136. Karunajeewa, H. A. Artemisinins: Artemisinin, dihydroartemisinin, artemether and artesunate. *Milestones Drug Ther.* **41**, 157–190 (2012).

137. Meshnick, S. R., Taylor, T. E. & Kamchonwongpaisan, S. Artemisinin and the antimalarial endoperoxides: From herbal remedy to targeted chemotherapy. *Microbiol. Rev.* **60**, 301–315 (1996).

138. Robert, A., Benoit-Vical, F., Claparols, C. & Meunier, B. The antimalarial drug artemisinin alkylates heme in infected mice. *Proc. Natl. Acad. Sci. U. S. A.* **102**, 13676–13680 (2005).

139. Moore, C. M. *et al.* Selective Inhibition of Plasmodium falciparum ATPase 6 by Artemisinins and Identification of New Classes of Inhibitors after Expression in Yeast. *Antimicrob. Agents Chemother.* **66**, (2022).

140. Dondorp, A. M. *et al.* Artemisinin Resistance in Plasmodium falciparum Malaria . *N. Engl. J. Med.* **361**, 455–467 (2009).

141. Ariey, F. *et al.* A molecular marker of artemisinin-resistant Plasmodium falciparum malaria. **505**,.

142. Imwong, M. *et al.* The spread of artemisinin-resistant Plasmodium falciparum in the Greater Mekong subregion: a molecular epidemiology observational study. *Lancet Infect. Dis.* **17**, 491–497 (2017).

143. Takala-Harrison, S. *et al.* Independent Emergence of Artemisinin Resistance Mutations Among Plasmodium falciparum in Southeast Asia. *J. Infect. Dis.* **211**, 670–679 (2015).

144. Birnbaum, J. *et al.* A Kelch13-defined endocytosis pathway mediates artemisinin resistance in malaria parasites. *Science (80-.).* **367**, 51–59 (2020).

145. Mok, S. *et al.* Population transcriptomics of human malaria parasites reveals the mechanism of artemisinin resistance. *Science (80-.).* **347**, 431–435 (2015).

146. Rocamora, F. *et al.* Oxidative stress and protein damage responses mediate artemisinin resistance in malaria parasites. *PLOS Pathog.* **14**, e1006930 (2018).

147. Gibbons, J. *et al.* Altered expression of K13 disrupts DNA replication and repair in

Plasmodium falciparum. *BMC Genomics* **19**, 1–14 (2018).

148. Egwu, C. O. *et al.* Resistance to artemisinin in falciparum malaria parasites: A redox-mediated phenomenon. *Free Radic. Biol. Med.* **179**, 317–327 (2022).

149. Karelle, D. L. *et al.* Computational Study of the Interactions between Antimalarial Chemotherapies with Folate Pathway Receptors and Telomerase Reverse Transcriptase. *Comput. Chem.* **9**, 197–214 (2021).

150. Hyde, J. E. Drug-resistant malaria − an insight. *FEBS J.* **274**, 4688–4698 (2007).

151. Winstanley, P. & Ward, S. Malaria chemotherapy. *Adv. Parasitol.* **61**, 47–76 (2006).

152. Mikomangwa, W. P. *et al.* Effect of sulfadoxine-pyrimethamine doses for prevention of malaria during pregnancy in hypoendemic area in Tanzania. *Malar. J.* **19**, 1–11 (2020).

153. Lynch, C. A. *et al.* Travel and the emergence of high-level drug resistance in Plasmodium falciparum in southwest Uganda: results from a population-based study. *Malar. J.* **16**, 1–9 (2017).

154. Ahmed, A. *et al.* Plasmodium falciparum Isolates in India Exhibit a Progressive Increase in Mutations Associated with Sulfadoxine-Pyrimethamine Resistance. *Antimicrob. Agents Chemother.* **48**, 879 (2004).

155. Tan, K. R., Magill, A. J., Parise, M. E. & Arguin, P. M. Doxycycline for Malaria Chemoprophylaxis and Treatment: Report from the CDC Expert Meeting on Malaria Chemoprophylaxis. *Am. J. Trop. Med. Hyg.* **84**, 517 (2011).

156. Okada, M., Guo, P., Nalder, S. A. & Sigala, P. A. Doxycycline has distinct apicoplast-specific mechanisms of antimalarial activity. *Elife* **9**, 1–11 (2020).

157. Dahl, E. L. *et al.* Tetracyclines Specifically Target the Apicoplast of the Malaria Parasite Plasmodium falciparum. *Antimicrob. Agents Chemother.* **50**, 3124 (2006).

158. Gaillard, T., Madamet, M. & Pradines, B. Tetracyclines in malaria. *Malar. J.* **14**, 1–10 (2015).

159. Schuck, D. C. *et al.* Biological evaluation of hydroxynaphthoquinones as anti-malarials. *Malar. J.* **12**, 1–6 (2013).

160. Nixon, G. L. *et al.* Antimalarial pharmacology and therapeutics of atovaquone. *J. Antimicrob. Chemother.* **68**, 977 (2013).

161. Siregar, J. E. *et al.* Direct evidence for the atovaquone action on the Plasmodium cytochrome bc1 complex. *Parasitol. Int.* **64**, 295–300 (2015).

162. Lalève, A. *et al.* The antimalarial drug primaquine targets Fe-S cluster proteins and yeast respiratory growth. *Redox Biol.* **7**, 21–29 (2016).

163. Ribbiso, K. A. *et al.* Artemisinin-Based Drugs Target the Plasmodium falciparum Heme Detoxification Pathway. *Antimicrob. Agents Chemother.* **65**, (2021).

164. Burrows, J. N. *et al.* New developments in anti-malarial target candidate and product profiles. *Malar. J.* **16**, 26 (2017).

165. MMV's pipeline of antimalarial drugs | Medicines for Malaria Venture. https://www.mmv.org/research-development/mmvs-pipeline-antimalarial-drugs.

166. Baragaña, B. *et al.* A novel multiple-stage antimalarial agent that inhibits protein synthesis. *Nature* **522**, 315 (2015).

167. McCarthy, J. S. *et al.* Safety, pharmacokinetics, and antimalarial activity of the novel plasmodium eukaryotic translation elongation factor 2 inhibitor M5717: a first-in-human, randomised, placebo-controlled, double-blind, single ascending dose study and volunteer infection study. *Lancet Infect. Dis.* **21**, 1713–1724 (2021).

168. Rottmann, M. *et al.* Preclinical Antimalarial Combination Study of M5717, a Plasmodium falciparum Elongation Factor 2 Inhibitor, and Pyronaridine, a Hemozoin Formation Inhibitor. *Antimicrob. Agents Chemother.* **64**, (2020).

169. Tse, E. G., Korsik, M. & Todd, M. H. The past, present and future of anti-malarial medicines. *Malar. J. 2019 181* **18**, 1–21 (2019).

170. Spillman, N. J. & Kirk, K. The malaria parasite cation ATPase PfATP4 and its role in the mechanism of action of a new arsenal of antimalarial drugs. *Int. J. Parasitol. Drugs Drug Resist.* **5**, (2015).

171. Phillips, M. A. & Rathod, P. K. Plasmodium dihydroorotate dehydrogenase: a promising target for novel anti-malarial chemotherapy. *Infect. Disord. Drug Targets* **10**, 226 (2010).

172. Sulyok, M. *et al.* DSM265 for Plasmodium falciparum chemoprophylaxis: a randomised, double blinded, phase 1 trial with controlled human malaria infection. *Lancet Infect. Dis.* **17**, 636–644 (2017).

173. De Clercq, E. The acyclic nucleoside phosphonates (ANPs): Antonín Holý's legacy. *Med. Res. Rev.* **33**, 1278–1303 (2013).

174. De Clercq, E. Tanovea® for the treatment of lymphoma in dogs. *Biochem. Pharmacol.* **154**, 265–269 (2018).

175. Doleželová, E. *et al.* Evaluation of the Trypanosoma brucei 6-oxopurine salvage pathway as a potential target for drug discovery. *PLoS Negl. Trop. Dis.* **12**, e0006301 (2018).

176. Doleželová, E. *et al.* Acyclic nucleoside phosphonates with adenine nucleobase inhibit Trypanosoma brucei adenine phosphoribosyltransferase in vitro. *Sci. Reports 2021 111* **11**, 1–27 (2021).

177. Downie, M. J., Kirk, K. & Mamoun, C. Ben. Purine Salvage Pathways in the Intraerythrocytic Malaria Parasite Plasmodium falciparum. *Eukaryot. Cell* **7**, 1231 (2008).

178. Cassera, M. B., Zhang, Y., Hazleton, K. Z. & Schramm, V. L. Purine and Pyrimidine Pathways as Targets in Plasmodium falciparum. *Curr. Top. Med. Chem.* **11**, 2103 (2011).

179. Berman, P. A. & Human, L. Hypoxanthine depletion induced by xanthine oxidase

inhibits malaria parasite growth in vitro. *Adv. Exp. Med. Biol.* **309**, 165–168 (1991).

180. Booden, T. & Hull, R. W. Nucleic acid precursor synthesis by Plasmodium lophurae parasitizing chicken erythrocytes. *Exp. Parasitol.* **34**, 220–228 (1973).

181. Hocková, D. *et al.* Antimalarial activity of prodrugs of N-branched acyclic nucleoside phosphonate inhibitors of 6-oxopurine phosphoribosyltransferases. **23**, 5502–5510 (2015).

182. Česnek, M. *et al.* Synthesis of 9-phosphonoalkyl and 9-phosphonoalkoxyalkyl purines: evaluation of their ability to act as inhibitors of Plasmodium falciparum, Plasmodium vivax and human hypoxanthine-guanine-(xanthine) phosphoribosyltransferases. *Bioorg. Med. Chem.* **20**, 1076–1089 (2012).

183. Hocková, D. *et al.* Synthesis of branched 9-[2-(2-phosphonoethoxy)ethyl]purines as a new class of acyclic nucleoside phosphonates which inhibit Plasmodium falciparum hypoxanthine-guanine-xanthine phosphoribosyltransferase. *Bioorg. Med. Chem.* **17**, 6218–6232 (2009).

184. Keough, D. T. *et al.* Inhibition of hypoxanthine-guanine phosphoribosyltransferase by acyclic nucleoside phosphonates: a new class of antimalarial therapeutics. *J. Med. Chem.* **52**, 4391–4399 (2009).

185. T, C. *et al.* β-Hydroxy- and β-Aminophosphonate Acyclonucleosides as Potent Inhibitors of Plasmodium falciparum Growth. *J. Med. Chem.* **63**, 8069–8087 (2020).

186. Collins, C. R. *et al.* Malaria Parasite cGMP-dependent Protein Kinase Regulates Blood Stage Merozoite Secretory Organelle Discharge and Egress. *PLoS Pathog.* **9**, e1003344 (2013).

187. Kim, J. J. *et al.* Crystal Structures of the Carboxyl cGMP Binding Domain of the Plasmodium falciparum cGMP-dependent Protein Kinase Reveal a Novel Capping Triad Crucial for Merozoite Egress. *PLOS Pathog.* **11**, e1004639 (2015).

188. Ashman, D. F., Lipton, R., Melicow, M. M. & Price, T. D. Isolation of adenosine 3', 5'-monophosphate and guanosine 3', 5'-monophosphate from rat urine. *Biochem. Biophys. Res. Commun.* **11**, 330–334 (1963).

189. Pasmanter, N., Iheanacho, F. & Hashmi, M. F. Biochemistry, Cyclic GMP. *StatPearls* (2022).

190. Patra, C., Foster, K., Corley, J. E., Dimri, M. & Brady, M. F. Biochemistry, cAMP. *StatPearls* (2022).

191. Ying, W. *et al.* Associations Between the Cyclic Guanosine Monophosphate Pathway and Cardiovascular Risk Factors: MESA. *J. Am. Hear. Assoc. Cardiovasc. Cerebrovasc. Dis.* **8**, (2019).

192. Baker, D. A. *et al.* Cyclic nucleotide signalling in malaria parasites. **7**, (2017).

193. Potter, L. R. *Guanylyl cyclase structure, function and regulation*. vol. 23 (NIH Public Access, 2011).

194. Mergia, E., Russwurm, M., Zoidl, G. & Koesling, D. Major occurrence of the new

alpha2beta1 isoform of NO-sensitive guanylyl cyclase in brain. *Cell. Signal.* **15**, 189–195 (2003).

195. Derbyshire, E. R. & Marletta, M. A. Structure and regulation of soluble guanylate cyclase. *Annu. Rev. Biochem.* **81**, 533–559 (2012).

196. Meigs, T. E. *et al.* Guanylyl Cyclase Receptors. *Encycl. Signal. Mol.* 843–847 (2012) doi:10.1007/978-1-4419-0461-4_434.

197. Nofal, S. D., Patel, A., Blackman, M. J., Flueck, C. & Baker, D. A. Plasmodium falciparum guanylyl cyclase-alpha and the activity of its appended P4-ATPase domain are essential for cGMP synthesis and blood-stage egress. *MBio* **12**, 1–19 (2021).

198. Nofal, S. D., Patel, A., Blackman, M. J., Flueck, C. & Baker, D. A. Plasmodium falciparum guanylyl cyclase-alpha and the activity of its appended P4-ATPase domain are essential for cGMP synthesis and blood-stage egress. *MBio* **12**, 1–19 (2021).

199. Gao, H. *et al.* ISP1-Anchored Polarization of GCβ/CDC50A Complex Initiates Malaria Ookinete Gliding Motility. *Curr. Biol.* **28**, 2763-2776.e6 (2018).

200. Hopp, C. S., Bowyer, P. W. & Baker, D. A. The role of cGMP signalling in regulating life cycle progression of Plasmodium. *Microbes Infect.* **14**, 831–837 (2012).

201. Manganiello, V. C., Fontana, J., Degerman, E. & Ahmad, F. CYCLIC NUCLEOTIDE PHOSPHODIESTERASES. *Encycl. Respir. Med. Four-Volume Set* 589–594 (2006) doi:10.1016/B0-12-370879-6/00104-6.

202. Francis, S. H. & Corbin, J. D. Cyclic GMP Phosphodiesterases. *Encycl. Biol. Chem. Second Ed.* 567–573 (2013) doi:10.1016/B978-0-12-378630-2.00343-1.

203. Richter, W. 3',5'-Cyclic nucleotide phosphodiesterases class III: Members, structure, and catalytic mechanism. *Proteins Struct. Funct. Bioinforma.* **46**, 278–286 (2002).

204. Omori, K. & Kotera, J. Overview of PDEs and Their Regulation. *Circ. Res.* **100**, 309–327 (2007).

205. Delhaye, S. & Bardoni, B. Role of phosphodiesterases in the pathophysiology of neurodevelopmental disorders. *Mol. Psychiatry 2021 269* **26**, 4570–4582 (2021).

206. Francis, S. H., Blount, M. A. & Corbin, J. D. Mammalian cyclic nucleotide phosphodiesterases: Molecular mechanisms and physiological functions. *Physiol. Rev.* **91**, 651–690 (2011).

207. Kong, G. *et al.* Functional characteristics and research trends of PDE11A in human diseases (Review). *Mol. Med. Rep.* **26**, 1–10 (2022).

208. Yuasa, K. *et al.* PfPDE1, a novel cGMP-specific phosphodiesterase from the human malaria parasite Plasmodium falciparum. *Biochem. J.* **392**, (2005).

209. Shakur, Y. *et al.* Membrane Localization of Cyclic Nucleotide Phosphodiesterase 3 (PDE3): TWO N-TERMINAL DOMAINS ARE REQUIRED FOR THE EFFICIENT TARGETING TO, AND ASSOCIATION OF, PDE3 WITH ENDOPLASMIC RETICULUM. *J. Biol. Chem.* **275**, 38749–38761 (2000).

210. Houslay, M. D., Baillie, G. S. & Maurice, D. H. cAMP-Specific Phosphodiesterase-4 Enzymes in the Cardiovascular System. *Circ. Res.* **100**, 950–966 (2007).

211. Kerr, N. M. & Danesh-Meyer, H. V. Phosphodiesterase inhibitors and the eye. *Clin. Experiment. Ophthalmol.* **37**, 514–523 (2009).

212. Azevedo, M. F. *et al.* Clinical and Molecular Genetics of the Phosphodiesterases (PDEs). *Endocr. Rev.* **35**, 195–233 (2014).

213. Barone, I., Giordano, C., Bonofiglio, D., Andò, S. & Catalano, S. Phosphodiesterase type 5 and cancers: progress and challenges. *Oncotarget* **8**, 99179 (2017).

214. Kim, G. E. & Kass, D. A. Cardiac Phosphodiesterases and their Modulation for Treating Heart Disease. *Handb. Exp. Pharmacol.* **243**, 249 (2017).

215. Cheitlin, M. D. *et al.* Use of Sildenafil (Viagra) in Patients With Cardiovascular Disease. *Circulation* **99**, 168–177 (1999).

216. Keating, G. M. & Scott, L. J. Vardenafil: a review of its use in erectile dysfunction. *Drugs* **63**, 2673–2702 (2003).

217. How and when to take tadalafil - NHS. https://www.nhs.uk/medicines/tadalafil/how-and-when-to-take-tadalafil/.

218. Manallack, D. T., Hughes, R. A. & Thompson, P. E. The next generation of phosphodiesterase inhibitors: Structural clues to ligand and substrate selectivity of phosphodiesterases. *J. Med. Chem.* **48**, 3449–3462 (2005).

219. Wentzinger, L. *et al.* Cyclic nucleotide-specific phosphodiesterases of Plasmodium falciparum: PfPDEα, a non-essential cGMP-specific PDE that is an integral membrane protein. *Int. J. Parasitol.* **38**, 1625–1637 (2008).

220. Flueck, C. *et al.* Phosphodiesterase beta is the master regulator of cAMP signalling during malaria parasite invasion. **17**, e3000154 (2019).

221. N'Dri, M. E. *et al.* Phosphodiesterase delta governs the mechanical properties of erythrocytes infected with Plasmodium falciparum gametocytes. *Microbes Infect.* **25**, (2023).

222. Lourido, S., Tang, K. & David Sibley, L. Distinct signalling pathways control Toxoplasma egress and host-cell invasion. *EMBO J.* **31**, 4524–4534 (2012).

223. Taylor, C. J., McRobert, L. & Baker, D. A. Disruption of a Plasmodium falciparum cyclic nucleotide phosphodiesterase gene causes aberrant gametogenesis. *Mol. Microbiol.* **69**, 110–118 (2008).

224. Schlossmann, J., Feil, R. & Hofmann, F. Insights into cGMP signalling derived from cGMP kinase knockout mice. *Front. Biosci.* **10**, 1279–1289 (2005).

225. Hofmann, F., Bernhard, D., Lukowski, R. & Weinmeister, P. CGMP regulated protein Kinases (cGK). *Handb. Exp. Pharmacol.* **191**, 137–162 (2009).

226. Wall, M. E. *et al.* Mechanisms associated with cGMP binding and activation of cGMP-dependent protein kinase. *Proc. Natl. Acad. Sci. U. S. A.* **100**, 2380–2385 (2003).

227. Sellak, H., Choi, C., Dey, N. B. & Lincoln, T. M. Transcriptional and post-transcriptional regulation of cGMP-dependent protein kinase (PKG-I): pathophysiological significance. *Cardiovasc. Res.* **97**, 200–207 (2013).

228. Francis, S. H., Busch, J. L. & Corbin, J. D. cGMP-Dependent Protein Kinases and cGMP Phosphodiesterases in Nitric Oxide and cGMP Action. *Pharmacol. Rev.* **62**, 525 (2010).

229. Aley, K. O., McCarter, G. & Levine, J. D. Nitric Oxide Signaling in Pain and Nociceptor Sensitization in the Rat. *J. Neurosci.* **18**, 7008 (1998).

230. Hofmann, F., Bernhard, D., Lukowski, R. & Weinmeister, P. *CGMP regulated protein Kinases (cGK)*. *Handbook of Experimental Pharmacology* vol. 191 137–162 (Springer, Berlin, Heidelberg, 2009).

231. Bakkouri, M. El *et al.* Structures of the cGMP-dependent protein kinase in malaria parasites reveal a unique structural relay mechanism for activation. *Proc. Natl. Acad. Sci. U. S. A.* **116**, 14164–14173 (2019).

232. Byun, J. A., VanSchouwen, B., Huang, J., Baryar, U. & Melacini, G. Divergent allostery reveals critical differences between structurally homologous regulatory domains of Plasmodium falciparum and human protein kinase G. *J. Biol. Chem.* **298**, (2022).

233. Gurnett, A. M. *et al.* Purification and Molecular Characterization of cGMP-dependent Protein Kinase from Apicomplexan Parasites: A NOVEL CHEMOTHERAPEUTIC TARGET. *J. Biol. Chem.* **277**, 15913–15922 (2002).

234. Donald, R. G. K. *et al.* Anticoccidial kinase inhibitors: identification of protein kinase targets secondary to cGMP-dependent protein kinase. *Mol. Biochem. Parasitol.* **149**, 86–98 (2006).

235. Alam, M. M. *et al.* Phosphoproteomics reveals malaria parasite Protein Kinase G as a signalling hub regulating egress and invasion. **6**, 1–15 (2015).

236. McRobert, L. *et al.* Gametogenesis in malaria parasites is mediated by the cGMP-dependent protein kinase. **6**, 1243–1252 (2008).

237. Panchal, D. & Bhanot, P. Activity of a Trisubstituted Pyrrole in Inhibiting Sporozoite Invasion and Blocking Malaria Infection. *Antimicrob. Agents Chemother.* **54**, 4269 (2010).

238. Baker, D. A. *et al.* A potent series targeting the malarial cGMP-dependent protein kinase clears infection and blocks transmission. *Nat. Commun.* **8**, 430 (2017).

239. Donald, R. G. K. *et al.* Toxoplasma gondii cyclic GMP-dependent kinase: chemotherapeutic targeting of an essential parasite protein kinase. *Eukaryot. Cell* **1**, 317–328 (2002).

240. Baker, D. A., Matralis, A. N., Osborne, S. A., Large, J. M. & Penzo, M. Targeting the Malaria Parasite cGMP-Dependent Protein Kinase to Develop New Drugs. *Front. Microbiol.* **11**, (2020).

241. Cowell, A. N. & Winzeler, E. A. Advances in omics-based methods to identify novel targets for malaria and other parasitic protozoan infections. *Genome Med. 2019 111*

11, 1–17 (2019).

242. Jiang, F., Zhou, K., Ma, L., Gressel, S. & Doudna, J. A. STRUCTURAL BIOLOGY. A Cas9-guide RNA complex preorganized for target DNA recognition. *Science* **348**, 1477–1481 (2015).

243. Bopp, S. E. R. *et al.* Mitotic Evolution of Plasmodium falciparum Shows a Stable Core Genome but Recombination in Antigen Families. *PLoS Genet.* **9**, 1003293 (2013).

244. Lasonder, E. *et al.* The plasmodium falciparum schizont phosphoproteome reveals extensive phosphatidylinositol and cAMP-protein kinase A signaling. *J. Proteome Res.* **11**, 5323–5337 (2012).

245. Rotella, D., Siekierka, J. & Bhanot, P. Plasmodium falciparum cGMP-Dependent Protein Kinase – A Novel Chemotherapeutic Target. *Front. Microbiol.* **11**, 3489.

246. Collins, C. R., Hackett, F., Atid, J., Tan, M. S. Y. & Blackman, M. J. The Plasmodium falciparum pseudoprotease SERA5 regulates the kinetics and efficiency of malaria parasite egress from host erythrocytes. **13**, e1006453 (2017).

247. Nyalwidhe, J. & Lingelbach, K. Proteases and chaperones are the most abundant proteins in the parasitophorous vacuole of Plasmodium falciparum-infected erythrocytes. *Proteomics* **6**, 1563–1573 (2006).

248. Hale, V. L. *et al.* Parasitophorous vacuole poration precedes its rupture and rapid host erythrocyte cytoskeleton collapse in Plasmodium falciparum egress. *Proc. Natl. Acad. Sci. U. S. A.* **114**, 3439–3444 (2017).

249. Berenbaum, M. C. A Method for Testing for Synergy with Any Number of Agents. *J. Infect. Dis.* **137**, 122–130 (1978).

250. Cooper, G. M. Cell Membranes. (2000).

251. Ginsburg, H. & Stein, W. D. The new permeability pathways induced by the malaria parasite in the membrane of the infected erythrocyte: comparison of results using different experimental techniques. *J. Membr. Biol.* **197**, 113–122 (2004).

252. Bouyer, G. *et al.* Plasmodium falciparum sexual parasites regulate infected erythrocyte permeability. *Commun. Biol.* **3**, (2020).

253. RIVADENEIRA, E. M., WASSERMAN, M. & ESPINAL, C. T. Separation and concentration of schizonts of Plasmodium falciparum by Percoll gradients. *J. Protozool.* **30**, 367–370 (1983).

254. Synchronization of Plasmodium falciparum erythrocytic stages in culture - PubMed. https://pubmed.ncbi.nlm.nih.gov/383936/.

255. Witkowski, B. *et al.* Novel phenotypic assays for the detection of artemisinin-resistant Plasmodium falciparum malaria in Cambodia: in-vitro and ex-vivo drug-response studies. *Lancet. Infect. Dis.* **13**, 1043–1049 (2013).

256. Fidock, D. A. & Wellems, T. E. Transformation with human dihydrofolate reductase renders malaria parasites insensitive to WR99210 but does not affect the intrinsic activity of proguanil. *Proc. Natl. Acad. Sci. U. S. A.* **94**, 10931–10936 (1997).

257. Deitsch, K. W., Driskill, C. L. & Wellems, T. E. Transformation of malaria parasites by the spontaneous uptake and expression of DNA from human erythrocytes. *Nucleic Acids Res.* **29**, 850 (2001).

258. Desjardins, R. E., Canfield, C. J., Haynes, J. D. & Chulay, J. D. Quantitative assessment of antimalarial activity in vitro by a semiautomated microdilution technique. *Antimicrob. Agents Chemother.* **16**, 710 (1979).

259. Keough, D. T. *et al.* Acyclic nucleoside phosphonates containing a second phosphonate group are potent inhibitors of 6-oxopurine phosphoribosyltransferases and have antimalarial activity. *J. Med. Chem.* **56**, 2513–2526 (2013).

260. Keough, D. T. *et al.* Inhibition of hypoxanthine-guanine phosphoribosyltransferase by acyclic nucleoside phosphonates: A new class of antimalarial therapeutics. *J. Med. Chem.* **52**, 4391–4399 (2009).

261. (PDF) The Role of Acyclic Nucleoside Phosphonates as Potential Antimalarials. https://www.researchgate.net/publication/287957393_The_Role_of_Acyclic_Nucleoside_Phosphonates_as_Potential_Antimalarials.

262. Gimode, W. R. *et al.* Fitness cost of resistance for lumefantrine and piperaquine-resistant Plasmodium berghei in a mouse model. *Malar. J.* **14**, 1–11 (2015).

263. Rosenthal, P. J. The interplay between drug resistance and fitness in malaria parasites. *Mol. Microbiol.* **89**, 1025 (2013).

264. Franz, E., Knape, M. J. & Herberg, F. W. CGMP Binding Domain D Mediates a Unique Activation Mechanism in Plasmodium falciparum PKG. *ACS Infect. Dis.* **4**, 415–423 (2018).

265. Kim, C. & Sharma, R. Cyclic nucleotide selectivity of protein kinase G isozymes. *Protein Sci.* **30**, 316 (2021).

266. Cooper, G. M. Cell Membranes. (2000).

267. Wein, S. *et al.* Transport and pharmacodynamics of albitiazolium, an antimalarial drug candidate. *Br. J. Pharmacol.* **166**, 2263 (2012).

268. Vanaerschot, M. *et al.* Inhibition of Resistance-Refractory P. falciparum Kinase PKG Delivers Prophylactic, Blood Stage, and Transmission-Blocking Antiplasmodial Activity. *Cell Chem. Biol.* **27**, 806-816.e8 (2020).

269. Tripathi, A. K., Mlambo, G., Kanatani, S., Sinnis, P. & Dimopoulos, G. Plasmodium falciparum Gametocyte Culture and Mosquito Infection Through Artificial Membrane Feeding. *J. Vis. Exp.* **2020**, 1–23 (2020).

270. Thompson, T. A., Chahine, Z. & Roch, K. G. Le. The role of long noncoding RNAs in malaria parasites. *Trends Parasitol.* **39**, 517–531 (2023).

271. Zhang, Y., Gao, Y., Wen, X. & Ma, H. Current prodrug strategies for improving oral absorption of nucleoside analogues. *Asian J. Pharm. Sci.* **9**, 65–74 (2014).

272. Krylov, I. S., Kashemirov, B. A., Hilfinger, J. M. & McKenna, C. E. Evolution of an amino acid based prodrug approach: stay tuned. *Mol. Pharm.* **10**, 445–458 (2013).